SURFACE CHARACTERIZATION OF PRETREATED AND MICROBIAL-TREATED *POPULUS* CROSS-SECTIONS

A Dissertation
Presented to
The Academic Faculty

by

Allison K. Tolbert

In Partial Fulfillment
of the Requirements for the Degree
Doctor of Philosophy in the
School of Chemistry and Biochemistry

Georgia Institute of Technology
May 2017

SURFACE CHARACTERIZATION OF PRETREATED AND MICROBIAL-TREATED *POPULUS* CROSS-SECTIONS

Approved by:

Dr. Arthur J. Ragauskas, Advisor

Departments of Chemistry and Biochemistry & Forestry, Wildlife, and Fisheries

University of Tennessee, Knoxville

Dr. Yulin Deng

School of Chemical and Biomolecular Engineering

Georgia Institute of Technology

Dr. Facundo Fernandez

School of Chemistry and Biochemistry

Georgia Institute of Technology

Dr. Preet Singh

School of Materials Science and Engineering

Georgia Institute of Technology

Dr. Stefan France

School of Chemistry and Biochemistry

Georgia Institute of Technology

Date Approved: April 11, 2017

ACKNOWLEDGEMENTS

White for your companionship. I am appreciative towards Dr. Norman Marsolan and Lloyd Williams for your guidance and support. Thanks to the BioEnergy Science Center for supporting my research.

I am also grateful for my internship in the Civil & Mechanical Engineering department at the United States Military Academy. Thank you to Mike Boss and Rod Wilson for supporting me and demonstrating true leadership. I am so thankful for LTC Phillip Root who showed me what it is like to invest in someone solely for their wellbeing and growth. I would like to thank MAJ Celio Biering for challenging me and helping me learn new skills. Special thanks to all the men on C level.

Most importantly, I would like to thank my family, friends, and God. I could not have accomplished this journey without the love, guidance, and support from my parents, Sam and Margo. Thanks to Jonathan, Luke, Patty, Anna Kate, Caroline, and Eleanor for believing in me. I am grateful for all my friends from Georgia Tech, Greenwood, and Knoxville who kept me grounded and helped me live life to the fullest. However, none of this would be possible expect through God, and I give Him all of glory and honor.

TABLE OF CONTENTS

LIST OF TABLES

LIST OF FIGURES

with Direct Red 23 (formerly, Pontamine Fast Scarlet 4B), lignin was autofluorescent.

LIST OF SYMBOLS AND ABBREVIATIONS

2D   Two dimensional

3D   Three dimensional

AAS   Aqueous ammonia soaking

AFM   Atomic force microscopy

Ar   Sum of ToF-SIMS aromatic peaks

ARP   Ammonia recycle percolation

CAZy   Carbohydrate-active enzymes

CBM   Carbohydrate-binding module

CBP   Consolidated bioprocessing

CLMS   Confocal laser scanning microscopy

DA   Dilute acid

DI   Deionized

DHP   Dehydrogenation polymer

DNA   Deoxyribonucleic acid

DP   Degree of Polymerization

DR23   Direct Red 23 dye

FTIR   Fourier transform infrared

G   Guaiacyl lignin unit

G-layer   Gelatinous layer

GH   Glycoside hydrolase

GPC   Gel Permeation chromatography

H	*p*-Hydroxyphenyl lignin unit
HPLC	High-performance liquid chromatography
HSQC	$^{13}C - ^{1}H$ heteronuclear single quantum coherence
L	Sum of ToF-SIMS lignin ion peaks
LCC	Lignin-carbohydrate complex
LHW	Liquid hot water
LMIG	Liquid metal ion gun
LOD	Low osmolarity defined
m/z	Mass-to-charge ratio
M_w	Weight average molecular weight
MSAFM	Mode-synthesizing atomic force microscopy
MTC	Medium for thermophilic clostridia
MWL	Milled wood lignin
NMR	Nuclear magnetic resonance
OCT	Optimum cutting temperature
PB	*p*-hydroxylbenzoate
PCA	Principal component analysis
PDMS	Poly-dimethyl-siloxane
PS	Sum of ToF-SIMS polysaccharide ion peaks
PTFE	Polytetrafluoroethylene
RFS	Renewable Fuel Standard
RIO	Region of interest
S	Syringyl lignin unit

S1   Outer layer of secondary cell wall

S2   Middle layer of secondary cell wall

S3   Inner layer of secondary cell wall

SXS   Sodium xylene sulfonate

SEM   Scanning electron microscopy

STXM   Scanning transmission X-ray microscopy

TEM   Transmission electron microscopy

ToF-SIMS   Time-of-flight secondary ion mass spectrometry

UV   Ultraviolet

Vis   Visible

XPS   X-ray photoelectron spectroscopy

SUMMARY

With the finite supply of fossil fuels and the contribution they have made to greenhouse gas emissions, one of the most promising alternative renewable energy sources for fuel is bioethanol. Lignocellulosic biomasses (e.g. woody biomass, grasses, and agriculture/forestry residues) are ideal feedstock since they avoid the "food versus fuel" debate of the first-generation biofuels from food-based crops. However, the challenge of utilizing the lignocellulosic biomass lies in overcoming its natural recalcitrance in order to ferment the sugars into ethanol. Various methods have been developed to increase cellulose accessibility by altering the physical and chemical structure of the plant cell wall. Optimizing chemical or biological treatments requires enhanced characterization techniques to analyze biomass changes. In this dissertation, time-of-flight secondary ion mass spectrometry (ToF-SIMS) is used to analyze the surface chemistry of chemically pretreated or microbial treated juvenile poplar stem sections.

The first objective of this thesis is to illustrate the advantages of surface characterization in biomass utilization studies. Untreated, ammonia-treated, and organosolv-treated poplar samples were analyzed for their chemical composition, lignin syringyl-to-guaiacyl ratio, and sugar release using surface and bulk characterization techniques. Surface chemical analysis can provide important information about specific lignocellulosic chemicals and cellulose accessibility that is lost during bulk chemical characterization. Chapter 5 compares ToF-SIMS analysis to other bulk analysis methods to determine how the ToF-SIMS might further enhance biomass characterization.

The second objective is to gain insight into the workings of potential consolidated bioprocessing microorganisms on the surface of poplar samples. Surface characterization of biomass in microbial studies is often neglected despite the common knowledge that enzymes first interact and bind to the sample's surface. Scanning electron microscopy and ToF-SIMS analysis provide insight into how *Caldicellulosiruptor bescii* and its enzymes alter the surface of the biomass in Chapter 6. The ToF-SIMS along with confocal laser scanning microscopy determines how *Clostridium thermocellum* hydrolysis impacts the surface chemistry of the poplar cross-sections (Chapter 7).

The third objective is to determine the impact biomass recalcitrance has on enzymatic hydrolysis and microbial fermentation in relation to the surface chemistry. The influence lignin content, lignin S/G ratio, and cellulose content has on the glucose release of pretreated biomass is addressed in Chapter 5. Chapter 7 goes into further detail about potential causes for the limited solubilization of poplar by *C. thermocellum* through chemical analysis, enzymatic hydrolysis, and surface characterization.

CHAPTER 1:   INTRODUCTION

With rising global energy demand along with growing concerns about global climate change and energy security, it is important to identify a renewable alternative to fossil-based fuels that is affordable and environmentally friendly.[1-2] One promising renewable fuel source is derived from biomass, which is organic material generated from crops, plants, and trees.[3] Not only is biomass a renewable resource, biomass-derived fuels could reduce greenhouse gas emissions and alleviate some energy security concerns.[2-3] Global usage of biofuels is expected to grow approximately 3.5 times between 2010 and 2035.[3]

In 2005, the United States Congress passed the Energy Policy Act, which created the Renewable Fuel Standard (RFS) program geared towards reducing or replacing a certain volume amount of petroleum-based transportation fuel with renewable fuel. The Energy Independence and Security Act of 2007 expanded the RFS program and the projected amount of renewable fuel produced by 2022 is 36 billion gallons. In 2010, the U.S. became the world's leading producer and exporter of biofuel with 13.5 billion gallons.[4] During that year, there were nearly 200 working biofuel production plants creating corn-based ethanol.[4]

Corn-based ethanol is considered a first-generation biofuel since it is derived from food crops. Other first-generation biofuel crops include: sugarcane, sugar beet, and wheat.[5] While these feedstocks are attractive due to their high sugar content that can readily be converted into biofuel, the problem lies with choosing between using the crops for biofuels or food and feed.[5] This issue can be addressed with second-generation biofuels produced from non-food crops of lignocellulosic biomass, including woody crops,

herbaceous crops, and agricultural/forest residues.[6] Specifically, *Populus deltoides* and other native North American poplar are fast growth trees that are capable of growing in various climates, such as the Great Lakes, the Northwest U.S., and the Mississippi Delta, making them promising feedstock for second-generation biofuel.[7-8]

Lignocellulosic biomass is structurally composed of an intricate network of biopolymers bound inter- and intra-molecularly together; the major chemical polymers are cellulose, hemicellulose, and lignin. This complex chemical matrix within the cell walls provides structural support to the plant, and assists in water transportation, and inhibits microbial degradation of its structural sugars.[6, 9] This natural defense, known as the biomass recalcitrance, hinders efficient biofuel production by making it difficult to easily access the sugars in the biomass.

Various pretreatment and microbial technologies have been developed to help overcome the biomass recalcitrance and improve sugar accessibility. With improvements in utilizing biomass through a number of different methods, it is imperative to obtain detailed chemical and physical information about the biomass sample using advanced analytical techniques. Conventional bulk chemical analyses (e.g. Dionex/high-performance liquid chromatography, gel permeation chromatography, nuclear magnetic resonance, and ultraviolet-visible spectroscopy) are the typical characterization methods for biomass treatment or utilization studies, but they neglect an important part of the biomass sample: the surface.

Bioconversion of lignocellulosic biomass into biofuels uses microorganisms and/or enzymes, whose first point of contact with the sample is at the surface. Time-of-flight

secondary ion mass spectrometry (ToF-SIMS) is a powerful tool capable of detecting major chemical components directly from the plant cell wall, which results in valuable knowledge of the specific chemical species and even their spatial distribution on the sample's surface. This type of information is typically lost with bulk compositional analysis.

The primary goal of this thesis is to a) illustrate the advantages of surface characterization in biomass utilization studies, b) gain insight into the workings of potential consolidate bioprocessing (CBP) microorganisms on biomass, and c) determine how the biomass recalcitrance and the surface chemistry impacts enzymatic hydrolysis and microbial fermentations. Few studies have used the ToF-SIMS in addition to bulk chemical analysis of a pretreated sample;[10-11] Jung et al.[12] performed a detailed study for dilute acid pretreated poplar where it was discovered that the surface and bulk chemistry can contradicted each other. ToF-SIMS analysis has not been applied to basic or organic solvent-based pretreatments or directly compared with other bulk characterization methods. Also, surface characterization could provide important information for microbial studies of potential CBP microorganisms. Therefore, a hypothesis was formed stating that surface lignin significantly impacts the bioconversion of pretreated biomass and the efficiency of microbial activity on lignocellulosic biomass. Part of this hypothesis was tested with a comprehensive study of the polysaccharide and lignin content, lignin syringyl-to-guaiacyl ratio, and glucose release of ammonia and organosolv pretreated poplar using ToF-SIMS and other bulk analytical methods in Chapter 5. The second part involving potential CBP microorganisms is addressed in Chapters 6 and 7. Scanning electron microscopy and ToF-SIMS analyze the physical and chemical impact

Caldicellulosiruptor bescii has on the surface of *Populus* cross-sections after long incubation times (Chapter 6). Assessment of *Clostridium thermocellum* conversion efficiency of *Populus* cross-sections and how biomass recalcitrance contributes to the premature cessation of microbial hydrolysis through ToF-SIMS and confocal laser scanning microscope occurs in Chapter 7.

CHAPTER 2:   LITERATURE REVIEW: BIOETHANOL FROM LIGNOCELLULOSIC BIOMASS

2.1   Lignocellulosic Biomass

One of the most abundant resources for the production of renewable fuels is biomass. The general classifications for biomass include terrestrial, aquatic, residues, and waste (Figure 1).[2] Food-based grain crops include corn, sugar cane, and sweet sorghum, while rapeseed and sunflower are designated oil crops.[2] "Lignocellulosic biomass" refers to plants primarily composed of cellulose, hemicellulose, and lignin that are not food-based crops, like hardwoods, softwoods, and grasses;[13] it is an abundant, nonfood-based feedstock that is relatively easily to grow and harvest when compared to biomass in other categories.[2]
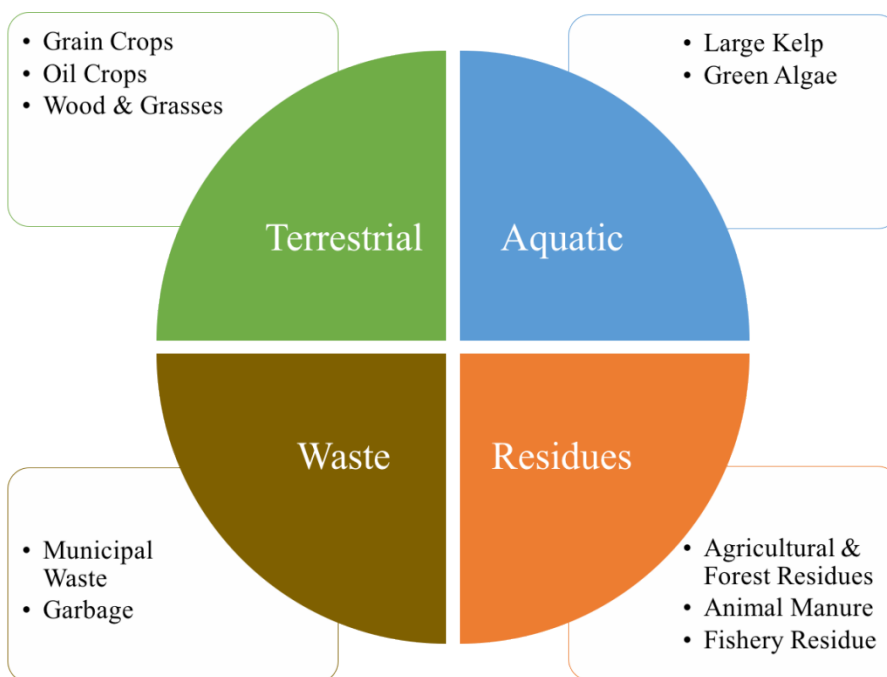
Figure 1. General biomass resource classification.[2]

All lignocellulosic biomasses are comprised of plant cell walls that provide structural support and protection to the cell membrane it surrounds. This cell wall is a complex matrix of cross-linked polysaccharide and lignin networks that make up the various layers: primary cell wall, secondary cell wall, and the middle lamella (Figure 2). In woody biomass, cellulose, hemicellulose, and pectin comprise the primary cell wall.[14] While secondary cell walls also contain cellulose and hemicellulose in addition to lignin, the cellulose microfibrils are aligned and spaced more loosely than those within the primary cell walls.[14] The secondary cell wall contains three different layers – outer (S1), middle (S2), and inner (S3) – which are differentiated from each other based on their cellulose microfibril orientation.[15] The middle lamella is composed of pectin and lignin that connects adjoining primary cell walls together and forms highly lignified cell corners.[16]
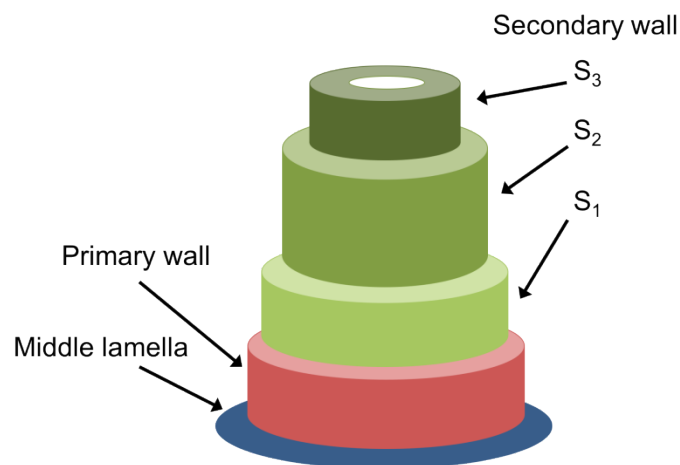
Figure 2. Cell wall schematic comprised of middle lamella, primary cell wall, and secondary cell wall layers.[17]

While different lignocellulosic biomasses possess similar cell wall structure, the chemistry can differ drastically. In order to develop biomass conversion technologies, it is vital to have a strong understanding of the chemical composition of lignocellulosic biomass.

2.1.1   Chemical Composition of Lignocellulosic Biomass

Lignocellulosic biomass is primarily composed of cellulose, hemicellulose, and lignin, which are biopolymers found within plant cell walls (Figure 3).[18] The amount of cellulose, hemicellulose, and lignin in common biomass feedstock can vary significantly, as summarized in Table 1. Cellulose and hemicellulose typically account for around 66% of the dry cell wall; other cell wall components are pectin, salts, and extractives, including fatty acids, fats, terpenes, and resins.

Table 1. Cellulose, hemicellulose, and lignin composition of common lignocellulosic biomass (%, dry basis).

	Cellulose	Hemicellulose	Lignin
Corn Stover[19]	38	26	19
Eucalyptus[20]	48	14	29
Miscanthus[19]	43	24	19
Monterey pine[7]	42	21	26
Populus deltoides[7]	42	17	26
Rice Straw[21]	35	25	12
Switchgrass[19]	37	29	19

| Wheat Straw[22] | 30 | 22 | 17 |
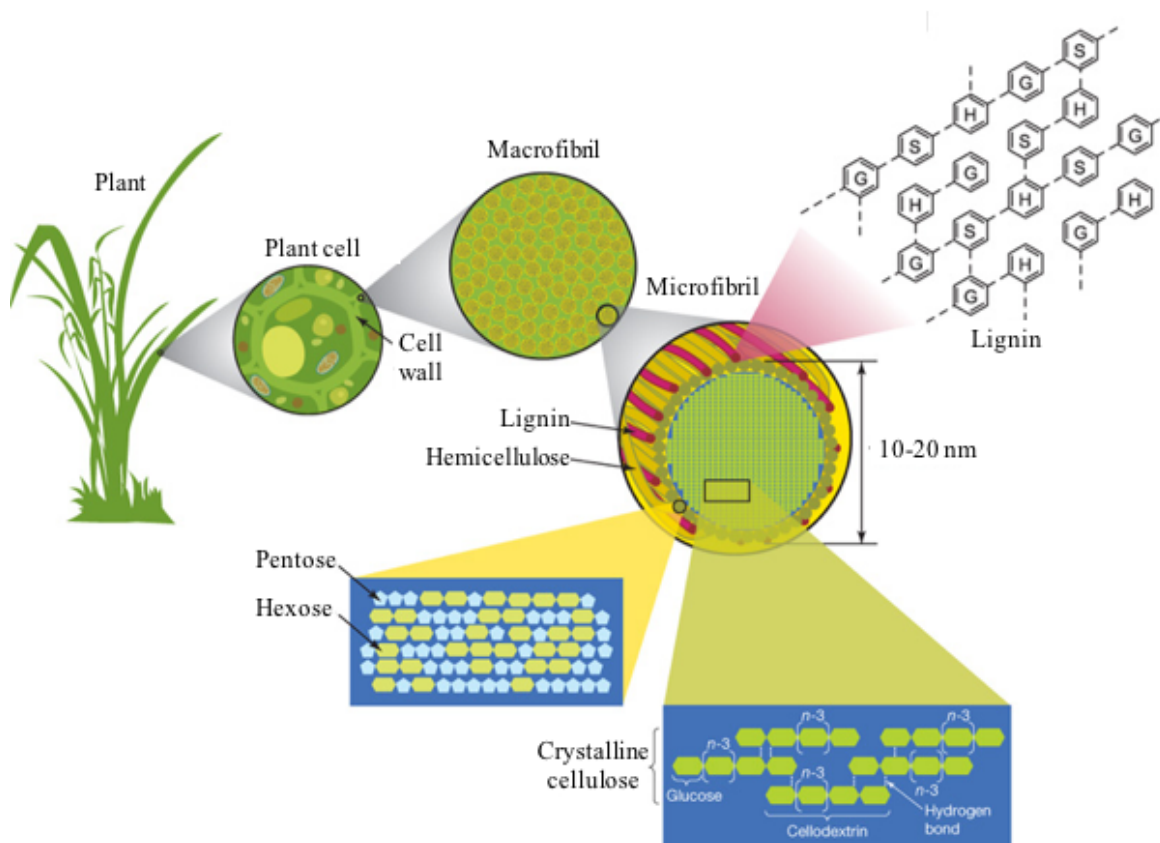
Figure 3. Schematic diagram of lignocellulosic biomass, including plant cell, macrofibrils, and microfibrils within plant cell wall. (Adapted from ref. 18)

2.1.1.1 Cellulose

Cellulose is the most abundant, naturally occurring terrestrial biopolymer and constitutes ~35 to 50% of lignocellulosic biomass.[1] Potentially thousands of glucose units connected by β-(1-4) glycosidic linkages form this linear chain polymer (Figure 4).[7, 23] The chain lengths vary between biomass; from regenerated cellulose fibers to almost cellulose-pure cotton, the degree of polymerization (DP) of cellulose can range from 250 to 10,000 and

sometime up to 15,000.[1, 24] Cellulose DP values for some common lignocellulosic biomass are listed in Table 2.
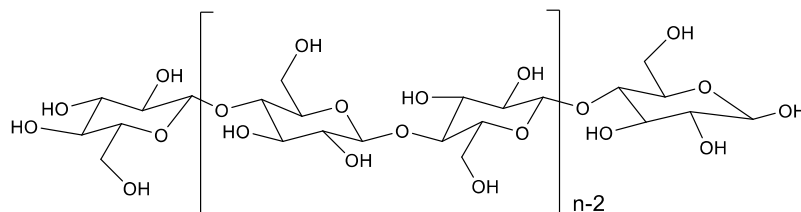
Figure 4 Molecular structure of cellulose.[24]

Table 2. Degree of polymerization for common lignocellulosic biomass cellulose.[25-26]

	Degree of Polymerization
Aspen	4581
Cotton	8000-15,000
Cotton Stalk	1820
Corn Stover	2520
Poplar	3500
Rice Straw	1820
Southern Pine	1450
Wheat Straw	2660

Cellulose microfibrils are composed of crystalline and amorphous regions (Figure 5). The highly ordered, crystalline structures are formed through the strong inter- and intra-molecular hydrogen bonding of the hydroxyl groups.[24, 27] Native cellulose possesses two

distinct crystalline forms (cellulose I_α and cellulose I_β) which are based on hydrogen-bonding patterns.[28] Cellulose I_α forms a triclinic structure with one cellulose chain per unit cell, while cellulose I_β has a monoclinic unit cell structure containing two chains.[29-30] Both cellulose I_α and cellulose I_β can be found in the same biomass, but algae and bacteria are predominantly composed of the cellulose I_α and higher plants mainly contain cellulose I_β.[28] Cellulose I can be modified into other crystalline cellulose polymorphs (cellulose II, III, IV). Cellulose II forms after cellulose I either undergoes regeneration involving solubilizing and recrystallization or mercerization via alkaline treatment. Liquid ammonia treatment of cellulose I and II will result in cellulose III, and treating cellulose III with heat in glycerol will form cellulose IV.[31] Cellulose crystallinity and relative proportions of cellulose I from Loblolly pine, poplar, and switchgrass are listed in Table 3.
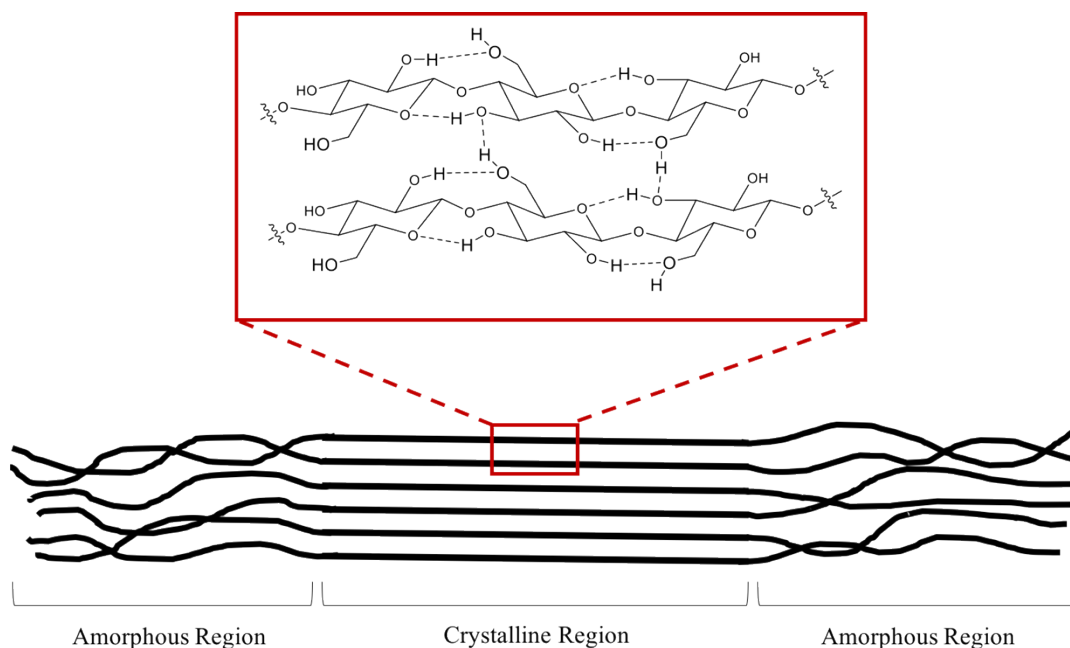
Figure 5. Schematic representation of amorphous and crystalline regions of cellulose along with an example of the inter- and intramolecular hydrogen bonding occurring in crystalline cellulose.[32]

Table 3. Cellulose crystallinity determined by cross polarization/magic angle spinning ^{13}C NMR.

	Loblolly Pine[33]	Poplar[a,34]	Switchgrass[b,35]
Cellulose crystallinity (%)	62.5	63	44
Cellulose I_α (%)	0.1	5.0	2.3
Cellulose $I_{\alpha+\beta}$ (%)	30.7	14.2	8.0
Cellulose I_β (%)	6.9	19.8	4.8
Accessible fibril surface (%)	33.1	10.2	6.2
Inaccessible fibril surface (%)	15.6	18.3	51.4

[a]*Populus trichocarpa x deltoides*; [b]Alamo.

2.1.1.2   Hemicellulose

Hemicelluloses are non-cellulosic, heterogeneous, polysaccharide polymers composed of pentose (xylose, arabinose), hexose (galactose, mannose), and uronic acids.[21, 36] They form linear and branched chains, which lead to more of an amorphous structure.[27] The different hemicelluloses can have different and important roles within the biomass; for example: mannans provide structural rigidity to the plant cell wall, xyloglucan form strong cross-linked networks with cellulose microfibrils, and xylans assist with water transportation and plant growth.[36] Overall, hemicellulose makes up approximately 25 to

30% of the dry biomass matter;[1] the individual monosaccharide distribution for various biomass is presented in Table 4.

Table 4. Hemicellulose compositions (% dry basis).

	Glucan	Galactan	Mannan	Xylan	Arabinan
Corn Stover[37]	38.3	0.6	ND	21.0	2.7
Miscanthus[a,38]	49.1	0.4	0.3	21.7	1.8
Populus deltoides[7]	39.2	0.9	1.8	13.1	0.9
Rice Strawn[37]	31.1	ND	ND	18.7	3.6
Switchgrass[b,38]	33.6	1.3	0.1	24.7	3.9
Wheat Straw[22]	30.2	0.8	ND	18.7	2.8

ND: Not Detected; [a]Without prehydrolysis; [b]Extracted with hot H_2O and C_6H_6/EtOH.

The building units of hemicellulose are many times composed of two or more different monosaccharides; for example, the main hemicellulose in hardwoods is glucuronoxylan, while softwoods contain significant amounts of both galactoglucomannan and arabinoglucuronoxylan (Figure 6).[39] The degree of polymerization for these polysaccharides and two others, arabinogalactan and glucomannan, found within dry biomass is listed in Table 5. Glucuronoxylan and galactoglucomannan can be present in amounts as high as 30% and 25%, respectively, while the others make up 10% or less of the dry biomass.[40] The DP of hemicellulose may only be a small fraction of the DP of cellulose, but these polysaccharides are capable of increasing the biomass recalcitrance by covalently binding with lignin and forming lignin-carbohydrate complexes (LCC).[41-42]

Table 5. Main types of polysaccharides in hemicellulose with corresponding amounts and degree of polymerization.[40]

	Biological Origin	Amount (% dry)	DP
Arabinogalactan	Softwood	1-3	100-600
Arabinoglucuronoxylan	Grasses, Softwood	5-10	50-185
Galactoglucomannan	Softwood	10-25	40-100
Glucomannan	Softwood, Hardwood	2-5	40-70
Glucuronoxylan	Hardwood	15-30	100-200
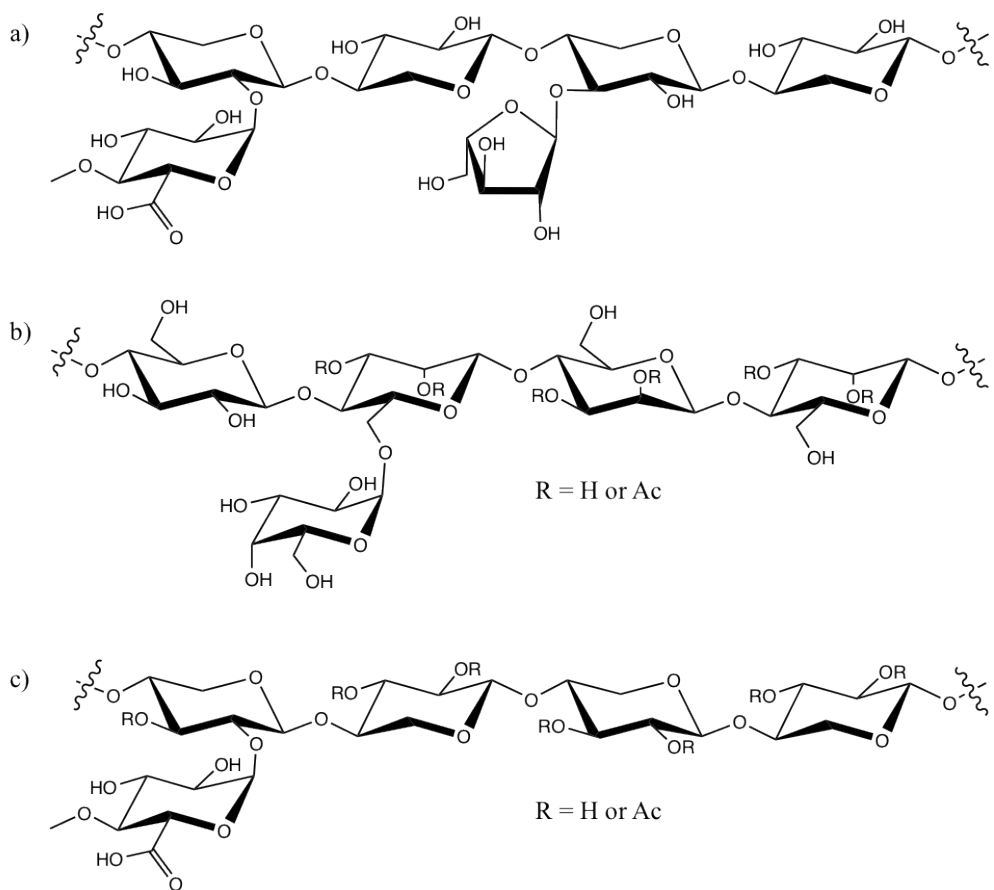
Figure 6. Chemical structures for the major hemicelluloses in softwoods, a) arabinoglucuronoxylan and b) galactoglucomannan, along with the major hemicellulose in hardwood, c) glucuronoxylan.[27]

2.1.1.3 Lignin*

Lignin usually contributes between 15 wt% and 40 wt% of woody plants' dry matter.[43] This polyphenolic polymer is primarily derived from three or less monolignols, including *p*-coumaryl alcohol, coniferyl alcohol, and sinapyl alcohol (Figure 7).[44-46] These alcohols give rise to the structural units of lignin: *p*-hydroxyphenyl (H), guaiacyl (G), and syringyl (S).[43-44] Low levels of H lignin structural unit are present in softwoods, like spruce, and herbaceous species, like alfalfa.[47] G lignin is the primary component of softwoods, while hardwoods are composed chiefly of G and S lignin structural units.[44, 16, 17] Table 6 presents H:G:S values for lignin found in various biomass.
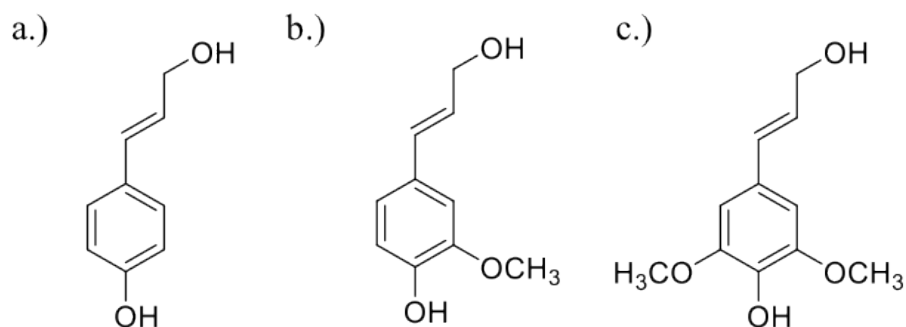
Figure 7. Three monolignol monomers: (a) *p*-coumaryl alcohol, (b) coniferyl alcohol, and (c) sinapyl alcohol.

Table 6. Relative distributions of *p*-hydroxyphenyl (H), guaiacyl (G), and syringyl (S) lignin monomers in various biomass (%).[47-49]

	H	G	S
Alfalfa[a]	5	56	39
Birch[b]	—	22	78
Miscanthus[c]	4	52	44
Poplar[b]	—	37	63
Spruce[b]	2	98	Trace
Wheat[b]	5	49	56

[a]Thioacidolysis and acetyl bromide treatment; [b]Thioacidolysis of extractive-free cell walls; [c]MWL.

These phenylpropane monomers are connected by various carbon-carbon bonds and ether linkages (Figure 8), the most abundant being the aryl ether bond, β-O-4.[44, 50] Interestingly, there are over 20 identified lignin linkages,[51] but major linkages found in softwoods and hardwoods are β-O-4, β-1, 4-O-5, 5-5, α-O-4, β-β, β-5, and dibenzodioxocin linkages (Table 7). Dibenzodioxocin is formed by oxidizing coniferyl alcohol with 5-5 biphenyl, and is found in smaller quantities in hardwood than softwood, where it contributes to 10% or more of the lignin structure.[46, 52] Dibenzodioxocin, 4-O-5, and 5-5 linkages are also branching points for this three-dimensional polymer.[51] Branching typically occurs using G lignin units, while S-rich lignin forms more linear structures.[51] The weight average molecular weight (M_w) of milled wood lignin (MWL) can range from 5900 g/mol for redwood to 23,500 g/mol for Norway spruce, as seen in

Table 8.[38, 53] It is important to note that the actual structure of lignin remains unknown,[46] but a representation of hardwood lignin is presented in Figure 9. The distribution of lignin within the biomass, its structure, and its degree of polymerization (i.e., molecular weight) can inhibit enzyme hydrolysis.[54] Overall, lignin is one of the most recalcitrant biopolymers found in the cell wall.[44]

β-O-4

β-1

4-O-5

Dibenzodioxocin

5-5'

α-O-4

β-β

β-5
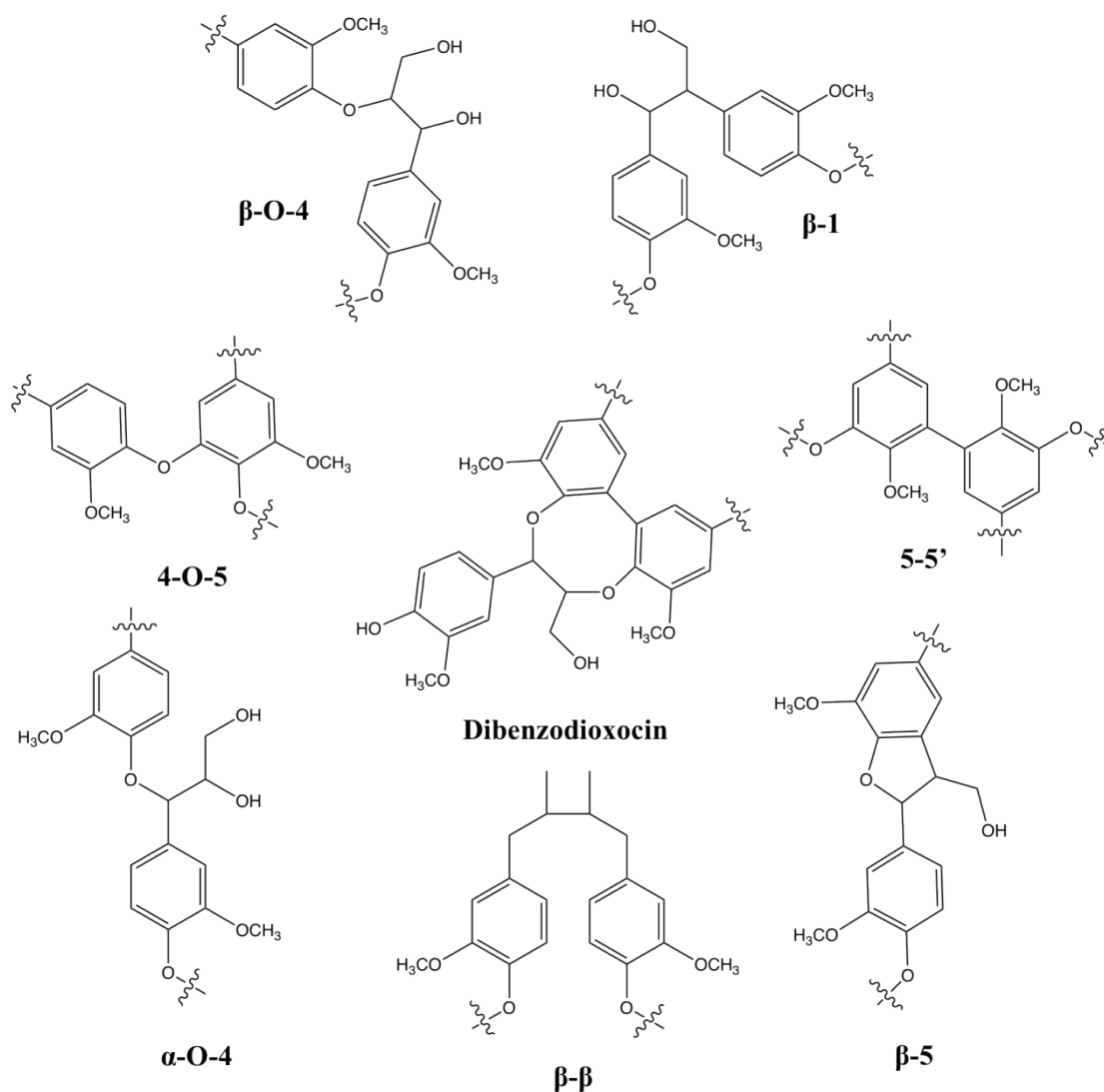
Figure 8. Softwood and hardwood major lignin linkages: β-O-4, β-1, 4-O-5, dibenzodioxocin, 5-5, α-O-4, β-β, and β-5.[46, 52, 55-56]

Table 7. Major linkages proportions (%) in softwood (spruce) and hardwood (birch) lignin.[55]

	β-O-4	β-1	4-O-5	5-5	β-β	α-O-4	β-5	Other
Softwood	46	7	3.5-4	9.5-11	2	6-8	9-12	13
Hardwood	60	7	6.5	4.5	3	6-8	6	5
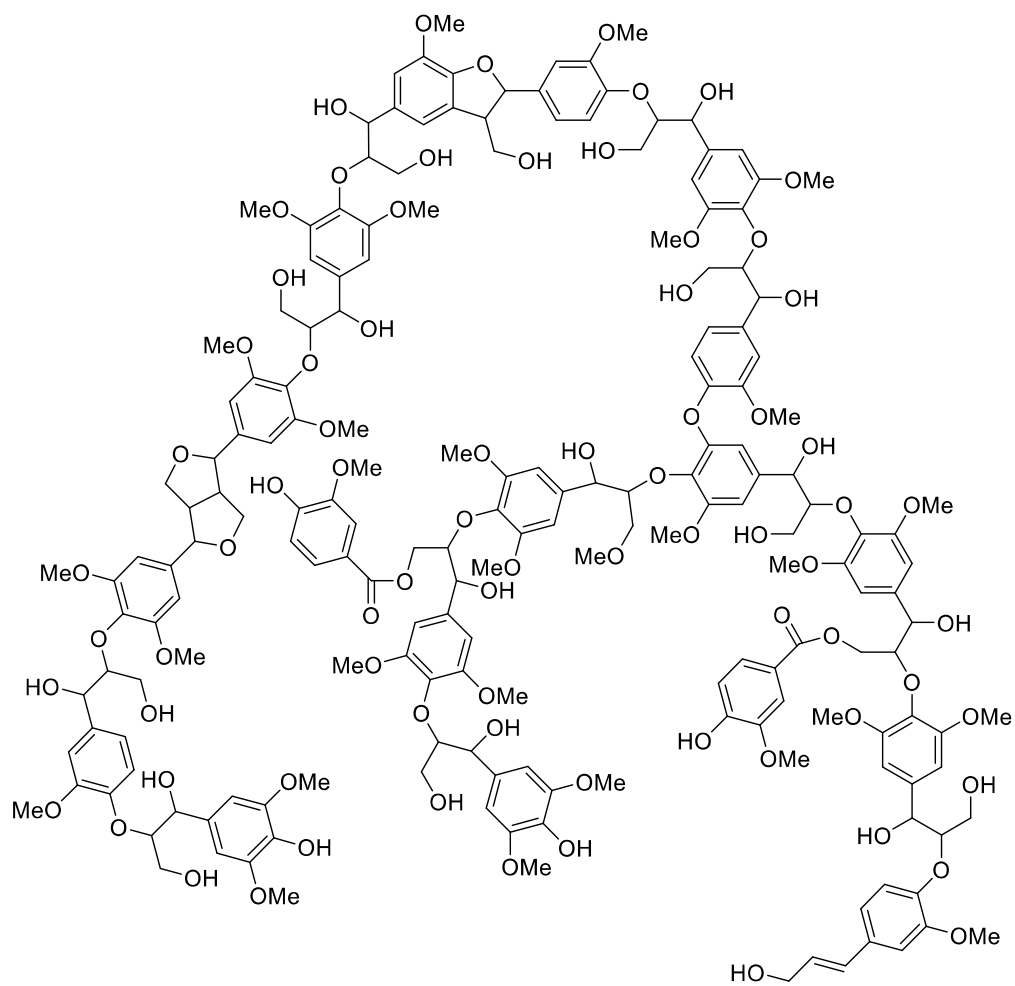
Figure 9. Schematic representation of hardwood lignin.

Table 8. Weight average molecular weight from milled wood lignin of various biomasses. (Adapted from ref. 38 and 53)

Biomass	M_w (g/mol)
Bamboo	12,090
Douglas Fir[a]	7400
Eucalyptus[a]	6700

Miscanthus[b]	13,700
Norway Spruce[c]	23,500
Poplar	10,000
Redwood[a]	5900
Southern Pine[a]	14,900

[a]Ball mill for 28 days; [b]Values corrected from the original manuscript after a personal discussion with the author; [c]Vibratory-milled.

2.1.1.4   Lignin-Carbohydrate Complexes

As mentioned previously, lignin and carbohydrates can form covalent and non-covalent bonds, known as lignin-carbohydrate complexes (LCCs).[51] Covalent bonding typically occurs at the α-carbon or the C-4 of the benzene ring.[57] The four major lignin-carbohydrate covalent bonds proposed are benzyl ether, benzyl ester, phenyl glycosides, and acetal linkages (Figure 10).[51, 57]
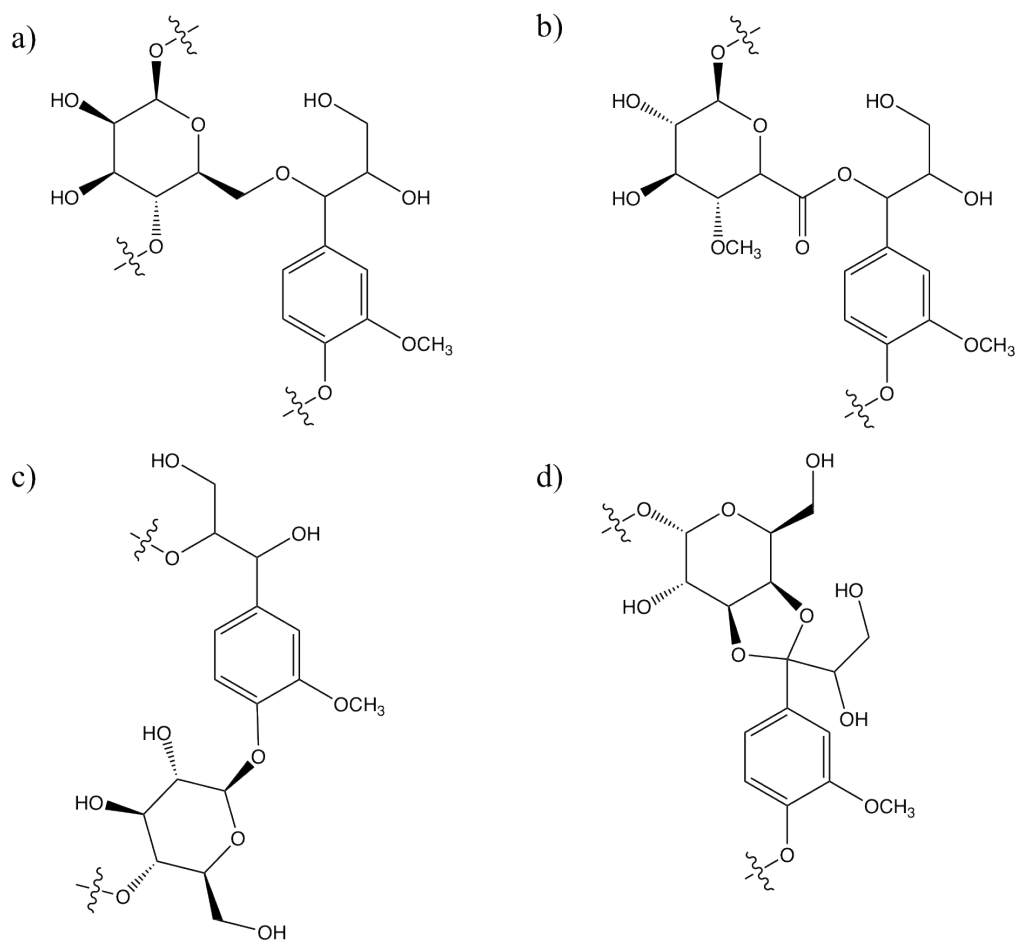
Figure 10. Major lignin-carbohydrate complex covalent bonds: a) benzyl ether, b) benzyl ester, c) phenyl glycoside, and d) acetal type.[51]

LCCs are different in woody biomass and grasses. The major carbohydrate in woody LCCs is xylose, while other sugars (arabinose, galactose, glucose, and mannose) make up the other 20%, as seen in Figure 11. Grasses LCCs are also known as lignin/phenolics-carbohydrate complexes due to the hydroxycinnamic acid (ferulic, *p*-coumaric, or sinapic acid, see Figure 12) bridges between lignin and carbohydrates, specifically arabinoxylans, at the ether or ester bond.[57] Rice straw LCCs contain 28% Klason lignin and 64% carbohydrate, along with uronic acid, ferulic acid, and *p*-coumaric acid.[57] Mild

acidic conditions can hydrolyze benzyl ethers and phenyl glycoside linkages,[58-59] in addition to cleaving lignin and ferulic acid at their ether bond.[57] Lignin-hemicellulose LCCs protect the cellulose by surrounding and forming hydrogen bonds with it,[51] thereby decreasing the cellulose accessibility and increasing the recalcitrance of the biomass.[42]
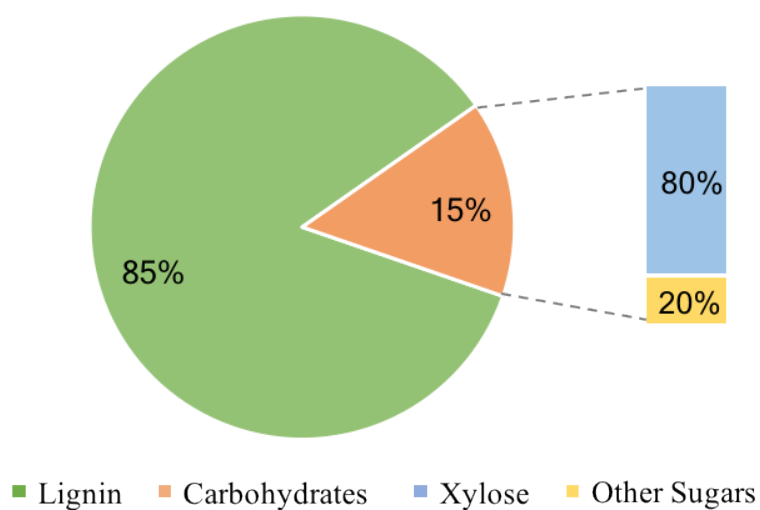
Figure 11. A general composition of lignin and carbohydrates of LLCs in woody biomass.[57]
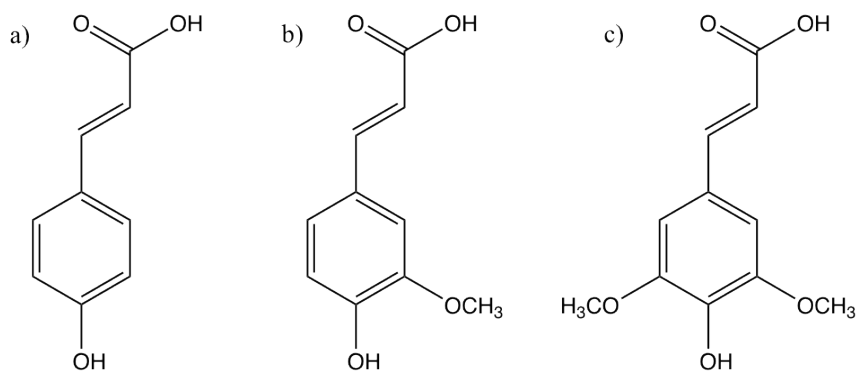
Figure 12. Structures of a) p-coumaric acid, b) ferulic acid, and c) sinapinic acid.

2.1.2 Biomass Recalcitrance

The complex matrix formed by interlocked lignocellulosic components within the plant cell walls produces a structural barrier that inhibits cellulose accessibility and biomass degradation from biological agents; this is known as the biomass recalcitrance.[37, 60] Some specific contributing factors impacting biomass digestibility include lignin and hemicellulose composition and structure, cellulose crystallinity and DP, and the surface area.[54, 61] Various pretreatments have been designed to disrupt the lignocellulosic structure to reduce or eliminate the recalcitrance and increase enzymatic hydrolysis of cellulose.[60, 62-63] Also, a number of microorganisms capable of utilizing lignocellulosic biomass have been studied and engineered as an alternative process towards overcoming the biomass recalcitrance.[64-65] Nevertheless, biomass recalcitrance remains a major impediment in developing cost-efficient bioethanol production.

2.2 Lignocellulosic Biomass Pretreatments and Consolidated Bioprocessing

2.2.1 Lignocellulosic Ethanol

Unlike the first-generation biofuel, the second-generation avoids food-based feedstock, like corn and sugar cane, by producing bioethanol from lignocellulosic biomass, one of the most abundant and renewable terrestrial resources. Well over a billion tons of woody and non-woody (agricultural residue, grasses, etc.) feedstock could be harvested in the U.S. each year to meet the demand of biofuel replacing 30% of petroleum-based transportation fuel;[1, 4] however, the cost of bioethanol production needs to be reduced, and one way is by increasing the cellulosic and hemicellulosic sugar yields from the biomass.[66] Isolating a high yield of fermentable carbohydrates from lignocellulosic cellulose and hemicellulose is a major challenge in producing lignocellulosic ethanol.[23] Overcoming the biomass recalcitrance to utilize the sugars typically requires a pretreatment or specific microorganisms capable of combined hydrolysis and fermentation technologies, a process known as consolidated bioprocessing (CBP).

Traditionally, ethanol production involves five major steps: pretreatment, enzymatic hydrolysis, fermentation, product separation, and liquid fraction treatment.[67] Lignocellulosic biomass is typically pretreated such that cellulose-rich residues are formed, which can be deconstructed by enzymes, like cellobiohydrolase, endoglucanase, and β-glucosidase.[14] While there are enzymes that also catalyze hemicellulose deconstruction, it usually requires a number of distinct enzymes to completely break down the heteropolysaccharide.[14] The hexose monosaccharides can easily be fermented by microorganisms, like yeast, into ethanol.[67]

2.2.2 Lignocellulosic Biomass Pretreatments

Lignocellulosic pretreatments assist in overcoming the biomass recalcitrance by disrupting the chemical matrix (Figure 13).[68] Dissociation of hemicellulose from cellulose, delignification or lignin redistribution, change in cellulose crystallinity and DP, and increase in surface area of substrate are a few desired results from pretreatments.[61, 69]
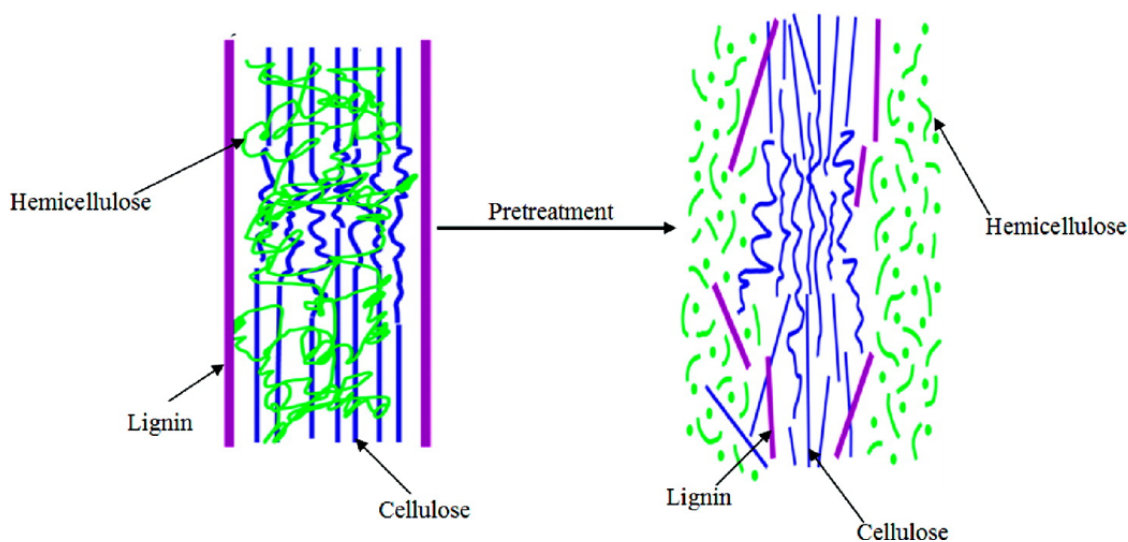
Figure 13. Schematic representation of the impact a pretreatment has on the cellulose, hemicellulose, and lignin. (Reprinted from ref. 71)

There are three different classifications for pretreatments: physical, chemical, and biological, as seen in Table 9. The majority of pretreatment methods impact the chemical and/or physical structure of the biomass.[61] Biological pretreatments are considered too slow (10-14 days) for industrial purposes, despite being some of the most environmentally friendly methods by using microorganisims, like white-rot fungi,

instead of chemicals.[37, 70] Physical treatment of milling reduces particle size and therefore increases the surface area, but milled biomass typically undergoes further chemical or biological pretreatments.[69] Another physical process is to use microwave irradiation to heat the sample, resulting in partial deligninification and disruption of LCCs.[37, 71]

Table 9. Lignocellulosic pretreatment classifications methods and specific treatment processes.[37-38]

Biological	▪ **Fungi** ▪ **Bacteria**
Physical	▪ Milling ▪ Microwave ▪ Thermophysical
Chemical	▪ Alkaline ▪ Dilute Acid ▪ Ionic Liquid ▪ Organosolv
Physico-chemical	▪ Ammonia Fiber Explosion (AFEX) ▪ CO_2 Explosion ▪ Liquid Hot Water ▪ Steam Explosion

Chemical and physico-chemical pretreatments typically involve solubilizing, at least partially, lignin, hemicellulose, or both. This makes it easier to isolate specific polymers or for enzymes to hydrolyze cellulose and hemicellulose into C_5 and C_6 sugar monomers.

Alkaline, dilute acid (DA), liquid hot water (LHW), and organosolv pretreatments are all leading technologies for overcoming the biomass recalcitrance. Common pretreatment conditions for these processes and others are summarized in Table 10.

Table 10. Summary of major chemical and/or physical impact different pretreatments have on lignocellulosic biomass.[63, 68-69, 72]

Pretreatment	General Conditions
Alkaline	NaOH, KOH, CaOH, or NH_4OH (temperature and time varies depending on base).
DA	$0.75 - 5\%$ H_2SO_4, HNO_3, H_3PO_4, or HCl (120-220°C).
Liquid Hot Water	Pressurized hot water (170-230°C, $p > 5$ MPa) for 1-46 min.
Organosolv	Methanol, ethanol, acetone, ethylene glycol and potentially with acid or base catalyst (100-250°C) for 30-90 min.
Steam Explosion	Saturated steam (160-290°C, $p = 0.69$-4.85 MPa) for several sec to min, then depressurized to atm pressure.

Different pretreatments impact biomass in different ways. LHW results in approximately all hemicellulose removal, some solubilization of cellulose (4-22%), and partial delignification;[69] however, it is possible for the lignin content to be greater than that of the starting material due to pseudo-lignin, lignin-like material derived from degraded polysaccharide and/or polymerization of solubilized lignin.[44, 73] DA pretreatment also removes the majority of hemicellulose, but it can also disrupt and redistribute lignin

26

within the plant cell wall and form pseudo-lignin spheres on the surface.[44, 69, 73] Significant delignification and hemicellulose removal occurs during alkaline and organosolv pretreatments.[74] Alkaline and organosolv pretreatments are briefly discussed in greater detail below.

2.2.2.1 Alkaline Pretreatment

Alkaline pretreatments target lignin in hardwoods, grasses, and some agricultural residues.[75] This pretreatment also significantly reduces the amount of hemicellulose within the biomass residue (Table 11).[63] The saponification at the ester bond link in LCCs can result in delignification and lead to an increased efficiency for enzymatic hydrolysis of cellulose.[74-76] However, lignin can be redistributed within the cell walls or recondensed on the biomass during the delignification process of the pretreatment.[67] While the solubilized hemicellulose and lignin can have an inhibitory effect on the fermentation microorganisms,[67] deacetylation of hemicellulose improves enzymatic hydrolysis by removing these sterically hindering functional groups.[69, 77] Depending on the pretreatment chemicals, cellulose I could be converted into cellulose II with sodium hydroxide or cellulose III with liquid ammonia.[31]

Table 11. General alkaline pretreatment conditions and effects.[78]

Reaction conditions	Hemicellulose Removal	Lignin Removal

Sodium hydroxide	0.5–10.0% NaOH, 10–30% solid loading, 60–180°C for 5–60 min.	50%	60-80%
Ammonium hydroxide	10–30% ammonia, 10–50% solid loading, 30–210°C for 5–60 min with ~2.3 MPa (ARP) or 4 – 24 h (AAS).	20-50%	60-80%

ARP: ammonia recycle percolation; AAS: aqueous ammonia soaking.

There are two general types of alkaline pretreatments: 1) those processes that use sodium, potassium, or calcium hydroxide, and 2) ammonia-based pretreatments.[79] Specifically, aqueous ammonia processes include aqueous ammonia soaking (AAS) and ammonia recycle percolation (ARP).[69, 74] Soaking in aqueous ammonia can occur at lower temperatures (30-60°C) for longer times (4-24 h).[70, 78, 80] ARP typically operates at 150-210°C using 10-15% aqueous ammonia for 10-90 min under pressure in a column reactor.[61, 68, 70, 78] Some advantages of using ammonia for the alkaline pretreatment of biomass are: 1) it is a non-corrosive, non-polluting chemical, 2) it will effectively cause the lignocellulosic material to swell, 3) it possesses higher selectivity for lignin reactions than reactions with carbohydrates, and 4) it can easily be recovered and recycled.[74] Overall, reaction temperature, length of pretreatment, and amount of alkali all impact the efficiency of the pretreatment.[63] Some limitations to this type of pretreatment include the cost of recycling the chemicals and the formation of salts during the pretreatment process that could be incorporated into the biomass substrate.[63, 68]

2.2.2.2 Organosolv Pretreatment

Organosolv pretreatment is another delignification process that use organic solvents to solubilizes significant amounts of lignin and hemicellulose.[69, 75] Delignification is possible through the cleaving ether linkages and lignin and hemicellulose LCC bonds.[37, 81] Solubilization of lignin and hemicellulose increases the surface area allowing for greater cellulase and enzyme absorption, thus significantly increasing enzymatic hydrolysis.[69, 82]

Some commonly used organic solvents for this type of pretreatment include methanol, ethanol, acetone, and ethylene glycol.[37] Methanol and ethanol are frequently used due to their low molecular weight, and that primary alcohols are typically better at delignification than secondary or tertiary alcohols; however, ethanol is less toxic than methanol and would be a more environmentally-friendly solvent to use.[81] Ethanol concentration for this pretreatment typically ranges between 35% and 70% (w/w).[68] Acid or base catalysts (e.g. HCl, H_2SO_4, NaOH) are added to the organic solvent to assist in lignin and hemicellulose solubilization.[37] The addition of acid catalysts results in higher delignification rate and xylose yields, but the need for them could be eliminated with a higher operating temperatures, 185-210°C.[81] At this temperature, it is believed that released organic acids from the biomass will become the catalyst for rupturing LCC bonds.[83] Ethanol pretreatment of hybrid poplar with a H_2SO_4 catalyst at 180°C can remove 73% of lignin, and methanol pretreatment with a HCl catalyst can remove 90% of pine lignin (Table 12). One disadvantage for this type of pretreatment is the high cost for the solvent recycling process[68] and equipment (e.g. pressurized reactor).

Table 12. Lignin removal for various organosolv pretreatment conditions.

	Solvent	Catalyst	Temperature (°C)	Time (min)	Lignin Removal
Hybrid poplar[a,84]	50% EtOH	1.25% H_2SO_4	180	60	73%
Miscanthus[b,85]	50% EtOH	0.9% H_2SO_4	170	60	75%
Eucalyptus[86]	75% EtOH	1.0% AA	200	60	88%
Pine[87]	90% MeOH	0.2% HCl	170	45	90%

[a]*Populus nigra x P. maximowiczii*; [b]Presoaking with H_2SO_4 and water at 100°C; AA: acetic acid.

2.2.3 Consolidated Bioprocessing (CBP)

Due to the expensive pretreatment step, researchers are attempting to genetically engineer microorganisms capable of consolidated bioprocessing (CBP), where enzymatic hydrolysis and sugar fermentation are combined into one step. Potential CBP microorganisms break down cellulose, typically through the activity of secreted cellulases, and therefore eliminate a production step used to add enzymes.[88-89] The current strategy, first generation CBP, still incorporates a pretreatment step, but researchers are working on developing a second generation CBP strategy that would use non-pretreated biomass.[90] For a CBP microorganism to be industrially relevant, it must be capable of decomposing biomass substrates polysaccharides and fermenting hexose and pentose sugars at a rate greater than 1g/L/h into ethanol with a 90%+ theoretical yield and a minimum of 40 g/L titer.[23, 89] Since, no known microorganism is capable of meeting these conditions, researchers have resorted to genetically engineering microorganisms fit for industrial use in biofuel production.[23] One way to accomplish this is by identifying a microorganism capable of degrading lignocellulosic biomass and engineering it (e.g.

through gene deletion) to produce ethanol or other desired products.[23, 91] *Clostridium thermocellum* and *Caldicellulosiruptor bescii* are widely considered to be potential CBP candidates due to their ability to naturally degrade lignocellulosic biomass, and are discussed in greater detail below.

2.2.3.1 *Clostridium thermocellum*

Clostridium thermocellum is a rod shaped, anaerobic, Gram positive cellulolytic thermophile that naturally produces lactate, acetate, ethanol, H_2, and formate from cellulose.[88, 92-95] In the presence of cellulose, this bacterium forms biofilms, where a monolayer of cells form that orient themselves parallel to the substrate's carbon fibers (Figure 14).[96] Optimum growth conditions for this microorganism occur at 60°C and between 6.7 and 7.0 pH.[23, 93] *C. thermocellum* growth conditions and corresponding ethanol and acetate product yields from various substrates can be found in Table 13. Glucose conversion during fermentation of DA pretreated *Populus* over 37 h was 58-64%, while only 43-49% of glucose was utilized for DA pretreated switchgrass.[97]
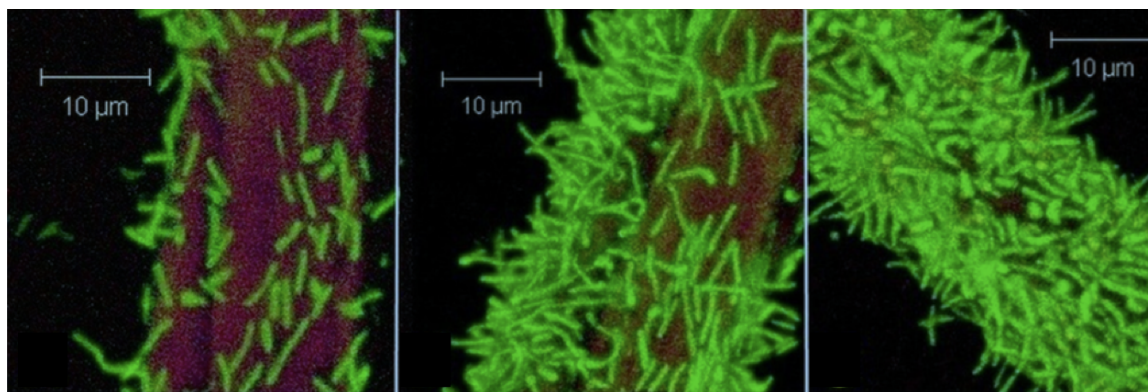
Figure 14. CLSM images of biofilm illustrating various degree of *Clostridium thermocellum* 27405 cell density on cellulose cotton fibers after 48 h incubation. (Reprinted from ref. 99)

This microbe possesses the ability to hydrolyze both hemicellulose and cellulose, in addition to fermenting six-carbon sugar cellodextrins at a fast rate;[23] however, it does not utilize hemicellulose for energy or growth.[98] *C. thermocellum* wild type (ATCC 27405) is capable of completely consuming cellobiose and 95% of Avicel cellulose.[92] While *C. thermocellum* is able to grow on untreated biomass,[99-100] only 32.5% of untreated switchgrass is converted.[101] Fermentation can solubilize 60% and 15% of carbohydrates in switchgrass and untreated *Populus*, respectively.[100, 102] Although the cause for this limited hydrolysis is not fully understood, pretreating the biomass can lead to an increase in glucan conversion during fermentation.[103]

Table 13. Growth conditions and fermentation products from treatment of various substrates with *C. thermocellum* strain 27405 in MTC medium.

Substrate[a]	Temperature (°C)	pH	Time	Ethanol (g/L)	Acetate (g/L)
Cellobiose[88]	58	6.8	Overnight + 2-3 h	1.02	1.43
Crystalline cellulose (Avicel)[104]	58	7.0	Overnight + 2-3 h	0.83	0.83
DA pretreated switchgrass[97]	58	6.8	12 h	0.10	0.30
			37 h	0.20	0.50
DA pretreated *Populus*[97]	58	6.8	12 h	0.20	0.40
			37 h	0.30	0.80

[a]Substrate loading: 5 g/L; MTC: medium for thermophilic clostridia.

To assist in solubilizing cellulose, *C. thermocellum* secretes a cell wall-bound multi-enzyme complex, known as a cellulosome.[92, 96] Its cellulosomes are composed of over 70 different types of glycoside hydrolases (GHs) capable of polysaccharide degradation.[88] The cellulosome's primary scaffoldin protein, known as CipA, contains nine Type I cohesion domains that bind the corresponding Type I dockerin modules of GHs, and which are connected through a linker to the carbohydrate-binding module (CBM), as represented in Figure 15.[23, 88] CipA connects to the bacterial cell surface through Type II dockerin and anchoring proteins.[23, 88] CBM within the CipA aids *C. thermocellum* in locating the lignocellulosic material, specifically cellulose.[65, 96, 105] The cellulosome tightly binds to both the solid substrate and the bacterial cell surface forming a tri-complex between the cellulose, cellulosome, and microbe; [65, 88] however, as the cell growth begins to slow down, the cellulosome can be released into the culture medium by the bacteria once it senses a decrease in available oligosaccharides.[88]
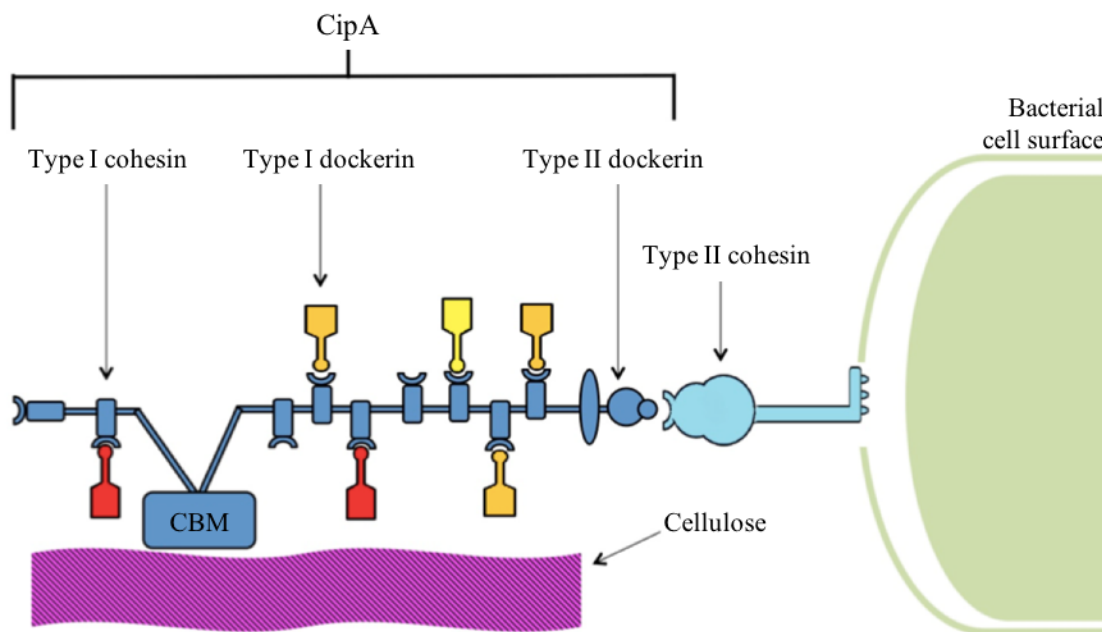
Figure 15. *C. thermocellum* cellulosome schematic structure. The primary scaffoldin protein CipA, which is composed of a lignocellulose locating carbohydrate-binding module (CBM), Type I cohesin binding Type I dockerins that assist in hemicellulose and cellulose digestion, and a Type II dockerin where the microbial binding Type II cohesin attaches to the CipA. (Reprinted from ref. 23)

Another cellulase system typically produced by fungi and aerobic bacteria is a system of noncomplex individual, free enzymes.[106] Interestingly, *C. thermocellum* also contains a cell-free cellulosomal system that does not attach to the bacterial cell wall or the primary cellulosomes.[106] This free cellulosomal system, like the cell-bound system discussed above, contains CipA scaffoldin protein, which is vital in the cellulose conversion process; knocking out CipA disrupts both types of systems leading to over 1000% increase in time required to convert Avicel.[106] The cell-free cellulosome complex is capable of degrading cellulose at a relative distance from the bacterial cell, and therefore is considered a longer-range cellulosome.[106]

While *C. thermocellum* is a promising CBP microorganism candidate, it currently does not produce the desired ethanol yield or titer for industrial processes.[89] Studies have shown that increasing the ethanol yield and/or titer is capable through metabolic or evolutionary engineering of *C. thermocellum*.[91, 95, 107] Engineering microorganisms typically involves replacing genes in the cell chromosome that alter the metabolic flux. An example of gene disruption using an allelic replacement, where a marker gene replaces the target gene, is illustrated in Figure 16.[108] One way of introducing DNA rings, known as plasmids, into a cell is through an electrotransformation process, where an electric field creates temporary pores in the cell membrane for the plasmids to enter.[108] The selected plasmid needs to have two homologous regions identical to those flanking the target gene in the chromosome, which will allow the plasmid to integrate onto the chromosome through a homologous recombination event (Figure 16 B-C). The marker gene will then replace the target gene in the chromosome DNA and the plasmid will be removed from the system (Figure 16 D-E).
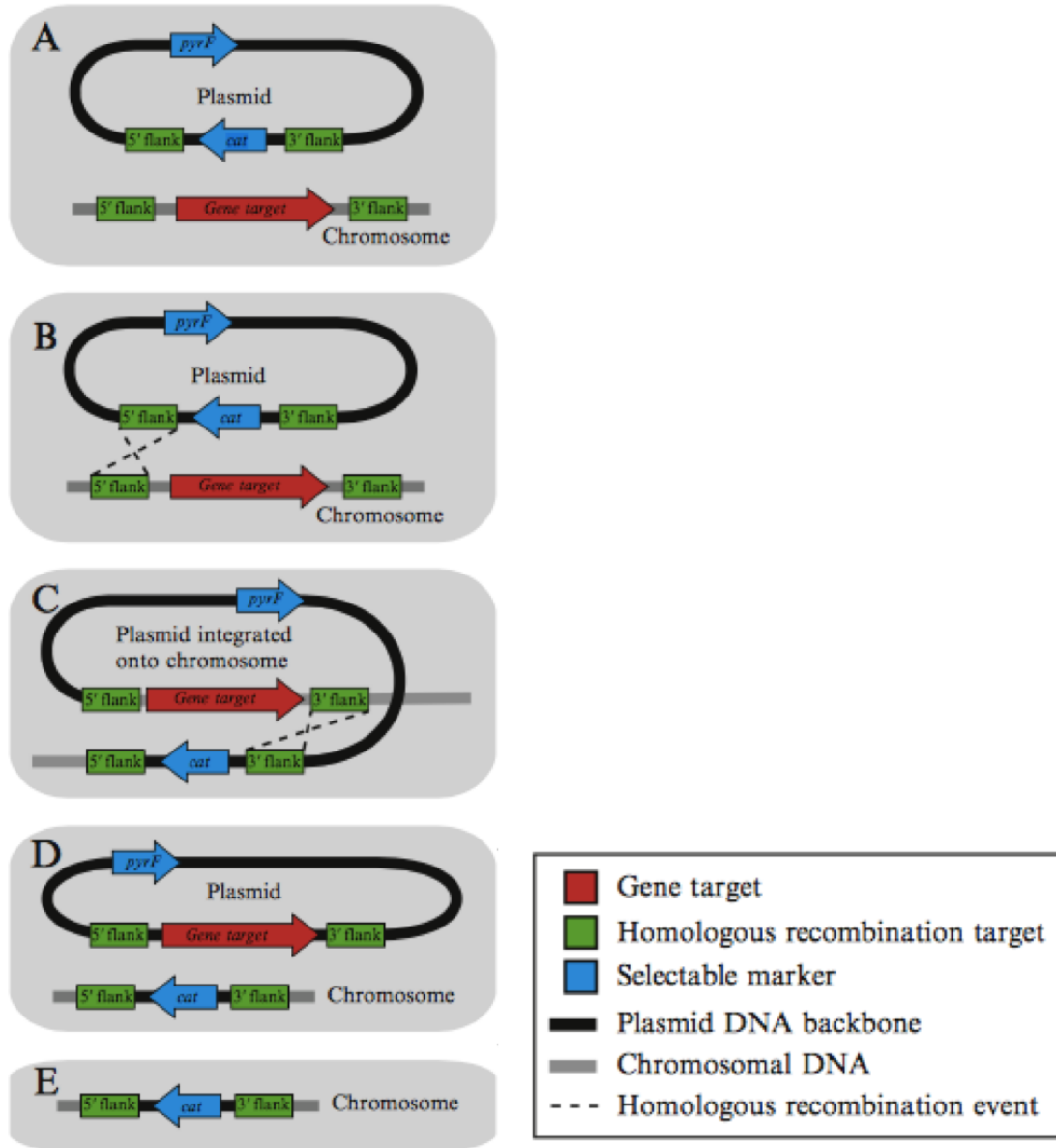
Figure 16. Schematic diagram of a gene disruption by allelic replacement. A) Plasmid enters cell through electotranformation, B-C) plasmid integrates onto chromosome through homologous recombination event, D-E) genetic marker inserted onto chromosome and plasmid exits cell. (Reprinted from ref. 111)

Biswas et al. deleted genes associated with the three [FeFe] hydrogenases and one ferrodoxin-dependent [NiFe] hydrogenase that catalyze H_2 production for *C. thermocellum.* While deleting genes *hydG* and *ech* blocked the metabolic flux for H_2 production (Figure 17, red X), there was a 90% increase in ethanol production compared to the wild type.[95] A spontaneous mutation of acetaldehyde/alcohol dehydrogenase *adhE* occurred when *hydG* was deleted, and resulted in a decreased acetate and lactate production and an increase in ethanol yield to 64% of its theoretical maximum (Figure 17, gray and red pathways).[95]
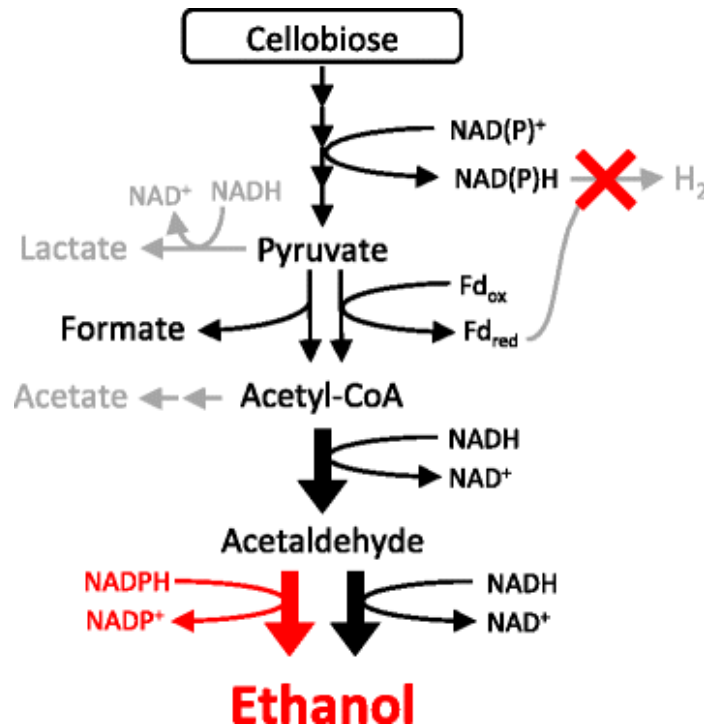
Figure 17. Overview of metabolic pathway for *C. thermocellum* with deleted *hydG* and *ech* genes, where H_2 production was eliminated (red X), lactate and acetate production decreased due to mutated alcohol dehydrogenase (grey pathways), and ethanol production increased (black and red pathway). (Reprinted from ref. 98)

Other engineering studies have focused on eliminating the acetate and lactate production pathways,[91, 94, 107] which could lead to an increase in the microorganism's ethanol tolerance.[65] The natural tolerance *C. thermocellum* has towards ethanol is poor, with *C. thermocellum* wild type becoming significantly inhibited when the ethanol amount exceeds 5 g/L;[23] however, researchers have made progress developing *C. thermocellum* strains with a higher ethanol tolerance.[109-111] *C. thermocellum* with a mutated acetaldehyde/alcohol dehydrogenase gene (*adhE*) was able to grow in the presence of 40 g/L ethanol.[111] While *C. thermocellum* wild type (ACCT 27405) has a well-studied genome and could be a baseline for the evolution or engineering of further strains, it does possess a high variability for efficient transformations (e.g. electrotransformations).[108, 112] *C. thermocellum* strain DSM 1313 is typically the main strain used for routine transformtions.[108]

2.2.3.2 *Caldicellulosirputor bescii*

Caldicellulosiruptor bescii is considered the most thermophilic anaerobic bacterium capable of digesting cellulose and other polysaccharides (simple and complex) to produce H_2, acetate, and lactate.[94, 98, 113-114] The optimum growth temperature for this rod-like microorganism (Figure 18) is 75°C.[94, 113] Interestingly, this microbe was originally misclassified as *Anaerocellum thermsophilum,* and therefore, *C. bescii* wild type is also referred to as *C. bescii* DSM6725,[115] which was the deposition number initially assigned.[116]

C. bescii is capable of converting cellulose into high concentrations of glucose and cellobiose, and can generate xylose and xylobiose from xylan.[114] *C. bescii* continues to convert glucose to pyruvate via the Embden-Meyerhof-Parnas pathway before producing fermentation end products (Figure 19).[90] This microorganism can successfully grow on untreated switchgrass and poplar,[114] but researchers were concerned that microbial growth on the untreated biomass was partially due to easily accessible sugars; therefore, water-soluble sugars were removed from the biomass with hot water, and *C. bescii* proved capable of utilizing insoluble biomass material.[98, 114, 117] *C. bescii* fermentation products for crystalline cellulose, xylan, switchgrass, and poplar are highlighted in Table 14. Once *C. bescii* stops growing at a high cell density, it no longer ferments glucose and cellobiose, but it does continue to produce those sugars by hydrolyzing cellulose.[98] Nevertheless, there remains a significant amount of biomass not utilized by the microorganism (Table 14).
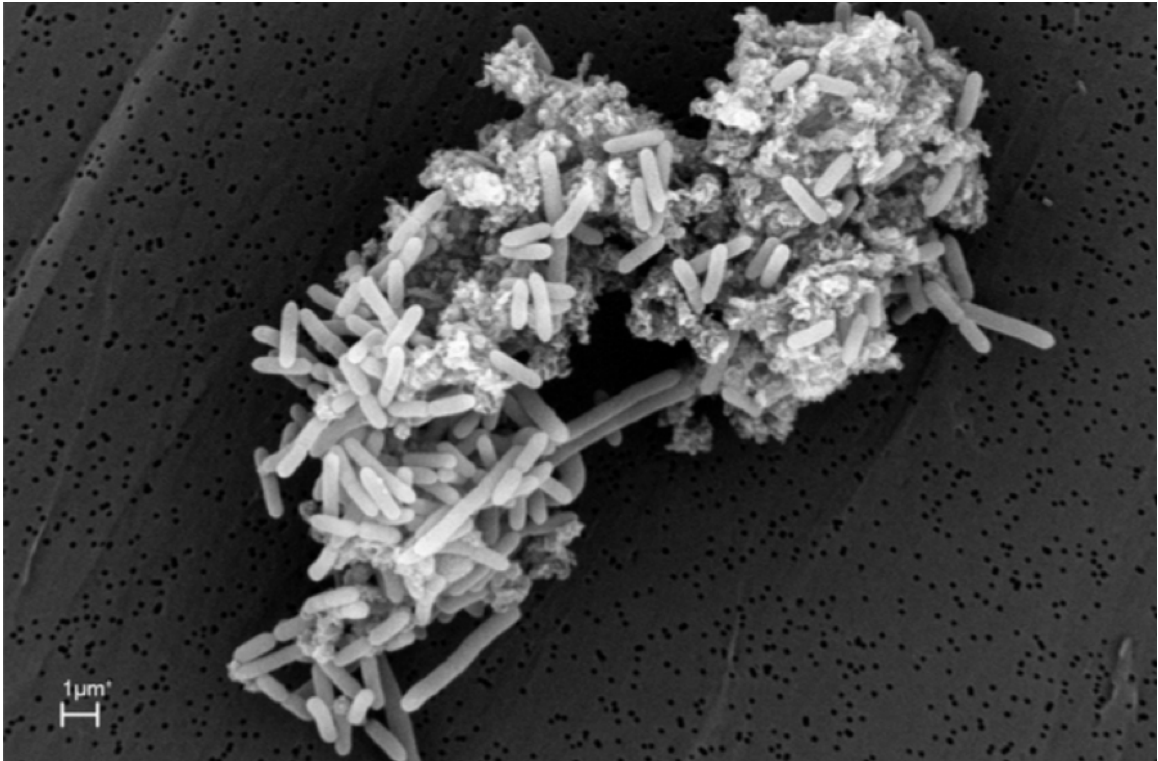
Figure 18. *C. bescii* cells attached to xylan in a SEM image. (Reprinted from ref. 116)
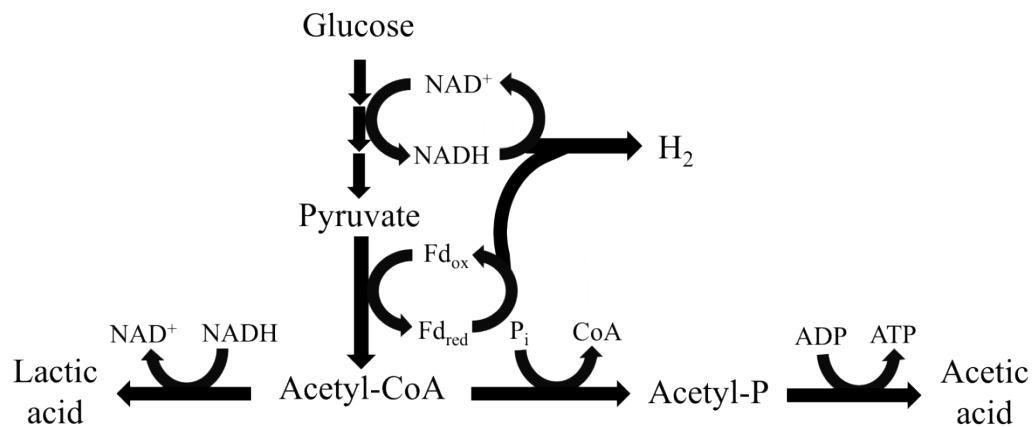
Figure 19. Overview of fermentation pathway for bioconversion of glucose by *C. bescii*.[90]

Table 14. Fermentation products from *C. bescii* incubation with various substrates at 75°C for 21 h.[114]

Substrate	pH	H$_2$ (mM)	Acetate (mM)	Lactate (mM)	Amount Remaining after 10 d
Crystalline cellulose[a]	7.1	4.5	2.2	2.8	10%
Xylan[b]	6.1	5.4	4.0	2.3	2%
Switchgrass	6.8	3.9	4.0	0.9	74%
Poplar	6.8	1.6	1.2	0.4	85%

[a]Avicel; [b]Oat spelt xylan.

Growth inhibitors could be contributing to the underutilization of 74% and 85% of switchgrass and poplar, respectively.[114] *C. bescii* fermentation of hot water washed switchgrass revealed the microorganism is solubilizing lignin, because phenolic acids (e.g. ferulic, coumaric, and sinapic acids) along with sinapyl and coniferyl alcohols (e.g. syringylglycerol and guaiacylglycerol) were detected in the soluble material.[117] Kataeva et al. determined that while these lignin-derived compounds are slowly released due to thermal degradation, *C. bescii* accelerates the release of the compounds.[117] Another study concluded that solubilized aromatic constituents may be a contributing factor inhibiting fermentation of DA and hot water pretreated switchgrass.[118] While additional research on these growth inhibitors and how they impact the fermentation process is necessary, it is known that these inhibitors originate from the plant biomass since *C. bescii* successfully grows on crystalline cellulose uninhibited.[98]

The major appeal towards using bacteria from the *Caldicellulosiruptor* genus is their high thermophilic properties (70-80°C).[98] Potential benefits of using elevated temperatures during fermentation, include increased rate of reaction, faster ethanol recovery, and

reduced risks for contamination.[119-120] Like *Clostridium thermocellum, C. bescii* is capable of hydrolyzing xylan, but it can go a step further and consume xylose.[113-114] Now, *C. bescii* does not naturally produce ethanol, but that has been addressed through gene deletion.[90, 94] The *adhE* gene from *C. thermocellum* is capable of converting acetaldehyde and then ethanol from acetyl-CoA; since *C. bescii* does not naturally contain this gene, a *C. thermocellum* plasmid containing *adhE* gene was inserted into a mutated *C. bescii* strain with a deleted lactate dehydrogenase gene (*ldh*) through electrotransformation.[90] Not only was the lactate production eliminated, the new mutant strain produced 14.8 mM, 14.0 mM, and 12.8 mM of ethanol from cellobiose, Avicel, and switchgrass, respectively.[90] Researchers have shown that it is possible for engineered *C. bescii* strains to produce ethanol, and now only need to develop a strain with increased yield and titer to be industrially relevant.[90]

Unlike *C. thermocellum*, *C. bescii* does not contain cellulosomes, but secretes mutlimodular cellulases, which can contain multiple CBMs.[98, 121] There are at least 15 primary carbohydrate-active enzymes (CAZy) that contain at least one CBM which targets xylan and/or cellulose.[113] The dominant cellulase *C. bescii* produces, CelA (gene Cbes1867), is stable at raised temperatures and possesses high specific activity.[121] This free enzyme (Figure 20) is composed of 3 CBM, an endoglucanase (GH9), and an exoglucanase (GH48), which allows it to target amorphous and crystalline cellulose.[113, 121-122]
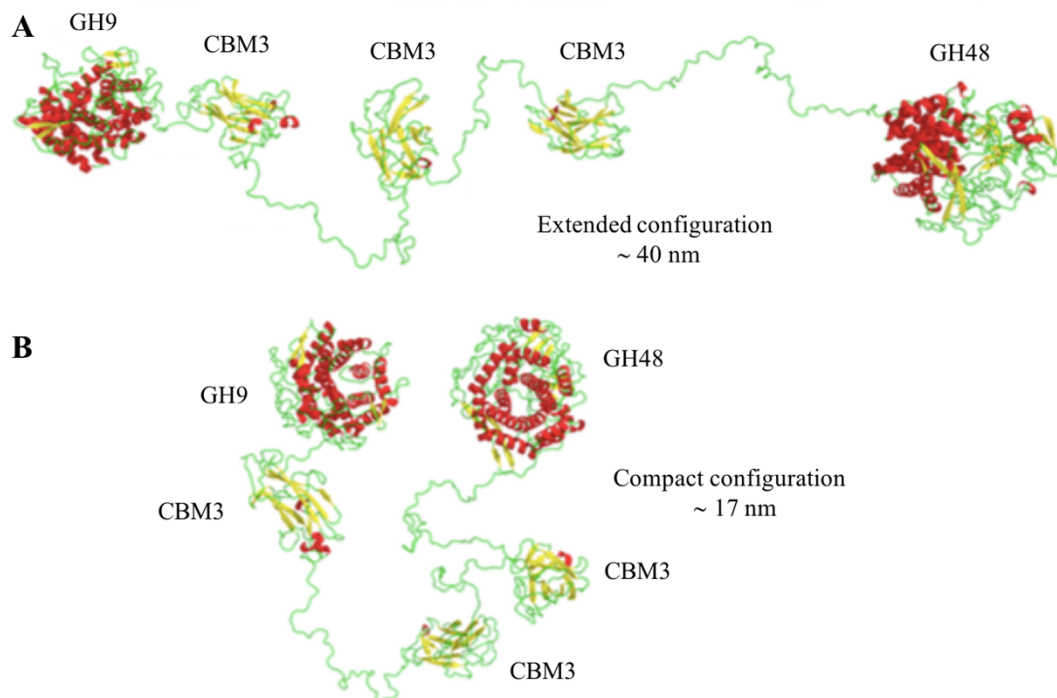
Figure 20. Typical extended (A) and compact (B) configurations of CelA. CelA is compose of a family 9 glycoside hydrolase (GH9), three family 3 carbohydrate-binding modules (CBM3), and family 48 glycoside hydrolase (GH48). (Reprinted from ref. 124)

CelA is more active than commercial cellulases, produces both glucose and cellobiose, and performs better on untreated biomass than pretreated biomass.[121] It has also digested 60% of xylan in native switchgrass.[121] CelA's tethered structure (the linked reducing end GH48 and non-reducing end GH9) allows for the formation of cavities in the substrate, as represented in Figure 21.[121-122] Since all cellulases experience some nonproductive binding, it is important to note that lignin and hemicellulose could trap CelA.[121]
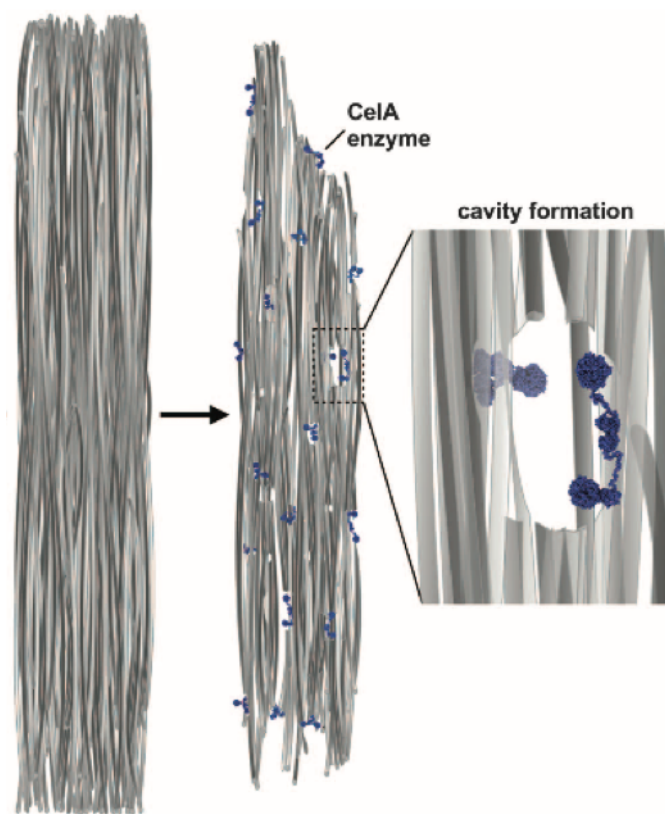
Figure 21. Schematic representation of CelA digesting cellulose microfibril bundles and forming cavities. (Reprinted from ref. 124)

2.3　Surface Characterization of Lignocellulosic Biomass

Advance surface analytical techniques can provide detailed information about the plant cell wall and any changes that occurred during a chemical or microbial treatment process that are not obtainable through conventional methods analyzing the bulk biomass. Microscopic imaging techniques (e.g. atomic force microscopy, confocal laser scanning microscopy, electron microscopy) assist in understanding the plant cell wall morphology and ultrastructure. Information pertaining to the chemistry of the plant cell wall can be determined using spectroscopic techniques, like Fourier transform infrared and time-of-

flight secondary ion mass spectrometry. These analytical techniques are described in greater detail below.

2.3.1   Microscopic Imaging Analysis

Atomic force microscopy (AFM) is an intermolecular force measuring tool that uses a cantilever probe and tip to scan the sample surface and measure the cantilever laser defections with a photodiode detector.[123-124]   This can provide topological information from the sample's surface at high lateral resolution of less than one angstrom.[124] AFM has been used to map the ultrastructures of the cell walls of various biomass and to understand the network connections between cellulose and hemicellulose.[125-127] Information obtained through AFM images assisted Ding and Himmel in developing a new molecular model for cellulose microfibril structure.[125]

Confocal laser scanning microscopy (CLSM) is a high spatial resolution instrument composed of a beam splitter for the laser, scanner mirrors, a pinhole to adjust the aperture, and a photomultiplier that amplifies the low light intensity signal.[128] Non-autofluorescent sample materials typically are stained with one or more fluorescent probes.[128] Lignocellulosic biomass samples stained with acriflavine will reveal green lignified tissue at 530 nm excitation and red unlignified tissue at 600 nm excitation.[129] Safranine stain produces red and green signals for lignin and cellulose-rich regions, respectively, at 488 nm excitation.[130] While lignin can be stained, it is also capable of autofluorescence (Figure 22).[131-132] In the presence of cellulose, Direct Red 23 (previously known as Pontamine Fast Scarlet 4B)[133-134] fluoresces red after green

exitation.[132, 134] Thomas et al. determined that this dye preferentially binds to S1 and S3 layers in the secondary cell wall and would be a useful tool in identifying cellulose microfibril orientation in those layers.[132] Zhu et al. used CLSM and fluorescence labeled cellulase solution to analyze the binding of *Thermobifida fusca* cellulases on hydrothermally pretreated wood particles over time.[135] While two fluorescently labeled species, like cellulose and lignin, are commonly analyzed visually, calculating the Pearson's *r* correlation coefficient reduces visual bias by quantifying the spatial correlation of two pixel intensities.[136-137] In the case of colocalization, *r* ranges from 0 to 1, where 0 represents random overlap and 1 signifies 100% colocalization.[136] Another quantification method determines the Mander's split coefficient, which measures the overlap of two different signals in an images.[138] CLSM and fluorescence labeling can provide visual images and line analyses of cellulose and lignin on the plant cell wall (Figure 22),[139] while additional statistical analysis can convert that information into quantitative values.
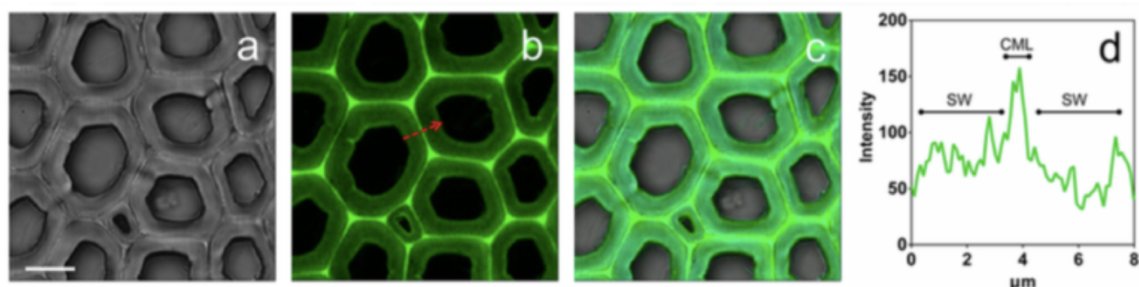
Figure 22. Cell wall bright field microscopy image (a), CLSM image of autoflouresing lignin (b), and superimposed bright field and CLSM images (c) of raw poplar sections. Line analysis (d) of cell wall marked by a red arrow in (b). Scalebar = 10 μm. (Reprinted from ref. 142)

High resolution electron microscopic techniques, like scanning electron microscopy (SEM) or transmission electron microscopy (TEM), are commonly used to analyze the plant cell wall morphology. SEM is an ideal instrument for determining structural features and cellular and nanometer scale resolution of biomass degradation.[130] SEM micrograph of DA pretreated maize revealed spherical lignin droplets on the surface.[140-141] Other images of pretreated biomass have revealed the loss of structural order due to the exposure and separation of microfibrils.[74, 142-143] TEM is capable of producing images that distinguish the different plant cell wall layers (primary, secondary, and middle lamella) from each other,[130] and have been used to elucidate the impact a pretreatment would have on the secondary cell walls, middle lamella, and cell corners (Figure 23).[143]
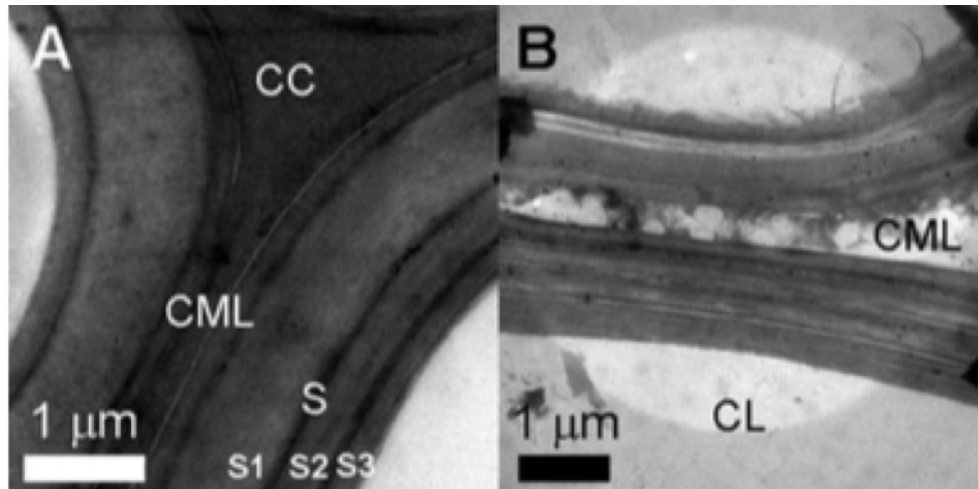
Figure 23. TEM cell wall images of untreated (A) and AFEX treated (B) corn stover. Cell corners (CC), compound middle lamella (CML), cell lumen (CL), and secondary cell wall layers (S) are labeled. (Reprinted from ref. 146)

2.3.2   Spectroscopic Analysis

Fourier transform infrared (FTIR) spectroscopic analysis produces an absorbance spectra based on specific chemical information from the plant cell wall. There are approximately 24 absorbance bands associated with lignocellulosic biomass that range from 875 to 3421 cm^{-1}.[144] For example the bands at 1155 cm^{-1}, 1270 cm^{-1}, 1327 cm^{-1} represent the C—O—C asymmetrical stretching of cellulose and hemicellulose,[145] the aromatic ring vibration of guaiacyl lignin, and the C—O of syringyl lignin, respectively.[144] It is possible to differentiate hardwoods and softwoods from each other by looking for spectral features in the fingerprint region.[146] Spatial IR absorbance images can be obtained with an imaging FTIR microscope, allowing for cell wall absorbance measurements from selected regions of interests (ROIs) which correspond to locations on the secondary cell wall. FTIR microscopy detected the degradation of chemical bonds in xylan, glucomannan, and lignin in spruce due to steam pretreatments at various temperatures.[147] This technique is capable of tracking the cellulose, hemicellulose, and lignin changes in the secondary cell walls of untreated and pretreated biomass.

Time-of-flight secondary ion mass spectrometry also produces high mass resolution spectra and images and is a powerful tool used to study the surface chemistry of lignocellulosic biomass. This technique is discussed in greater detail in Chapter 3.

CHAPTER 3: LITERATURE REVIEW: TIME-OF-FLIGHT SECONDARY ION MASS SPECTROMETRY[†]

Lignocellulosic biomass is a valuable renewable resource that is primarily composed of cellulose, hemicellulose, and lignin. The key hindrance to the utilization and conversion of these biopolymers into biofuels and bioproducts via the biological conversion platform is the natural recalcitrance of the biomass. Through chemical, physical, and/or biological pretreatments along with genetic modifications, progress has been made toward reducing biomass recalcitrance and accessing lignocellulosic polymers. These various processes modify the structure and/or chemistry of the plant cell walls by altering one or more of the polymers of the plant cell wall and increasing the accessibility to cellulose. Currently, the fundamental principles of biomass recalcitrance are under active investigation so as to facilitate practical conversion of plant polysaccharides to simple sugars that can readily be fermented to ethanol and related alcohols. It is generally acknowledged that comprehensive analytical biomass analysis is key to understanding the principles of recalcitrance. High-performance liquid chromatography (HPLC), gel permeation chromatography (GPC), nuclear magnetic resonance (NMR), FTIR spectroscopy, X-ray photoelectron spectroscopy (XPS), scanning transmission X-ray microscopy (STXM), and ultraviolet (UV) spectrophotometry are typical analysis instruments for characterizing biomass and its molecular components, for example, the

---

degree of polymerization, molecular weight distribution, cellulose crystallinity, accessibility, lignin structural characteristics, and cellulose accessibility to cellulase.[148-152] Electron microscopy tools, like TEM, SEM, and AFM have also been developed to analyze the morphological changes to biomass samples.[141, 153-155]

Time-of-flight secondary ion mass spectrometry (ToF-SIMS) is a mass spectrometry tool that is matrix-free in regards to ionization of a sample's surface and detects lower molecular weight fragmented species in high mass resolution spectra and spatial mapping.[156-157] Some advantages to using a ToF-SIMS are direct analysis of solid samples,[158] minimal sample preparation steps,[159] and low surface damage in the range of a few nanometers.[160] Also, the mass spectral imaging is extremely useful in mapping selected secondary ions on a heterogeneous surface, like lignocellulosic biomass.[157] The relative amounts of cellulose and lignin and their location in the cell walls on the surface of a biomass samples is important in understanding how the plant cell wall structure is impacted due to various treatments or modifications. In addition, the deconstruction of cellulose by cellulase is a surface dominated process and hence, there is a compelling need to understand the chemical structure of the surface of biomass. There have been a number of advances in the use of the ToF-SIMS since Belu et al. published a comprehensive review of ToF-SIMS covered basic principles and applications for the instrument.[161] This is especially true in relation to characterizing lignocellulosic biomass via ToF-SIMS. This paper covers the principles of the instrument used to study biomass along with sample preparation, key lignocellulosic secondary ions and their location in the cell wall, and detecting various biomass modifications using this methodology.

3.1   Instrumentation Principles

ToF-SIMS functions by emitting a pulsed primary ion beam from a liquid metal ion gun, which is rastered across the surface of the sample ejecting positive, negative, and neutral secondary ions (Figure 24).[161] There are different liquid metals for the pulsed primary ion beam, including gallium,[10-12, 157, 160] gold,[162-163] and bismuth.[156, 164-169] Clustered ion sources, like Bi_3^{2+}, are capable of increasing the yield of higher molecular weight secondary ions while not damaging the sample surface more.[161] It is important to be aware of the instruments' primary ion source since it can significantly impact the intensities of the secondary ion peaks in the resulting spectra.[161] The primary ion beam utilizes energy between 1 and 25 keV, which allows enough force to bombard the sample surface and eject the secondary ions from the top 1-2 nm of the sample.[160-161, 168]

The ToF-SIMS spectra are formed after the secondary ions are detected by the ToF-SIMS analyzer and separated according to their mass-to-charge (*m/z*) ratio. The specific secondary ion peaks are selected in the calibrated spectra and can result in relative ion counts/intensities or spatial mapping of ions, depending on the mode setting (bunched mode for high resolution spectra and burst/burst alignment mode for images, Figure 25).[170] Some of the ToF-SIMS settings depend on the type of sample being analyzed. For example, with biomass the ToF-SIMS analyzer is set to detect positive ions since all developed libraries for lignocellulosic biomass are for cations. Also, the bombardment of primary ions on a biomass sample easily results in surface charging, which is reduced by using a low-energy pulsed electron gun, or a floodgun.[160]

51
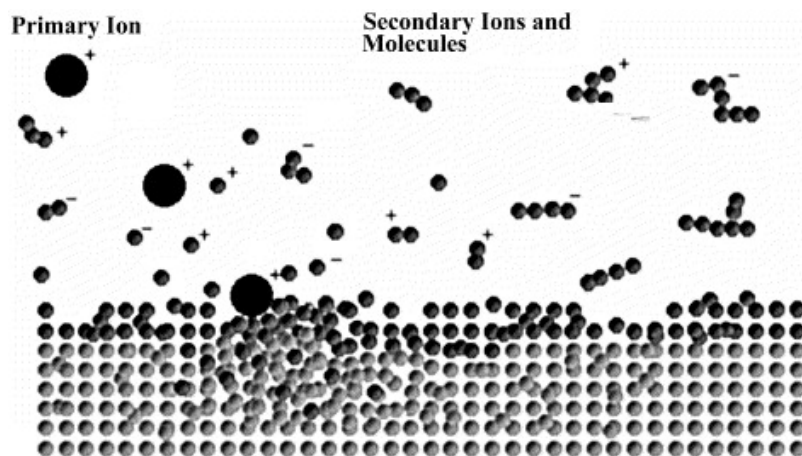
Figure 24. A schematic drawing of the formation of secondary ions from the sample surface after primary ion impact. (Reprinted from ref. 164)
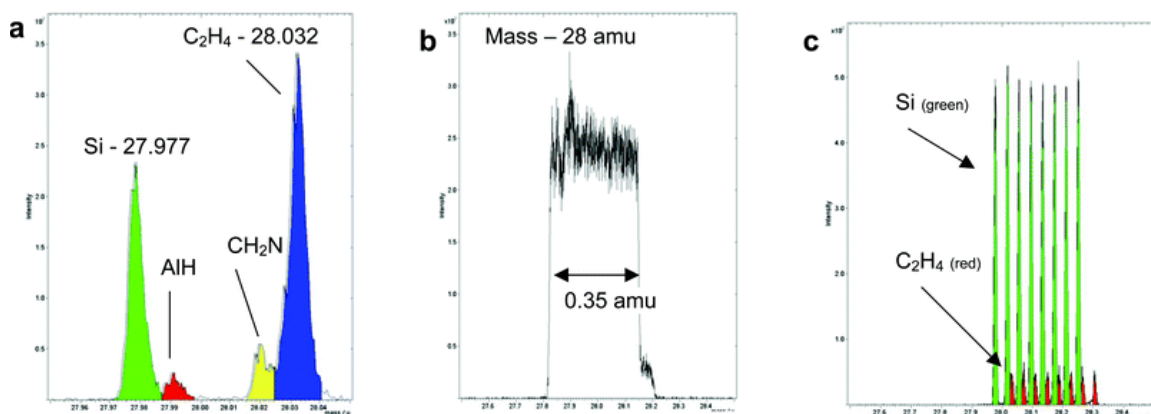
Figure 25. Mass spectra examples for the a) bunched spectral and b-c) burst/burst alignment imaging operational modes. (Reprinted from ref. 173)

While the settings need to be sample specific, the interpretation of the ToF-SIMS data is likewise dependent on the sample. Spectra of different locations on a sample are slightly

different in the total number of secondary ions detected, and as a reference, some studies report a mass resolution (M/ΔM) range. The mass resolution is dependent on the surface roughness, and varied roughness on a sample could result in different total ion counts. When analyzing biomass, the M/ΔM for *m/z* 23 or 91 have been reported;[156, 159] for example at *m/z* 91, Goacher et al. reported mass resolutions of ~3000-5000 and ~250-300 for bunched mode and burst alignment mode, respectively.[159] Prior to selecting specific peaks, ToF-SIMS spectra need to be calibrated. For lignocellulosic biomass analysis, a few typical ions used for calibration are CH_3^+, H_3O^+, $C_2H_3^+$, $C_3H_5^+$, and $C_5H_7^+$.[156, 159, 164-166, 169]

After the spectra are calibrated and the specific characteristic ion peaks selected, the ion intensities for these peaks are typically normalized to the total ion intensity detected by the analyzer. The normalized ion intensities can be used for further direct comparison analysis, ratios, and/or multivariate analysis, like principal component analysis (PCA) which was used by Groacher et al. to develop a lignocellulosic biomass library.[159] The spectra for spatial images likewise need to be calibrated prior to the characteristic ion peaks selection. ToF-SIMS 2D imaging can potentially spatially resolve the cell wall chemically to under 1 μm and occur up to distances of approximately 300-400 nm.[156, 167] ToF-SIMS detects the location of emitted secondary ions and creates pixels based on this information to form spatial mapping of the total ions or specifically selected ions. For biomass, an image based on chemical ions helps determine location of high or low intensity lignocellulose ions on the cell wall.

There have been several recent advances to the ToF-SIMS technique for analyzing biomass. Jung et al. stacked a series of 2D ToF-SIMS images to form a 3D molecular

image (Figure 26) by removing the previously analyzed top layer of the sample with a sputtering beam, like O_2^+ and C_{60}^+.[167-168] This method has the potential to be extremely valuable in gaining insight into the interaction between a biomass sample and enzymes or microbes, especially in detecting the vertical distance the enzyme/microbe penetrates.[167] It is also possible to conduct 3D analysis by cutting subsequent layers off of the biomass if the previous analysis position can be easily identified, but the layers would be tens of micrometers apart from each other.[162] Another advancement utilizes the development of a cryo-ToF-SIMS/SEM system that is capable of analyzing frozen-hydrated biomass samples to minimize the movement of water-soluble chemicals during the drying process.[162] This new system works by moving a holder that the biomass is mounted on between a glove box and a cryo-SEM or a cryo-ToF-SIMS.[162]

Figure 26. ToF-SIMS 3D image of poplar tension wood stem cross-section, where cellulose (green pixels) and lignin (red pixels) are spatially distributed. The square edges are 50 μm long and the image is composed of 30 2D images stacked. (Reprinted from ref. 170)
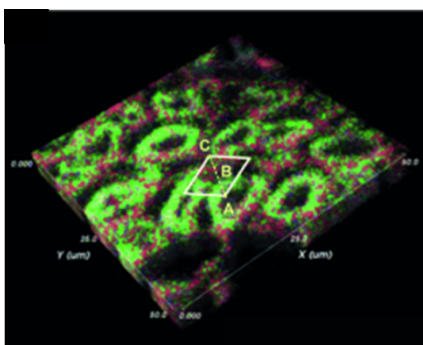
3.2   Biomass Sample Preparation

All analytical instruments require samples to be prepared in specific ways in order to accurately analyze them. The following are general preparation descriptions necessary for lignocellulosic biomass prior to ToF-SIMS analysis; specific details can be found in the subsections below. First, biomass samples need to fit correctly into the ToF-SIMS mounting stage either through milling or sectioning the sample to a smaller size. Second, the removal of extractives, non-structural biomass material, is necessary for most ToF-

SIMS analyses and this can be accomplished using a number of different procedures. Additional rinsing or washing might be required to remove any chemical residue after a pretreatment and/or enzymatic hydrolysis. Once the samples are dried, they are then ready for analysis via the ToF-SIMS. Below are various processes for milling and sectioning the biomass along with different biomass extractions, ways to rinse post-enzymatic hydrolysis, and drying techniques used in various studies.

3.2.1   Milling and Sectioning

ToF-SIMS can analyze biomass samples that are prepared in various ways, including milled wood or powder, sectioned tissue, and small blocks of wood.[10, 12, 157, 171] The size of milled biomass for ToF-SIMS studies has varied from 0.149 to 0.841 mm.[11-12, 164-165] A benefit to using milled wood is that it helps reduce the heterogeneous nature of the wood found within the different cell wall regions and different zones, like heartwood and sapwood.[165] Milled biomass can be compressed into wood powder pellets or attached to adhesive tape prior to ToF-SIMS analysis.[158, 165, 169] If the adhesive tape is used, it is important to know the ToF-SIMS spectra of the tape in order to identify any peaks that overlap with those characteristic of lignocellulose.[158] Saito et al. originally pressed the powdered milled wood lignin onto indium foil sheet, but to attain even a higher mass resolution, the sample mixed with acetone was dropped onto a silicone wafer where it dried; the drop-dried method resulted in a flatter, homogeneous milled biomass sample for ToF-SIMS analysis.[157, 160]

The sectioning of plant tissue from whole stems or small blocks of wood typically occurs on a cryotome or a microtome. It is important to be aware of the materials used to section the biomass so minimal damage occurs during the cutting process. A previous study showed that a cryo-microtome using a steel knife collapses the plant cell walls, while a double-edged razor blade results in varied section thickness.[172] Tokareva et al. determined that a disposable microtome blade can be used for biomass sectioning, but it must first be cleaned to remove any polytetrafluoroethylene (PTFE) on the blade that might contaminate the samples.[172] A cleaned diamond knife on a microtome is also a useful tool to cut biomass sections.[159] There are various methods used to clean blades and knives that typically involve solvents, including acetone,[156, 159] dichloromethane and ethanol,[12] and dichloromethane in a high intensity ultrasonic processor.[172] The cross- and transversal-sections can be cut to various micrometer thicknesses like 12 μm,[168] 20 μm,[173] and 50 μm.[12, 156] Note that different cutting techniques might result in microtome-induced smearing and debris leading to a loss in spatial resolution; to correct for this, the first few layers of the sample can be removed with a sputtering ion beam.[168]

Biomass studies incorporating a pretreatment followed by enzymatic hydrolysis typically utilizes milled biomass, sawdust, or woodchips. A study analyzing 0.841 mm ground poplar and 50 μm thick poplar cross-sections via FTIR and carbohydrate analysis determined that the ground and section poplar were comparable chemically. [12] This indicates that it is inconsequential whether the sample biomass is milled or sectioned, and the actual limiting factor for biomass size preparation is for it to fit in the ToF-SIMS mounting stage. While ToF-SIMS can analyze both milled and sectioned samples, the cell walls of sectioned biomass have greater probability of being intact for ToF-SIMS

imaging than the milled biomass. Otherwise, the milling or cutting process is dependent on the research study and the biomass; for example, switchgrass would have to be encased fully in embedding material to obtain cross-sections via a microtome, but a cryotome would easily section juvenile poplar that is mounted to a metal stage. Prior to analysis, the samples must have the extractives removed for accurate ToF-SIMS analysis.

3.2.2   Removing Extractives

Extractives are essentially chemicals that do not contribute to the structure of the cell walls in the biomass.[174] They typically fall into two categories, water soluble and ethanol soluble materials.[174] These materials can include inorganics, waxes, nitrogen-based compounds, and non-structural sugars.[174] Fardim and Durán proposed ToF-SIMS peak assignments for seven free fatty acids, eight fatty acid salts, and three sterols all over *m/z* 200,[175] while Goacher et al. developed a list of 32 low-mass peaks (under *m/z* 200) that "distinguished unextracted from extracted lignocelluloses samples."[158]

The main reason for the removal of biomass extractives is due to their ability to mask the detection of secondary ions from lignin and cellulose.[172] Goacher et al. compared unextracted and extracted spruce, aspen, and *Arabidopsis* and determined that an observed change in the number of lignin ions could actually be caused by a change in extractive content on the unextracted biomass sample.[158] Phenolic extractives, in particular, may be interfering with the instrument's ability to accurately detect lignin.[171]

For this reason, the analysis of unextracted biomass may result in mass interferences or alter peak proportions which could negatively impact peak assignments.[159]

Table 15. Various extraction techniques used on lignocellulosic biomass prior to ToF-SIMS analysis.

Solvent(s)	Extraction Method
Acetone	Soxhlet extract with acetone-water (9:1, v:v) overnight or for 48 h.[10, 159]
Dichloromethane	Soxhlet extracted with dichloromethane overnight.[12]
Ethanol, acetone, and water	Dehydration in a series of ethanol-water (20, 40, 60, 80, 100% v/v) for 10 min each, 1:1 acetone-ethanol solution, and pure acetone.[172]
Ethanol, toluene, and water	Soxhlet extract with 1.0 L absolute ethanol and 427 mL toluene for 4 h followed by ethanol for 4 h or longer.[158] 95% ethanol for 4-5 h, ethanol-toluene (2:1 or 7:3) for 6-8 h, and boiling water for 3 h.[156, 158]

This stresses the importance of extraction, especially when trying to identify lignin fragmentation ions of a sample's surface. Various biomass extraction techniques, which typically are performed for 4-12 h or even longer depending on the procedure, include solvent solutions using acetone, dichloromethane, ethanol, and toluene in different concentrations, some of which are detailed in Table 15. Samples need to be dried prior to analysis, but further rinsing might be required to remove any traces of buffers if the samples underwent enzymatic hydrolysis.

3.2.3   Rinsing after Enzymatic Hydrolysis

In enzymatic reactions, buffers maintain the pH, but they produce inorganic peaks that interfere with lignocellulosic peaks.[176] Salts can negatively impact the ToF-SIMS spectra since samples not exposed to buffers result in relatively low sodium ion peaks.[158] Buffers typically have been removed by rinsing with distilled water; Braham and Goacher determined that rinsing wood with acetic acid removes more buffer-related salt ions, specifically potassium and sodium, than distilled water.[176] Nevertheless, distilled water is still an effective way to reduce the buffer salts on the samples surface.[176] Using potassium salts instead of sodium salts to prepare pH buffers is better since both acetic acid and distilled water are more efficient in removing potassium salts and K-buffer produces fewer interferences with the characteristic lignocellulosic peaks.[176] After rinsing, biomass samples then undergo a drying process like other pretreated or extractive-free samples.

3.2.4   Drying the Sample

Biomass samples for ToF-SIMS analysis need to be dried prior to loading into the instrument. Different studies have dried the biomass through freeze-drying,[10, 173] critical point drying,[172] and air-drying,[12, 158, 165-166] in addition to oven drying at 60°C.[165] Tokareva et al. studied Norway spruce that was freeze-dried, air-dried, acetone extracted with nitrogen flow drying, and ethanol-acetone dehydration with critical point drying to determine what drying process gave better results (Table 16)[172] The analysis of the freeze-dried and air-dried samples revealed extractives on the sample surface that were

masking the ion signals from the major lignocellulosic components.[172] Therefore, the samples that were dried via critical point drying or nitrogen flow after extraction were accurately prepared for ToF-SIMS analysis and it was determined that either drying technique would be appropriate to use.[172] Other studies tend to differ the biomass drying process from those listed in Table 16, for example, Jung et al. air-dried poplar samples overnight.[12]

Table 16. Four drying technique and procedural details.[172]

Drying Technique	Details
Air drying	ambient temperature for 3 days
Critical point drying	CO_2 transition fluid
Freeze drying	20 h
Nitrogen flow drying	room temperature

3.3 Lignocellulosic Secondary Ion Peaks

Various studies were conducted to determine the key ion peaks characterizing lignocellulosic components and develop a ToF-SIMS library for biomass. In 2003, Fardim and Durán proposed a list of tentative peak assignments for the ToF-SIMS positive secondary ions from unbeaten and beaten pulp derived from *Eucalyptus grandis* wood chips.[175] Those peak assignments represented cellulose (*m/z* 127 and 145), xylan (*m/z* 115 and 133), and lignin (*m/z* 137, 151, 167, and 181).[175] The processes for deriving
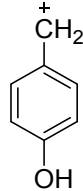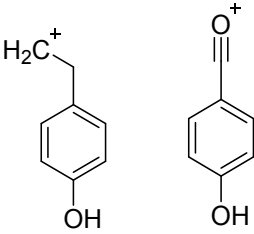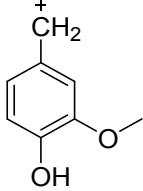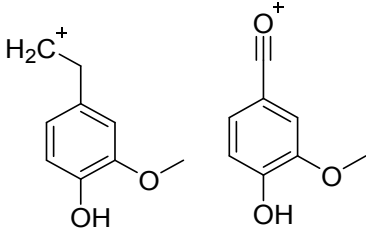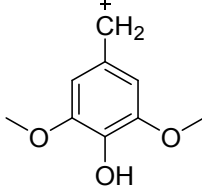
the representative peaks for lignin, cellulose, and hemicellulose from isolated lignocellulosic components are addressed below.

3.3.1   Lignin

Fardim and Durán tentatively proposed that the secondary ions representing lignin ToF-SIMS peaks of m/z 137, 151, 167, and 181 were $C_8H_9O_2^+$, $C_8H_7O_3^+$, $C_9H_{11}O_3^+$, and $C_9H_9O_4^+$, respectively.[175] To verify these peaks, it was necessary to first analyze isolated lignin samples and then the lignin in the biomass. Also, the sources of the biomass lignin were varied since softwoods predominately have guaiacyl (G) lignin, whereas hardwoods are primarily composed of guaiacyl (G) and syringyl (S) lignin, and grasses contain all three types – p-hydroxyphenyl (H), guaiacyl (G), and syringyl (S) lignin. The structures of the three monolignol that H, G, and S lignin are derived from are illustrated in Figure 7.

Various studies were conducted on milled wood lignin (MWL), [160, 163] Klason lignin,[177] and lignin model dimers.[157] The analysis of pine and spruce MWL revealed lignin characteristic peaks in the spectra at m/z 137 and 151, which correlates with G lignin.[160, 177] The peak at m/z 137 does represent $C_8H_9O_2^+$ as Fardim and Durán tentatively assigned;[160, 175] however, based on the spectra of pine MWL led Saito et al. to conclude that m/z 151 actually was two unresolved peaks, $C_8H_7O_3^+$ and $C_9H_{11}O_2^+$.[160] The two peaks were able to be resolved when they analyzed unlabeled coniferyl alcohol.[160] All of the ToF-SIMS G lignin ions were confirmed by using deuterium-labeled synthetic lignin, DHP.[160] The chemical structure for the G lignin ions can be found in Table 17.

Table 17. Mass-to-charge ratio, chemical formula, and chemical structure of lignin fragmentation ions in biomass for ToF-SIMS analysis.[163]

Mass-to-charge ratio (m/z)	Chemical formula	Chemical structure	Characterization
107	$C_7H_7O^+$		H lignin
121	$C_7H_5O_2^+$, $C_8H_9O^+$		H lignin
137	$C_8H_9O_2^+$		G lignin
151	$C_8H_7O_3^+$, $C_9H_{11}O_2^+$		G lignin
167	$C_9H_{11}O_3^+$		S lignin

181     $C_9H_9O_4^+$, $C_{10}H_{13}O_3^+$ S lignin
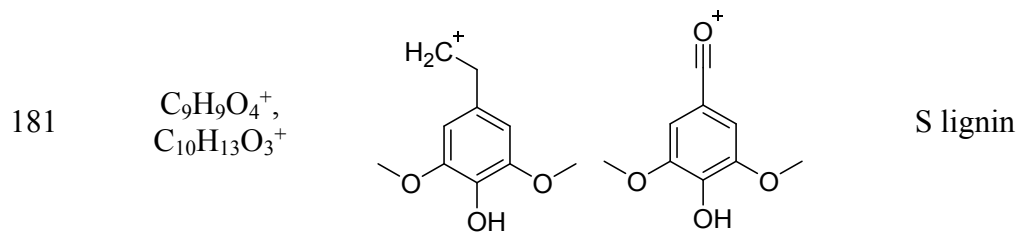
Using lignin model dimer compounds, it was determined that the interunit linkages of β-O-4, β-1, β-8, and β-5 contributed to the formation of G lignin fragmentation ions (*m/z* 137 and 151), and that those peaks can originate from the phenolic end group or the ether-linked phenolic unit of a lignin polymer with a β-O-4 linkage, as illustrated in Figure 27.[157]
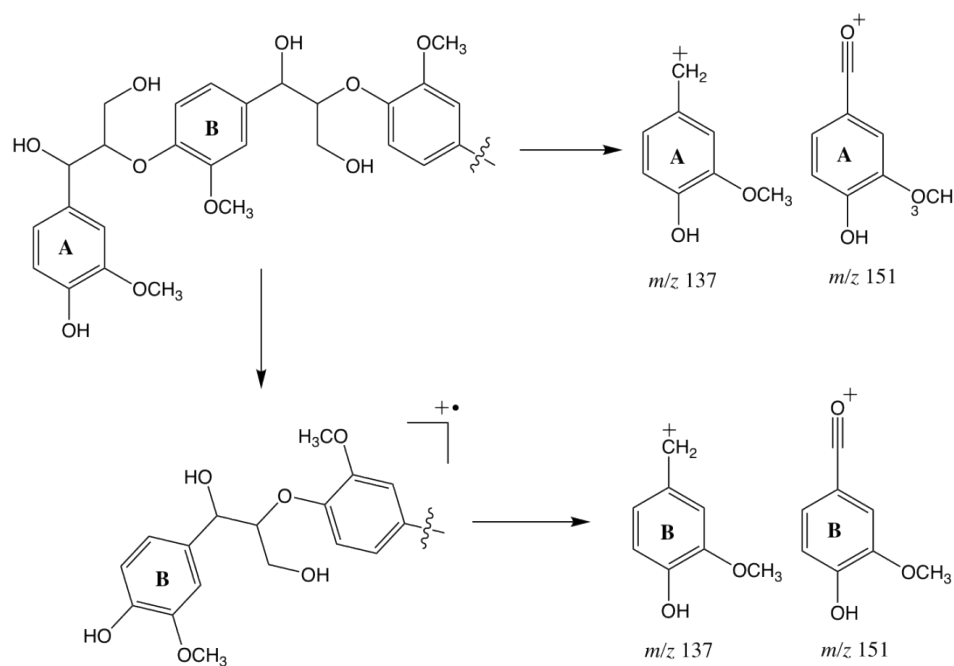
Figure 27. A postulated fragmentation pathway to the formation of G lignin ions at m/z 137 and 151 originating from the phenolic end group (A) or the ether-linked phenolic unit (B) with a β-O-4 linkage.[157]

Beech MWL also revealed G lignin ion peaks in addition to characteristic peaks of S lignin at *m/z* 167 and 181 (Figure 28). The former peak represents $C_9H_{11}O_3^+$ while the latter peak was also an unresolved double peak characterizing $C_9H_9O_4^+$ and $C_{10}H_{13}O_3^+$ (Table 17).[160]
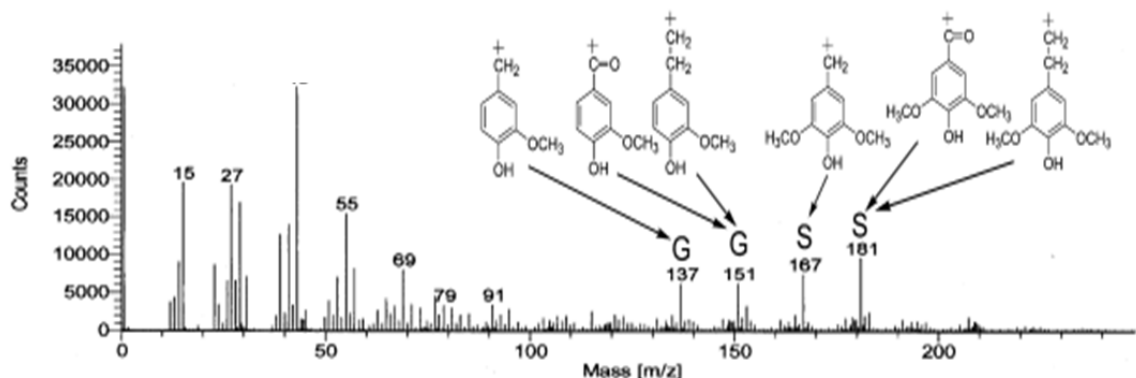
Figure 28. ToF-SIMS spectra of beech MWL. (Reprinted from ref. 163)

ToF-SIMS analysis of two lignin dimeric compounds composed of a G unit and H unit, 1-(4-hydroxyphenyl)-1-hydroxy-2-(2-methoxyphenoxy)-ethane and 1-(4-hydroxyphenyl)-1-ethoxy-2-(2-methoxyphenoxy)-ethane, resulted in distinct peaks at m/z 107 and 121.[177] Another ToF-SIMS study, the spectrum of wheat straw Klason lignin revealed peaks representing H, G, and S lignin, and where the ion counts for the H lignin peaks (m/z 107 and 121) were more intense than that of G and S lignin.[177] It was determined through high mass resolution that the H lignin ion peak (m/z 121) could be resolved into two peaks, $C_7H_5O_2^+$ and $C_8H_9O^+$ (Table 17).[163] Spectra of both aspen Klason lignin and a hardwood aspen section interestingly revealed the H lignin peak at m/z 121, but not m/z 107.[177]

Table 18. Lignin and polysaccharide peak list.[159, 165]

Lignin		Polysaccharide	
Mass	**Exact Mass**	**Mass**	**Exact Mass**
51	51.021	44*	44.023*
63	63.022	47	47.013
65	65.038	59*	59.015*
67	67.056	60*	60.021*
77	77.037	61	61.030
79	79.056	71	71.014
91	91.051	81	81.036
93	93.073	83*	83.013*
95*	95.092*	85*	85.034*
105	105.071	87*	87.051*
107	107.044	97	97.032
115	115.045	99	99.049
121	121.065	101*	101.029*
128	128.051	109	109.033
137	137.063	113	113.026
151	151.049	127	127.041
152	152.050	145	145.061
153	153.049		
165	165.059		
167	167.071[a]		
181	181.050[a]		
189	189.059		

*protein fragment interference, [a]theoretical mass.

Lignin ion peaks in the ToF-SIMS spectra for wood is less intense compared to the synthesized lignin, and most likely caused by the cell wall matrix.[163] This matrix contains both covalent and non-covalent cross-linkages between lignin and cellulose and hemicellulose.[163] Goacher et al. studied red pine and developed a more comprehensive list for lignin (Table 18) other than the six characteristic peaks that represent H, G, and S lignin ion.[159, 165] Polydimethyl siloxane (PDMS) contamination interference resulted the removal of a few of the peaks (*m/z* 15, 45, 73, 131, and 147) from the original list due to potential peak overlap.[165] Two peaks, *m/z* 19 and 31, were also removed from the original list due to dependence on the sample moisture content.[165] If the biomass sample was previously treated with proteins, like cellulase and laccase, there will also be protein interference with some lignocellulosic peaks; these peaks are noted by an asterisk in Table 18 and should not be included in the analysis under these or similar conditions.[165] The normalized ion intensities of the lignin ion peaks in Table 18 can be used to calculate the lignin peak fraction (Equation 1), the polysaccharide peak fraction (Equation 2), or lignin modification metric (Equation 3), where L and PS are the sums of lignin and polysaccharide peaks, respectively, in Table 18. The lignin modification metric (Equation 3) helps determine the relative amount of lignin benzene rings that lose methoxy groups that are present in G and S lignin units; the G and S in Equation (3) represent G lignin and S lignin peaks in Table 17, while Ar represents the sum aromatic peaks of *m/z* 77 and 91.[164-165]

$$Lignin\ peak\ fraction = \frac{L}{L + PS} \qquad (1)$$

$$Polysaccharide\ peak\ fraction = \frac{PS}{PS + L} \qquad (2)$$

$$Lignin\ modification\ metric = \frac{G + S}{Ar} \qquad (3)$$

The use of this comprehensive list (Table 18) is typically not used for ToF-SIMS images because it would result in an overwhelming number of selected ion images that would be difficult to sum up for PS and L images. For ToF-SIMS lignin ion images, the major contributing ions for H, G, and S lignin (Table 17) are used.

3.3.2   Cellulose and Hemicellulose

The ToF-SIMS peaks characterizing cellulose can be located in the spectra at *m/z* 127 and 145, which represents ($C_6H_7O_3^+$) and ($C_6H_9O_4^+$), respectively.[159] While there is one report that indicates other hexose compounds, like mannose and galactose, contribute to the assigned cellulose peaks, these two peaks are accepted as representative peaks of cellulose.[159, 177] Figure 29 illustrates the chemical structure of the cellulose-related ions at *m/z* 127 and 145.
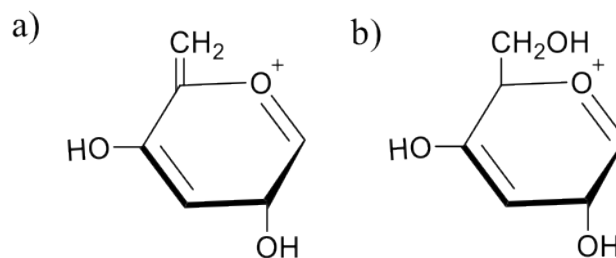
Figure 29. The chemical structures for cellulose ions a) m/z 127 and b) m/z 145.[178]

Tokareva et al. analyzed D(+)-xylose and D(−)-arabinose (Figure 30) and determined that peaks at m/z 115 ($C_5H_7O_3^+$) and 133 ($C_5H_9O_4^+$) originate from these isolated compounds.[177] With the use of PCA modeling (example seen in Figure 31), Goacher et al. determined that lignin contributed to m/z 115 and neither that peak nor m/z 133 distinguished holocellulose from α-cellulose or a pine wood.[159] This means that while these two peaks could be characteristic peaks for hemicellulose in isolated xylose, they cannot be used to represent carbohydrates when analyzing pine wood.[159] While this study occurred only with a softwood pine sample, it is not recommended to use m/z 115 and 133 to represent hemicellulose in any biomass.
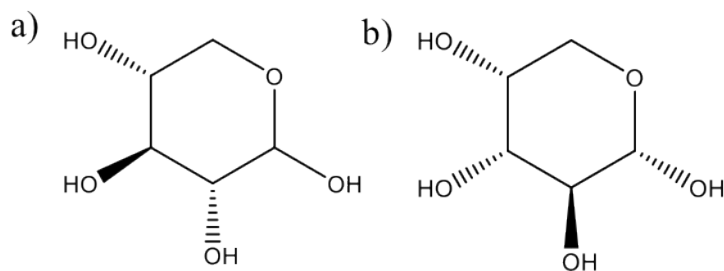
Figure 30. The chemical structures a) D(+)-xylose and b) D(−)-arabinose.

As mentioned above, while Goacher et al. developed a comprehensive ToF-SIMS peak list for lignin characteristic peaks, they also verified a list for polysaccharide characteristic peaks (Table 18) through PCA modeling.[159] This list can be used to calculate the lignin or polysaccharide peak fraction (Equation 1and 2). The original polysaccharide peak list, like the lignin list, had a few peaks removed due to PDMS contamination or their dependence on moisture content; similarly, specific peaks (denoted by an asterisk in Table 18) should not be used after enzymatic activity on the biomass because of protein interference with these polysaccharide ToF-SIMS peaks.[159, 165]
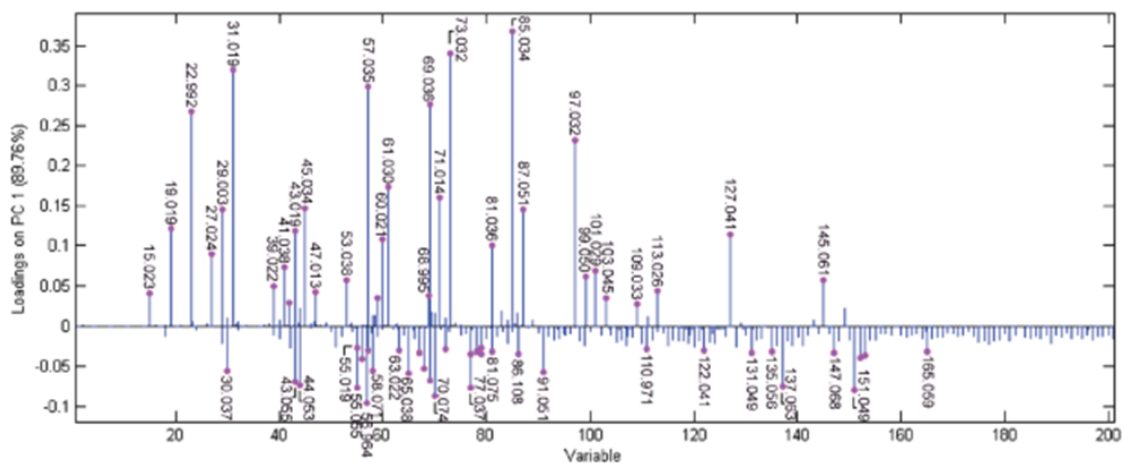
Figure 31. PC1 loading for the PCA model representing ToF-SIMS spectra of extracted red pine, holocellulose, and cellulose fractions. (Reprinted from ref. 162)

3.3.3 Extractives and Pectins

While biomass needs to be extracted to obtain accurate lignin and polysaccharide peaks intensities, there have been some studies conducted on identifying some of the fragmentation peaks for extractives. As mentioned in the biomass sample preparation section on removing the extractives, 18 extractives with proposed peak assignments over m/z 200 and a list of peaks under m/z 200 that "distinguished unextracted from extracted lignocelluloses samples" were determined by Fardim and Durán and Goacher et al.[158, 175] Imai et al. was able to identify a high intensity ion peak at m/z 285 in Sugi heartwood tissue that corresponds with the diterpene phenol ferruginol.[179] Since extractives overlap the lignin content peaks, this incorrect increase in lignin intensity would result in a decrease in the polysaccharide peak fraction (Equation 2) for unextracted biomass.[158]

Also, extractives can contribute to the aromatic peak intensity (Ar, *m/z* 77 and 91), resulting in a decrease in the biomass' lignin modification metric (Equation 3).[158]

Pectins are also naturally occurring heteropolysaccharides in native wood found in the primary cell walls, secondary cell walls, and the middle lamella.[177, 180] Tokareva et al. studied pectin by analyzing trigalacturonic acid, polygalacturonic acid, and methyl-esterified pectin.[177] The distinct peak associated with all polymeric pectin models was *m/z* 155, while *m/z* 111 correlates with methyl-esterified pectin.[177] Metal ions were also used as markers to label anionic groups, like the carbonyl groups found in some pectins.[181] Metal labeling, using metal ion markers, observed in ToF-SIMS images was most effective using Sr^{2+} ions, but that Cu^{2+} ion also identified itself as a useful marker.[181]

3.4   Origination of Components in the Cell Wall

Spatial mapping is extremely useful in identifying the location lignocellulosic fragmentation ions originate from within the cell wall (Figure 32). The cell wall thickness was automatically estimates by Gerber et al. through the combination of computational modeling and ToF-SIMS analysis to develop an "artificially created cell wall mask."[173] The average cell wall thickness of a five-year old field-grown poplar transversal section via ToF-SIMS analysis was 7.6 ± 0.4 μm.[173] This average includes the fiber cell walls of the thicker late wood, thus resulting in a slightly higher value than the 5.4 μm average found in literature.[173] This technique can further be used to differentiate cell wall thickness between wild-type and genetically modified biomass.
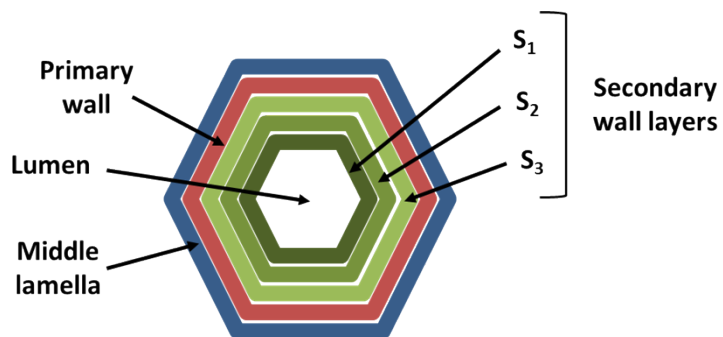
General Plant Cell Wall Layers

Figure 32. General locations of the plant cell walls layers: middle lamella, primary cell wall, secondary cell walls, and the lumen.

Typical locations for high intensity lignin ions are in the secondary cell wall and the cell corners regions.[167] More specifically, Zhou et al. used ToF-SIMS line intensity profiles (Figure 33) to illustrate the predominant locations of G lignin and S lignin in the cell walls, which are the middle lamella and the secondary cell walls, respectively.[168] In relation to specific cells, it was determined that poplar vessel cell walls have more G lignin than fiber cell walls.[168] A lower lignin S/G ratio is the result of higher G lignin in the vessel cells.[168] Vessel cells closer to fiber cells have a lignin S/G ratio of 0.7 compared to the 0.5 of those further from the fiber cells; the fiber cell walls have a 1.1 lignin S/G ratio.[168] These ratio values were interestingly comparable to the lignin S/G ratio for maple, where the vessel walls were approximately 0.6 and maple fiber walls ranged from 0.8 to 1.2.[182] A different poplar study reported lignin S/G ratio values for the vessel and fiber cells also to be 0.7 and 1.1, respectively.[183] These values are lower than the lowest natural variant poplar lignin S/G ratio of ~1.2 by pyrolysis molecular beam

mass spectrometry.[100] Lignin S/G ratio for different types of poplars determined by thioacidolysis were also significantly higher than those lignin S/G ratios by the ToF-SIMS above;[7] this difference is most likely a result of the heterogeneous nature of the biomass and the difference in chemistry content on the sample's surface compared to the bulk material. Studying the surface of biomass is important since the amount of cellulose and lignin on the surface differs from that detected by bulk chemical analysis. This is especially true for biological treatment of biomass, since enzymes and microorganisms typically bind to the surface of biomass.

Figure 33. Line intensity profiles for a) G lignin ions and b) S lignin ions across c) the fiber cell wall from A to B. (Reprinted from ref. 171)
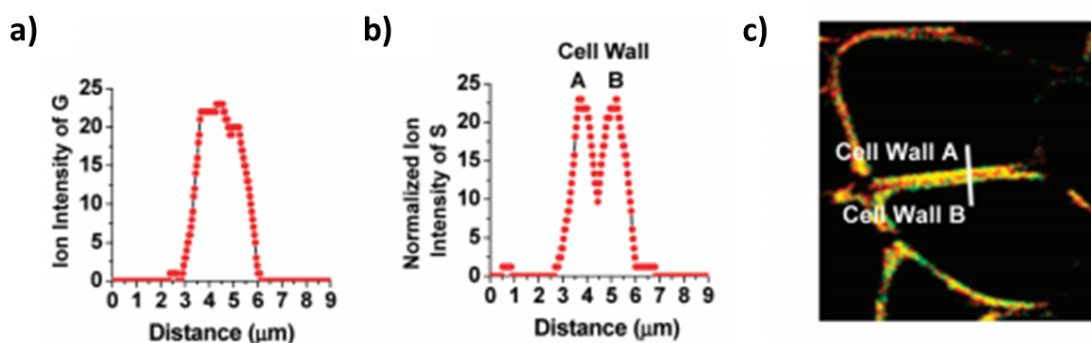
Most mature woody biomass has heartwood, transition zone, and sapwood, where the dark colored heartwood is found in the inner core and the pale sapwood is in the outer zone near the bark.[171] The paler transition zone is where extractives accumulate, living cells die, and sapwood becomes heartwood.[171] A study of these three different areas in Hinoki cypress (*Chamaecyparis obtusa*) revealed that the formation of extractives during the sapwood to heartwood transition occured within the ray parenchyma cells.[171] The ToF-SIMS was used to track the relative intensity of elements Na, Mg, Al, K, and Ca from heartwood to sapwood.[171] Saito et al. showed that heartwood had a higher concentration of K and relatively lower concentrations of Na, Mg, Al, and Ca compared to the sapwood with a "drastic increase or decrease" of Na, Al, and Ca distribution in the transition zone.[171]

As mentioned above in the section on extractives and pectins, Tokareva et al. used metal ion markers to determine the location of anionic groups within the biomass; these anionic groups can provide insight into the location of pectins and xylan.[181] Sr^{2+}-labeled anionic groups were detected in the ray cells and pit membranes of spruce using ToF-SIMS images.[181] ToF-SIMS images further suggested that more methyl-esterified pectin can be found in the ray cells than the pit membrane regions.[181] Analysis with Sr^{2+} labeling revealed that pectins remain in the ray cells and pit membranes of spruce even after delignification.[181] In general, pectin can be found in ray cells, primary cell walls, cell corners, and near the pits of biomass.[181] ToF-SIMS images of the ferruginol fragment peak at *m/z* 285 revealed it is distributed relatively evenly throughout the inside and along the walls of the axial and ray parenchyma cells in addition to the tracheid cell walls.[179]

3.5 Chemical, Biological, and Genetic Modification in Biomass

Biomass modification can occur through chemical pretreatments, microbial treatments, and genetic modifications. A list of softwoods, hardwoods, and grasses analyzed by ToF-SIMS can be seen in Table 19.

Table 19. List of softwoods, hardwoods, and grasses analyzed by the ToF-SIMS.

Softwoods	Hardwoods	Grasses
Pine[10, 159, 166]	Poplar[12, 167-168, 173]	Rice straw[164]
Spruce[158, 165, 172, 176-177]	Birch[10]	Reed[11]
Cedar[162]	Aspen[158, 165, 172, 177]	*Arabidopsis*[156]
Fir[166]		
Cypress[171]		
Beech MWL[163]		

3.5.1 Chemical Pretreatment

Oftentimes, chemical pretreatments are needed to reduce the natural recalcitrance of the biomass in order to facilitate subsequent enzymatic deconstruction. Pretreatments tend to solubilize lignin and/or hemicellulose, but different methods could alter the properties of lignin and negatively impact the glucan digestibility.[184] The changes to the physical cell walls also can occur during pretreatments and research showed that increasing the sample surface area is more important than lignin removal when striving for higher sugar yields

after enzymatic hydrolysis.[153] The biomass chemistry and/or cell walls morphology alterations depend on the chemical treatments; analysis of the surface chemistry provides insight into the efficiency of the pretreatment and the impact it has on the cell walls by detecting the changes to the cell wall chemistry. ToF-SIMS can also reveal lignin migration from one area of the cell wall to another and through an increase of cellulose ions on the surface it can indicate if the pretreatment improved the accessibility of cellulose. The different chemical pretreatments and conditions for biomass that have been subsequently analyzed by the ToF-SIMS are listed in Table 20.

Table 20. Chemical pretreatments and conditions of biomass, where the biomass samples are later analyzed by the ToF-SIMS.

Pretreatment	Conditions
Alkaline	NaOH (1.5g/g sample) in pressure tube at 121°C for 1 h.[164]
	NaOH (0.2g/g substrate), liquor/solid (w/w) 10:1, 60°C for 2 h.[11]
Alkaline peroxide	NaOH (0.2g/g substrate) and H_2O_2 (0.25g/g substrate), liquor/solid (w/w) 10:1, dark place at room temperature for 24 h.[11]
Dilute Acid (DAP)	1 vol% H_2SO_4 in batch reactor at 160°C for 10 min.[12]
Severe DAP	2 vol% H_2SO_4 in batch reactor at 175°C for 10 min.[12]
Holocellulose	$NaClO_2$ (1.30g/g sample) in 0.14 M CH_3OOH at 70°C for 1 h (x3).[12]
Severe Holocellulose	$NaClO_2$ (1.30g/g sample) in 0.14 M CH_3OOH at 70°C for 1 h (x6).[12]
Hydrotropic[a]	30% (w/v) SXS at 150°C for 30 min or 2 h.[10]
	30% (w/v) SXS and 0.17% (w/v) formic acid, liquor solid

(w/w) 10:1) at 160°C 60 min, pH = 3.5 ± 0.05.[11]

[a]Sodium xylene sulfonate (SXS).

Generally, mild thermochemical alkali pretreatment improves enzymatic digestibility through the solubilization of lignin and hemicellulose.[164] A study analyzed the impact of washing with water or HCl of rice straw after an alkaline pretreatment (Table 20).[164] It was determined that lignin was removed through the alkali pretreatment process, but was redeposited onto the surface due to the acid wash; this can be seen in the increase of approximately 9.7% in acid-washed lignin peak fraction (Equation 1) compared to water-washed sample.[164] The ToF-SIMS analysis was useful for providing insight into the changes occurring on the surface of the sample that is not always clear from the bulk compositional analysis.

A comparison study between alkaline, alkaline peroxide, and hydrotropic pretreated common reed samples revealed that hydrotropic pretreatment was more efficient at removing hemicelluloses and increasing the glucan percentage through bulk compositional analysis.[11] ToF-SIMS analysis revealed that the most efficient enzymatic hydrolysis occurred with the hydrotropic pretreated sample; the enzymatically hydrolyzed hydrotropic sample was 58.1% and 64.3% lower for the carbohydrates/lignin ratio and the guaiacyl/total lignin ratio, respectively, compared to the pretreated sample.[11] Through ToF-SIMS images, it was determined that residual lignin location on the surface fiber changed after the pretreatments and that decrease in lignin allowed for more carbohydrates to be exposed.[11] Now, the carbohydrate ToF-SIMS data should be used carefully since the authors used m/z 115 and 133 peaks in addition to m/z 127 and 145,[11]

and Goacher et al. determined that *m/z* 115 and 133 do not uniquely identify hemicelluloses in wood.[159] Overall, it was shown through bulk analysis, ToF-SIMS ion intensity ratios, and ToF-SIMS images that hydrotropic pretreatment reduced and even re-localized lignin in the fiber cells of reed.[11] Also, ToF-SIMS analysis was instrumental in determining which pretreatment would work best for enzymatic hydrolysis.[11]

Another pretreatment comparison study determined that hydrotropic pretreatment was better at removing lignin and increasing enzyme accessibility than hydrothermal and ionic liquid pretreatments; therefore, birch and pine samples that underwent hydrotropic pretreatment with sodium xylene sulfonate (SXS) for 30 min and 2 h followed by enzymatic hydrolysis were analyzed via ToF-SIMS to determine the changes in surface chemical compositions.[10] The ToF-SIMS analysis of hydrotropic pretreated birch revealed that both lignin and some polysaccharides, most-likely low mass hemicelluloses, were being removed from the surface; the loss of polysaccharides mostly occurred in the first 30 min.[10] Comparison between the enzymatically pretreated birch samples and the pretreated birch samples showed that the enzyme treatment possesses the capability of breaking bonds between polysaccharides and lignin as seen in the decrease in lignin ratio (lignin/total ions).[10] A similar comparison between pretreated and enzymatically pretreated pine lead Mou et al. to believe that lignin-carbohydrate-complexes could be influencing the lignocellulosic component fragmentation by the ToF-SIMS.[10] The polysaccharide peak fraction (Equation 2) did not change after enzymatic hydrolysis for the birch samples, the pine samples did see a 5.0% decrease after enzymatic hydrolysis.[10] There was a 56.1% decrease in lignin/total and a decrease of 18.4% in cellulose/total on the surface after enzymatic hydrolysis of the 2 h hydrotropic pretreated pine sample.[10]

For both the birch and the pine, longer pretreatment times reduce the lignin S/G ratio on the surface.[10]

Dilute acid (DA) pretreatment changes the chemistry and cell wall structure of biomass which improves the enzyme accessibility.[12] The conditions for the DA and severe DA pretreatment are in Table 20. Severe DA sample showed a significant decrease is S lignin normalized ion counts when compared to the DA sample; this indicates that S lignin units are easier to breakdown than G lignin units during pretreatment.[12] Cellulose normalized ion counts stayed relatively the same when comparing DA and severe DA pretreatment.[12] Jung et al. did report a 30% increase of xylan on the surface of the sample after DA pretreatment, and compositional analysis indicates there is actually a significant decrease in xylose; ToF-SIMS images also revealed what appeared to be xylan migration from the cell wall to middle lamella and the lumen.[12] The lignin contribution to m/z 115 might explain the supposed xylan migration to the middle lamella, a typical lignin concentrated region.

Jung et al. also determined there was not a significant difference between holocellulose and severe holocellulose pulping treatment on poplar in regards to the major lignocellulosic compounds via the ToF-SIMS.[12] When compared to the extractive-free poplar sample, the holocellulose and severe holocellulose S lignin relative intensity dropped significantly, while the relative G lignin intensity decreased only slightly.[12]

3.5.2   Biological Treatment with Microorganisms

A few studies addressed in the previous section looked at the efficiencies of various pretreatments and pretreatments followed by enzymatic hydrolysis.[10-11, 164] Enzyme activity will result in modification or degradation of biomass and the ToF-SIMS is a useful tool to monitor the changes that occur.[176] The adjustments to the lignocellulosic library (Table 18) that would account for protein interference in the ToF-SIMS spectra as a result of enzyme activity was determined by studying the impact both laccase and cellulase had on white spruce and trembling aspen.[165] Cellulase treatment increased lignin and decreased polysaccharides on the surface, as seen by the 19% and 34% drop in polysaccharide peak fraction (Equation 2) for aspen and spruce, respectively.[165] Laccase activity, with a mediator, cleaved the "hydroxyl and methoxy groups from lignin benzoid units" and resulted in a reduction in both G and S lignin peak intensity.[165] Another study reported that high laccase dosage allows the protein to penetrate the biomass and reduce the polysaccharide content.[169]

While biomass extractives will alter the analysis of surface lignocellulose peaks by overlapping with lignin peaks, a cellulase enzyme treatment can still be detected on unextracted wood.[158] The cellulase enzyme activity was detected using PCA modeling of the ToF-SIMS ions from Celluclast treated unextracted and extracted red spruce.[158]

A way to significantly minimize or even eliminate contamination during processing, is to conduct the fiber-based enzyme assays in a 96-well filter plate.[158] Another potential issue with enzymatic activity on biomass is through buffer interference, which was addressed by rinsing in the section on sample preparation.[176]

PCA modeling of ToF-SIMS spectra and images from white-rot fungus (*Phanerochaete carnosa*) treated balsam fir and lodgepole pine wood detected prominent polysaccharide peaks, while lignin peaks strongly characterized the control samples; this indicates lignin degradation on the surface of the treated sample.[166] The decrease in lignin simultaneously results in an increase of polysaccharide ions on the wood surface.[166] The ToF-SIMS images indicate that lignin removal does not occur predominately in the middle lamella and cell corners, but across the cell walls.[166] Interestingly, Mahajan et al. were able to determine that the fungal decay of pine occurred "more rapidly" than with fir.[166] Since softwood lignin is predominantly composed of G lignin and the study showed *P. carnosa*'s ability at targeting and modifying the G lignin, this fungus is a prime candidate at minimizing softwood species' natural recalcitrance.[166]

3.5.3   *Physical and Genetic Modification*

Stress-induced tension and opposite wood on poplar were studied to determine the chemical differences when compared to normal poplar wood.[167] As expected, there is a relatively low lignin intensity in the gelatinous layer (G-layer) of the tension wood, which is predominately composed of crystalline cellulose; high concentration of lignin was found in the secondary cell wall and the cell corner regions.[167] Other than the increased intensity of cellulose ions in the G-layer, cellulose is rather evenly distributed over the tension wood surface.[167] Jung et al. conducted 3D analysis from 30 sputtering cycles with O_2^+ on the tension wood and a line scan across a region of interest. The line scan bisects a

G-layer, secondary cell wall, and a cell corner, and confirms that cellulose is observed in the G-layer and lignin signal is relatively high in the other two areas.[167]

Genetically modified biomass will typically have anatomical changes, which will usually impact the chemistry of the biomass.[173] PCA modeling of the ToF-SIMS spectra data was able to determine that wild-type *Arabidoposis* (*A. thaliana* Col-0) was enriched in S lignin, while the *Arabidopsis fah1* mutant had a significant amount of G lignin; this data is consistent with our understanding that the *fah1* lines halts the production of S lignin and its incorporation into the cell wall.[156] The high S lignin content found in the fiber cells of the wild-type contributes to the higher lignin S/G ratio compared to the *fah1* mutant.[156] The polysaccharide peak fraction (Equation 2) indicates that the difference between the wild-type and the mutant is not associated with carbohydrates.[156] Now, the *Arabidopsis irx3* mutation does result in an approximate 20% depletion of cellulose, and the polysaccharide peak fraction ratio similarly reports a decrease of 15% between the wild-type and this mutant.[156] This shows that the ToF-SIMS is capable of differentiating genetic mutations of herbaceous plants.

Genetic modifications of poplar by downregulating the *PdKOR2* gene resulted in a lignin S/G ratio decrease of approximately 50% on the fiber cell walls and a less than 10% lignin S/G ratio increase on the vessel cell walls. The ToF-SIMS analysis of the overall lignin S/G ratio for the transgenic sample compared to the control was lower. It was shown that while the bulk chemical analysis can provide insight into the changes to a plant due to genetic modifications, surface characterization can reveal alterations occurring in specific types of plant cells and cell wall layers.[183]

CHAPTER 4: EXPERIMENTAL MATERIALS AND PROCEDURES

4.1   Chemicals and Materials

4.1.1   Chemicals and Materials

Chemicals and materials were procured from Sigma-Aldrich (St. Louis, MO) or VWR (West Chester, PA), and used as received. All gases were acquired from Airgas (Radnor Township, PA). Cryotome sectioning required embedding material (OCT Compound, Tissue-Tek®) and disposable blades (Accu-Edge® Low Profile Blades 4689) made by Sakura® Finetek (Alphen aan den Rijn, Netherlands) and Feather Safety Razor Co, LTD (Osaka, Japan), respectively. Precleaned glass slides came from VWR and Thermo Fisher Scientific. G8 glass fiber filters for carbohydrate analysis were purchased from Thermo Fisher Scientific (Madison, WI). Double sided carbon adhesive tabs (12 mm diameter) for SEM analysis were purchased from Electron Microscopy Sciences (Hatfield, PA). SlowFade Diamond Antifade Mountant was the antifade oil purchased from Thermo Fisher Scientific for CLSM analysis.

4.1.2   Biomass Substrate

Poplar and hybrid poplar were grown in greenhouses at different locations for six months. *Populus deltoides* were harvested at Oak Ridge National Laboratory (ORNL, Oak Ridge, TN) and *Populus. deltoides x nigra* (DN34) was grown at National Renewable Energy Lab (NREL, Golden, CO), where greenhouses were maintained at 25°C and 30-60% humidity. The plants were watered automatically four times a day and received 16 h of

light daily. The poplar stems were cut approximately 15 cm above the soil and then stored at -20°C.

4.1.2.1   Milled Poplar Stems

Fresh poplar stems were freeze-dried (VirTis Sentry 2.0 Freezemobile) at -80 °C for 24 h prior to milling. A Thomas-Wiley Laboratory Mill machine was used to mill the dried poplar stems through a 40 mesh screen to a particle size of 0.42 mm or less. Milled samples were stored at -20°C until further treatment.

4.1.2.2   Cryotome Sectioned Poplar Stems

A poplar stem approximately 4 cm in length and 2 cm or less in diameter was cross-sectioned by either a LEICA CM 1850 cryostat or a LEICA CM 3050S cryostat (Leica Microsystems Nussioch GmbH, Nussioch, Germany). The cryostat was used under manual control at approximately -10°C chamber temperature and equipped with a disposable steel blade cleaned with dichloromethane and ethanol or acetone to remove any lubricant. The stem was attached to the 40 mm specimen disc with embedding material (OCT compound, Tissue-TEK®) surrounding the bottom and approximately 0.5 cm of the stem base. The cross-sections were cut to 60 or 80 μm thickness.

4.1.3 Microorganisms

Caldicellulosiruptor bescii wild type was purchased from DSMZ (Braunschweig, Germany). *C. bescii* was grown anaerobically at 75 °C in low osmolarity defined (LOD) medium (described 4.2.3 *Caldicellulosiruptor bescii* Incubation).

Clostridium thermocellum (ATCC 27405) was maintained in the laboratory in 20% glycerol stocks at -80°C over time.

Enzymatic hydrolysis occurred with either Novozymes CTec2 (Franklinton, NC) or purified *C. thermocellum* cellulase exoproteome[106] (donated by Yannick J. Bomble from National Renewable Energy Laboratory, CO). Commercial *Aspergillus niger* β-glucosidase (Novozyme 188) was obtained from Sigma-Aldrich (St. Louis, MO).

4.2   Experimental Procedures

4.2.1   Soxhlet Extraction

Non-structural material, like solvent soluble compounds (resins, waxes, fatty acids, etc.) can potentially interfere with analytical analysis and techniques and, therefore, are removed prior to chemical analysis.[7] Less than 5% dry weight of poplar is attributed to extractives.[7] The extraction method was adapted from TAPPI method T 204 cm-97, where extractives of the milled and cross-sectioned poplar samples were removed with dichloromethane (CH_2Cl_2) using a Soxhlet apparatus and extraction thimbles. Approximately 150 mL of CH_2Cl_2 was refluxed for either 4 h at a rate of 6 solvent cycles

per h or overnight at a slower rate. The extractive free solids were air-dried over night with the cross-sections stored between glass slides.

4.2.2 Ammonia and Organosolv Pretreatments

Milled (0.75 g) and cross-sectioned (0.012 g) samples were loaded with 25 mL of pretreatment solution in a batch 5460 mini-Parr 300 mL reactor (internal volume: 300 mL). Ammonia pretreatment was conducted with 5.0% ammonia hydroxide, and organosolv pretreatment occurred with 65.0% ethanol and 1.0% sulfuric acid as an acid catalyst. The same reaction temperature (180 °C) and reaction time (20 min) were applied in both pretreatments. Ramp up time was approximately 25 min and reaction was quenched in an ice bath. After the pretreatment, solid residues were filtered by Whatman #1 filter paper and rinsed by deionized (DI) water until the pH reached ~7. The milled pretreated samples were collected and air-dried, while the pretreated cross-sectioned samples were separated from the milled biomass, rinsed, and placed between glass slides to air-dry.

4.2.3 Caldicellulosiruptor bescii Incubation

C. bescii was grown anaerobically at 75°C in low osmolarity defined (LOD) medium with either maltose (0.5% wt/v) as sole carbon source for routine growth or juvenile poplar stem cross-sections. LOD medium contained 0.25 g/L NH_4Cl, 0.0136 g/L NaCl, 0.33 g/L KCl, 0.33 g/L $MgCl_2$ x $6H_2O$, 0.14 g/L $CaCl_2$ x $6H_2O$, 1 g/L $NaHCO_3$, 5 g/L maltose, 1 g/L cysteine HCl x H_2O, and trace element solution SL-10 at a pH of 7.2.[185]

Trace element solution SL-10 contained 1.5 g/L $FeCl_2$ x $4H_2O$, 0.07 g/L $ZnCl_2$, 0.1 g/L $MnCl_2$ x $4H_2O$, 0.006 g/L H_3BO_3, 0.19 g/L $CoCl_2$ x $6H_2O$, 0.002 g/L $CuCl_2$ x $2H_2O$, 0.024 g/L $NiCl_2$ x $6H_2O$, 0.036 g/L Na_2NoO_4 x $2H_2O$, 0.015 g/L Na_cWO_4, 0.015 g/L Na_2SeO_3 x $5H_2O$, and 10 mL/L of 25% HCl.[186]

Sample cross-sections were incubated with and without *C. bescii* in LOD media (0.5% w/v) at 75ºC for 0, 72, and 288 h. Cultures were periodically sampled with needle and syringe to monitor the cell growth after characterization. After incubation, poplar cross-sections were washed with DI water (3 x 50 mL) and ethanol (2 x 50 mL). Each section was air dried between glass slides before further surface characterization.

4.2.4   *Clostridium thermocellum Fermentation*

Microtome-sections of extractive-free poplar were used (at 10g/L, dry weight basis) as the carbohydrate source in the anaerobic preparation of MTC media for batch microbial bioconversions. MTC medium was a mixture of independently sterilized solutions: solution B + M (2 g/L potassium citrate, 1.25 g/L citric acid monohydrate, 1 g/L sodium sulfate dibasic, 1 g/L potassium phosphate monobasic, 2.5 g/L sodium bicarbondate), solution C (1.5 g/L ammonium chloride, 2 g/L urea), solution D (1 g/L magnesium chloride hexahydrate, 0.2 g/L calcium chloride dehydrate, 0.1 g/L ferrous chloride tetrahydrate, 1 g/L L-cysteine hydrochloride monohydrate), solution E (0.02 g/L pyridoxamine dihyrochloride, 0.001 g/L riboflavin, 0.001 g/L nicotinamide, 0.5 mg/L lipoic acid, 0.004 g/L 4-aminobenzoic acid, 0.004 g/L D-biotin, 0.025 mg/L folic acid, 0.002 g/L cyanocobalamin, 0.2 mg/L thiamine hydrochloride), and solution F (0.5 mg/L

manganese chloride tetrahydrate, 0.5 mg/L cobalt chloride hexahydrate, 0.2 mg/L zinc sulfate heptahydrate, 0.05 mg/L copper sulfate pentahydrate, 0.05 mg/L boric acid, 0.05 mg sodium molybdenum oxide dehydrate, 0.05 mg nickle chloride hexahydrate, 0.01 g/L citric acid monohydrate).[100]

To obtain fermented poplar samples, freshly grown *C. thermocellum* was used as inoculum at 10% v/v and the bottles incubated at 60 °C for 92 h with gentle shaking (MaxQ™ 6000 Incubator Shaker, ThermoFisher Scientific, MA). Fermentations were performed in triplicate biological replication. Control poplar biomass was processed similarly in a single bottle without receiving a microbial inoculum. Replicate processing of control poplar was not needed, as a previous study[15] indicated that short-term storage in buffered medium does not induce significant changes in the solids to warrant investigation of variation. However, all further analysis of control poplar biomass was performed in technical replication as indicated. Aliquots of liquid supernatant of incubated cultures were collected at ~24 h intervals for further analysis.

4.2.5 *Enzymatic Hydrolysis*

Enzymatic hydrolysis of samples with Novozymes CTec2 (10 FPU per gram biomass) occurred at a consistency of 1.0% (w/v) in 50 mM citrate buffer solution (pH 4.8). The enzymatic hydrolysis was conducted at 50 °C and 200 rpm in an incubator shaker and then quenched in boiling water for 10 min. The hydrolysate was periodically collected (1.0 mL) at 0, 3, 6, 12, 24, 48, and 72 h. Released sugars in each hydrolysate were

analyzed using Dionex ICS-3000 ion chromatography system. Each analysis was conducted in duplicates. Error bars on the plotted data represent one standard deviation.

Enzymatic hydrolysis of samples with *C. thermocellum* cellulase exoproteome (20 mg protein/g biomass) took place in a freshly prepared buffer (pH = 5.5) made of 20 mM sodium acetate, 5 mM $CaCl_2$, 100 mM NaCl, 2 mM EDTA, 10 mM L-cysteine x HCl, and performed in five biological replicates each. The *C. thermocellum* cellulase exoproteome was then added at 20 mg protein/g biomass, a concentration range similar to published work,[106] where excellent activity was demonstrated on model cellulose and dilute-acid pretreated corn stover. Additionally, a commercial *Aspergillus niger* β-glucosidase (Novozyme 188 with 250 units/g) was added at 20 µL β-glucosidase solution/g biomass to avoid cellobiose inhibition of cellulases. Enzymatic hydrolysis was performed at 60 °C for 96 hours with shaking and the end-point solute sugars were quantified by (HPLC) with an Aminex™ HPX-87P column (Bio-Rad Laboratories Inc., CA).

4.3 Analytical Procedures

4.3.1 Chemical Compositional Analysis

Samples were treated by two-step acid hydrolysis process adapted from NREL/TP-510-42618 to analyze carbohydrates and lignin composition.[187] In short, biomass solids were acid hydrolyzed by 72% w/w H_2SO_4 at 30°C for 1 h, and then the mixture was diluted to 4% w/w H_2SO_4. The sample solution mixture was autoclaved at 121°C for 1h. After the two-step hydrolysis, solid residues and hydrolysate were separated using crucible with

glass filter. The hydrolysate was analyzed by Dionex ICS 3000 ion chromatography system or high precision liquid chromatography (HPLC) with an Aminex™ HPX-87P column (Bio-Rad Laboratories Inc., CA) to quantify carbohydrates against known standards. Acid soluble lignin was analyzed by ultraviolet-visible (UV-Vis) spectroscopy. The solid residues were further washed with DI water until neutralized and oven-dried for measuring acid-insoluble lignin. Error analysis was conducted by performing compositional analysis 2-3 times on the samples and calculating the standard deviation from the average value.

4.3.2   C. bescii Cell Growth Analysis

To monitor growth on the poplar slices (0.5% (w/v)), cultures for the *C. bescii* incubation were periodically sampled at 0, 3, and 6 h following by sampling every 6 h from 6 h to 30 h and every 12 h from 30 h to 124 h. The cultures were fixed in 3.7% formaldehyde, vortexed, and stored at -20 ºC for cell counts. Samples were appropriately diluted and stained with 0.1% Acridine Orange before visualizing using an epifluorescent microscope at 100x (oil immersion). Cell counts from 15 to 20 fields were averaged and error bars represent one standard deviation.

4.3.3   Fermentation Products of C. thermocellum

Aliquots of liquid supernatant of incubated cultures were collected at ~24 h intervals and the fermentation products and potential solubilized hydrolysis sugars determined by HPLC against known standards of ethanol, acetic acid, formic acid, lactic acid,

cellobiose, glucose and xylose. In short, samples were filtered (0.22 μm), then acidified to pH 2 with 2M H_2SO_4. Separation was made at 0.5 mL/min flow rate with 5 mM H_2SO_4 mobile phase through an Aminex HPX-87H column (Bio-Rad Laboratories Inc., CA) at 60ºC and the products quantified by refracting index at 50ºC (detector model L-2490, Hitachi High Technologies America Inc., IL). Error analysis was conducted by analyzing the liquid supernatant 2-3 times for each aliquot and plotting the average with error bars representing one standard deviation.

4.3.4   Confocal Laser Scanning Microscopy

Prior to CLSM analysis, the cellulose of the samples was fluorescently labelled by placing cross-sections in saline solutions with 18 μM Direct Red 23 and allowed to stain for 10 minutes in the dark. The dye solution was then replaced twice with fresh saline liquid to rinse the excess DR23 from biomass. Sample sections were then blot-dried gently and mounted with antifade oil onto microscope slides with coverslips. Confocal laser scanning microscopy (Zeiss LSM 710, Carl Zeiss AG, Germany) was used to acquire at least two z-stack volume scans at random positions in each poplar section.

To adhere to strict quantitative imaging principles, all samples were scanned with identical instrument settings using: Plan-Apochromat 63x/1.40 NA oil immersion objective, laser excitation at 405 nm wavelength and 45% power and 488 nm wavelength with 15% power; pinhole size of 1 AU (airy units), detector bandpass filters of 410-480 nm to capture lignin autofluorescence and 550-625 nm to capture DR23 fluorescence with the corresponding beam-splitters and detector gains set to 863 and 660, respectively.

Volume z-stack scans – ranging between 10 to 14 µm depth - were acquired by capturing images with 0.132 µm/pixel scaling at 0.600 µm z-step size (i.e., at an estimated 50% sectioning overlap between consecutive scans) and a 1.58 µs pixel dwell time. Digital gain and offset were set to default 1 and 0, respectively. These settings were pre-optimized (using real-time pixel intensity histograms) to capture sample emission with minimal pixel saturation (detector saturation, on an 8-bit scale) and to reduce noise, scan averaging of 2 in line mode was performed.

Volume 3D views were reconstructed in Zen Black 2.1 (Carl Zeiss AG, Germany) in transparency rendering mode using signal threshold of 5, ramp 9, maximum opacity of 80% and brightness 2.1.

For quantitative fluorescence and colocalization imaging, signal data was used raw, as acquired and extracted using ImageJ in the Fiji distribution package. First, a z-stack of 3 µm (5 frames of 0.600 µm each) was extracted from each independent volume scan to compare regions of identical size (i.e., x:y:z of 134.82 µm: 134.82 µm: 3.00 µm). To eliminate user bias, the extracted z-stack was always centered on the frame with highest average pixel intensity for cellulose (i.e., the middle slice in the 5-slice stack had the most intense fluorescence emission in the original z-stack). Signal was captured and analyzed in an 8-bit scale (i.e., a range of 0-255 pixel intensity distribution).

Pearson's r[136] and Manders'[138] coefficients were calculate according to user guideline (http://imagej.net/Coloc_2) using ImageJ plugin "coloc 2" (part of Fiji distribution package) for 6 different locations. Each image analyzed was composed of 5-frame z-

stacks. Pixel thresholds were auto-detected and all of Pearson's correlations were validated according to Costes theory and significance tests.[136]

Colocalization across plant cell walls were determined using volume scans made of 5 z-stack frames and identifying a region of interest of variable length in μm and of exactly 2.5 μm widths that was drawn across three adjacent plant cells, such that the length axis was intersecting the cell wall at a perpendicular axis. Pixel intensity was averaged in the width dimension and between the 5 frames of a z-stack and plotted against the length axis. The averages localization distance across plant cell walls were determined from the regions of interest shown by the histogram which measured the difference in μm between the start and the end of cellulose or lignin signals (minimum average intensity = 5).

To determine the spatially-resolved average fluorescence intensity, the background noise from non-tissue areas was reduced by setting the minimum thresholds for cellulose-DR23 and lignin signals to 17 and 26, respectively. Average signal fluorescence intensity was calculated as: $\sum_{i=1}^{5} \frac{\sum_{j=threshold}^{255}(pxI_j \cdot pxC_j)}{\sum_{J=threshold}^{255} pxC_j}$, where i is the frame number (for a total of 5 frames in a z-stack), j is the intensity scale in 8-bit, pxI is the pixel intensity and pxC is the pixel count. Calculations were made separately for each detection channel and the results of six randomly selected z-stacks were averaged.

4.3.5   Scanning Electron Microscopy

Samples were mounted to aluminum SEM disks using double sided carbon adhesive tape and coated with gold for 20 sec by SPI Module Sputter/Carbon Coater System. SEM

images were acquired via a Leo 1525 Field Emission (FE) SEM (Carl Zeiss AG, Oberkochen, Germany) at 3 kV and various resolving powers.

4.3.6   Solid-State NMR Analysis

Samples were ground by a planetary ball mill (Retsch PM 100) at 580 rpm with zirconium dioxide (ZrO_2) vessels (internal volume: 50 mL) and ZrO_2 ball bearings (10 mm × 10) for 2 h and 30 min (5 min grinding and 5 min break) for whole cell wall NMR analysis. Yoo et al. recently developed a new bi-solvent system, a mixture of dimethylsulfoxide (DMSO-d_6) and hexamethylphosphoramide (HMPA-d_{18}), which successfully caused swelling in the biomass and provided structural detail of the biomass at a good resolution.[188] Approximately 50 mg of ball-milled biomass (either untreated or pretreated) and DMSO-d_6/HMPA-d_{18} (4/1, *v/v*; ~0.5 mL) were loaded in a 5 mm NMR tube. The biomass samples were well dispersed and dissolved by vortexing and sonication for 1~2 h into a uniformed gel-state. NMR spectra of each sample were obtained by a Bruker Avance III 400-MHz spectroscopy equipped with a 5-mm Broadband Observe probe (5-mm BBO 400MHz W1 with Z-gradient probe, Bruker). Two-dimensional (2D) ^{13}C –^1H heteronuclear single quantum coherence (HSQC) spectra were collected at 298 K using a Bruker standard pulse sequence ('hsqcetgpsi2') with the following parameters: spectral width of 11 ppm in F2 (^1H) with 2048 data points and 190 ppm in F1 (^{13}C) with 256 data points; 128 scans (NS) and 1 s interscan delay (D1).

Chemical shift was calibrated with the central DMSO solvent peak at 2.49/39.5 ppm (δ_H/δ_C).

Volume integration of contours in HSQC spectra was conducted using Bruker's TopSpin 3.5 software. Lignin S/G ratio is calculated from the integration of S, S', and G areas (structures seen in Figure 34) using Equation 4, where $S_{2,6}$, $S'_{2,6}$ and G_2 represent the integrated area of the ^{13}C-^1H cross-signals in the HSQC NMR spectra. The untreated and pretreated ^{13}C-^1H cross-signal spectra assignment for $S_{2,6}$, $S'_{2,6}$ and G_2 were δ_C/δ_H 104.0/6.74 ppm, δ_C/δ_H 106.3/7.25 ppm, and δ_C/δ_H 111.0/7.03 ppm, respectively.
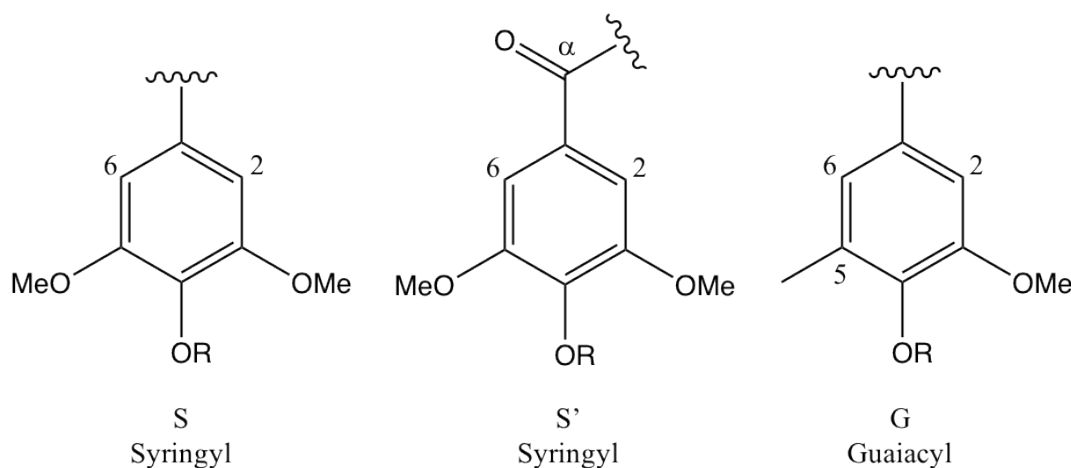
Figure 34. Labeled syringyl (S and S') and guaiacyl (G) lignin structures indicating the C-H locations detected by 2D HSQC NMR analysis that can be used to calculate lignin S/G ratio.

$$Lignin\ ^{S}/_{G}\ Ratio = \frac{S_{2,6} + S'_{2,6}}{2} \times \frac{1}{G_2} \qquad (4)$$

4.3.7   ToF-SIMS Analysis

99

TOF-SIMS analysis was performed using an ION-TOF TOF·SIMS V (ION-TOF, Münster, Germany) equipped with a bismuth liquid metal ion gun (LMIG) as a primary ion source. The pulsing primary ion gun (25 keV) disrupts the samples surface, ejecting secondary ions; the positive charged ions were detected and the information was converted into either high mass resolution spectra or high spatial resolution images using Measurement Explorer ionTOF software.

ToF-SIMS bunch mode produced high mass resolution spectra after bismuth primary ions randomly rastered various 500×500 μm areas (128 x 128 pixels) on the sample. The spectra were calibrated to CH^+, CH_2^+, CH_3^+, and $C_2H_3^+$. The ion intensities of selected peaks were normalized to the total ions detected and the average value for each ion fragmentation was used for further calculations. Error analysis was performed by averaging data from 6-9 random locations and calculating the standard deviation (represented by error bars in plotted data). The specific fragmentation ions peaks included: cellulose (*m/z* 127, 145), G lignin (*m/z* 137, 151), S lignin (*m/z* 167, 181), and additional ion peaks associated with polysaccharides and lignin (Table 18).[159, 165] This results in average cellulose, G lignin, and S lignin for each sample, and average sums of the lignin (L) and polysaccharides (PS) ion peaks are used to calculate the lignin and polysaccharide peak fractions (Equation 1 and 2). It is important to note that previously reported xylan ions peaks[175] does not in fact characterize hemicellulose. The total polysaccharide fraction reported in this study, which included cellulose and holocellulose, utilized all polysaccharide peaks identified in recent literature.[159]

ToF-SIMS images were obtained using the burst alignment mode, where the primary ions were randomly rastered across 100 x 100 μm areas (256 x 256 pixels) and the positive secondary ions detected. The spectra for the images were calibrated to CH^+, CH_2^+, CH_3^+, and $C_2H_3^+$ and the peaks corresponding to cellulose (m/z 127 and 145), G lignin (m/z 137 and 151), and S lignin (m/z 167 and 181) were selected. The ion intensities from each specific fragmentation ions peak were converted into a spatial map using a color scale, low (black) to high (yellow/white) intensity. The two cellulose images were added together for a mapping of the total cellulose. This was similarly done for the G and S lignin images, resulting in a single lignin ion image. In some cases, the cellulose or lignin ion image could be scaled green and overlaid on the total ion image in order to distinguish specific chemical characteristics of the lignocellulosic biomass sample.

CHAPTER 5: UNDERSTANDING THE CHANGES TO THE BIOMASS SURFACE AFTER AMMONIA AND ORGANOSOLV PRETREATMENT USING TOF-SIMS[‡]

5.1   Introduction

Lignocellulosic biomass is the most abundant and renewable natural resource on earth. Utilization of cellulose, hemicelluloses, and lignin in the biomass can facilitate in the production of biofuels and/or bio-based products. Biomass recalcitrance, like the structural complexity and heterogeneity of its chemical components within the cell wall, contributes to the plant's natural defense against biological degradation, but it also plays a negative role in biomass conversion and must be overcome for efficient biomass utilization.

One way to reduce biomass recalcitrance is change the physicochemical characteristics of the bioresource through pretreatments. Physical, chemical, and/or biological pretreatments can break down or solubilize one or more biomass components making the utilization of the treated biomass easier. Traditionally, cellulose-rich pretreated solids show higher yields and faster conversion rates during enzymatic hydrolysis and fermentation when compared to the untreated biomass.

Characterization of biomass is an essential step for designing effective biomass conversion processes, such as pretreatment and fermentation. In particular, biomass

characterization techniques are capable of providing insight into how the pretreatment impacts the physical structure and chemistry of the biomass. Chemical composition, syringyl (S)/guaiacyl (G) lignin ratio, molecular weight of each biomass fraction (cellulose, hemicellulose, and lignin), and cellulose crystallinity are typical biomass characteristics measured using HPLC, NMR, GPC, and other instrumentations.

Another biomass characterization method is surface characterization, which examines the morphology and chemistry of the plant cell walls on the surface of a sample. Surface characteristics of biomass are crucial factors for enzymatic hydrolysis and fermentation of biomass, because enzymes and microorganisms directly interact with the substrate's surface. Surface analysis revealing erosion and re-location of cell wall matrix components has assisted in explaining how enzyme accessibility increased and enzymatic hydrolysis was improved in pretreated biomass.[189] SEM,[153, 155] TEM,[141] Raman spectroscopy,[154, 190] FTIR spectroscopy,[12, 141, 154] and AFM[140, 191] are commonly used for biomass surface analysis.

Time-of-flight secondary ion mass spectrometry (ToF-SIMS) is another analysis technique for surface characterization that produces high mass resolution spectra and spatial mapping of the surface chemical ions. This analytical technique has been applied for analyzing the surface of neurobiological systems,[192] drug delivery,[193] and polymer films.[161] Recently, biomass characterization studies using ToF-SIMS were investigated.[159, 168, 182] In the early stage, studies focused on identifying key fragmentation peaks associated with cellulose and lignin.[160, 194] Application of ToF-SIMS characterization was expanded to understand the surface changes of woody biomass after pretreatments.[10, 12] Groacher et al. developed a list of approximately 40 secondary ion

peaks that correlate with polysaccharides and lignin found within lignocellulosic biomass.[159, 165] These values contain the common fragmentations for cellulose (*m/z* 127, 145), G lignin (*m/z* 137, 151), and syringyl (S) lignin (*m/z* 167, 181). The ion intensities (or counts) for each mass peak were normalized to the total ions to determine compositional ratio of specific peaks detected on the surface, including polysaccharide peak fraction, lignin peak fraction, and lignin S/G ratio.

To date, ToF-SIMS analysis has been applied to only a few types of pretreated biomass, such as hydrotropic pretreated birch and pine and dilute acid pretreated poplar.[10, 12] Herein, the application of ToF-SIMS analysis is expanded to ammonia-treated and organosolv-treated poplar to determine advantages and limitation of this analysis method compared to traditional analysis methods, including wet chemical compositional analysis by HPLC via two-step acid hydrolysis, lignin S/G ratio by 2D HSQC ^{13}C-^{1}H NMR analysis, and sugar release by enzymatic hydrolysis. Ammonia and organosolv pretreatments are considered lignin-targeting pretreatments,[74, 81, 195] but each has its own advantages and limitation. For instance, ammonia pretreatment partially removed lignin with minimal carbohydrates loss,[74, 195] while organosolv pretreatment significantly removed both lignin and hemicellulose.[81] Ammonia pretreatment showed effective delignification, in specific, on herbaceous plants or agricultural residues,[61] while organosolv pretreatment was applicable towards diverse biomass, including woody biomass.[196]

5.2   Experimental Section

5.2.1   Biomass Substrates and Extraction

Populus deltoides stems were grown at from ORNL and the six-month old stems were harvested, as described in Chapter 4 (4.1.2 Biomass Substrate). The poplar stems were milled to 0.42 mm or less and sectioned into 60 μm thick cross-sections using an acetone-cleaned disposable steel blade in a LEICA CM 1850 cryostat, as described in Chapter 4 (4.1.2.1-2 Milled Poplar Stems and Cryotome Sectioned Poplar Stems). Both milled and cross-sectioned samples were extracted for 16.5 h as describe in Chapter 4 (4.2.1 Soxhlet Extraction). Extractive-free poplar is referred to as untreated poplar in this chapter.

5.2.2   Ammonia and Organosolv Pretreatments

Ammonia and organosolv pretreatments occurred under the same conditions (180°C for 20 min) on extractive-free milled and cross-sectioned *Populus,* as described in Chapter 4 (4.2.2 Ammonia and Organosolv Pretreatments).

5.2.3   ToF-SIMS Analysis

ToF-SIMS spectra of cross-sectioned extractive-free (untreated), ammonia-treated, and organosolv-treated samples were obtained with a TOF·SIMS V, as described in Chapter 4 (4.3.7 ToF-SIMS Analysis). Six different, random locations on the three different

samples were rastered with a Bi_3^+ primary ion beam, resulting in average normalized intensities for cellulose, G lignin, and S lignin along with polysaccharide and lignin peak fractions ((PS/(PS+L) and L/(PS+L), respectively).

5.2.4   Chemical Compositional Analysis

The untreated and pretreated poplar samples underwent duplicate compositional analysis to quantify the carbohydrates, acid soluble lignin, and acid-insoluble lignin using the Dionex and UV-Vis, as described Chapter 4 (4.3.1 Chemical Compositional Analysis). The standard deviation was calculated for glucose (< 1.7%), xylan (< 0.9%), galactan (< 0.2%), arabinan (<0.4%), and lignin (0.8%). For direct comparison of the composition on the biomass surface with the bulk chemical composition of biomass, the polysaccharide and lignin contents from the chemical compositional analysis were normalized similar to the ToF-SIMS results, as seen in Equations 5 and 6.

$$Polysaccharides\ (\%) =$$
$$\frac{Glucan + Xylan + Galactan + Arabinan}{Glucan + Xylan + Galactan + Arabinan + Lignin} \times 100\% \qquad (5)$$

$$Lignin\ (\%) =$$
$$\frac{Lignin}{Glucan + Xylan + Galactan + Arabinan + Lignin} \times 100\% \qquad (6)$$

5.2.5   Solid-State NMR Analysis

NMR analysis of untreated and pretreated samples occurred as described in Chapter 4 (4.3.6 Solid-State NMR Analysis).

5.2.6 Sugar Release

Untreated, ammonia-treated, and organosolv-treated poplar samples were tested for sugar release measurement in duplicates. Poplar samples (250 mg oven-dry weight) underwent enzymatic hydrolysis with Novozymes CTec2, as described in Chapter 4 (4.2.5 Enzymatic Hydrolysis).

5.3   Results and Discussion

5.3.1 Chemical Composition

The impact the two pretreatments had on the surface and bulk chemical composition were determined using ToF-SIMS and wet chemical composition analysis methods. A ToF-SIMS bismuth ion beam was rastered across 6 different locations on each of the 60 μm thick untreated or pretreated cross-section poplar sample, and forty secondary ion peaks associated with polysaccharides and lignin from the ToF-SIMS total ion spectra of the poplar samples were quantified,[159, 165] normalized, and averaged. The polysaccharide and lignin peak fractions (Figure 35) reveal a 9% decrease in polysaccharides to the total polysaccharides and lignin ratio for the ammonia-treated poplar from the untreated sample, where the organosolv pretreatment resulted in a slightly higher fraction (2%). The ammonia-treated poplar cross-section possessed a higher lignin peak fraction than the others.
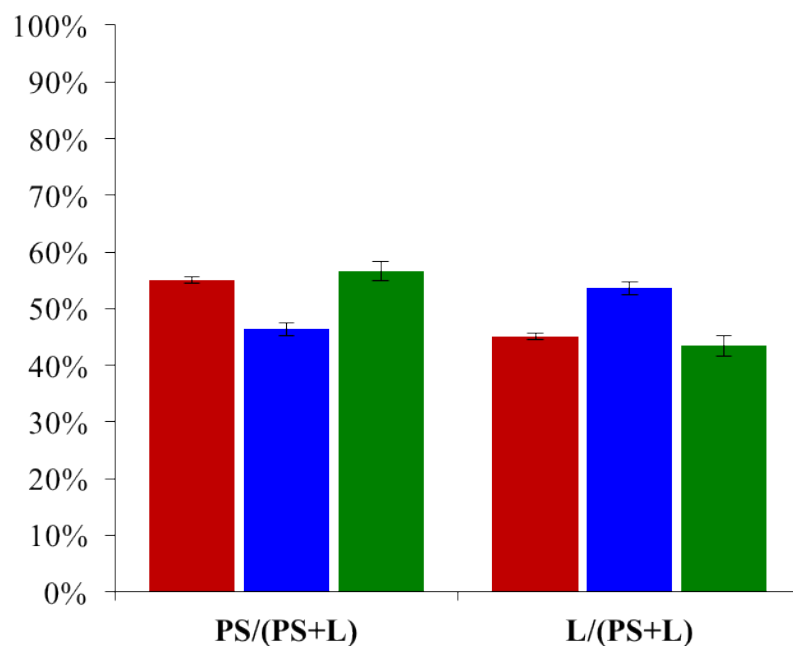
Figure 35. Polysaccharide and lignin peak fraction observed from untreated (red), ammonia-treated (blue), and organosolv-treated (green) poplar cross-sections. Derived from the sum of polysaccharide (PS) and lignin (L) ToF-SIMS peaks.[159, 165]

Untreated and pretreated samples also underwent a two-step sulfuric acid hydrolysis process in order to quantify the bulk composition of polysaccharides and lignin using an ion chromatography system. Compositional information based on the oven-dry weight of untreated samples (Figure 36) showed a removal of 40% hemicellulose and 19% lignin with minimal cellulose loss (~2%) for the ammonia-treated sample. Organosolv pretreatment removed 73% of hemicellulose and 42% of lignin, but it also caused 15% of cellulose loss. The results indicated that organosolv pretreatment possessed a greater efficiency at deconstructing and removing hemicellulose and lignin in poplar than ammonia pretreatment, but it solubilized more of the cellulose. For a better understanding

of the chemical compositions in the pretreated poplar solids, the results were calculated based on the oven-dry weight of each solid residue (Figure 37), where the values represent the actual amount of each composition in the pretreated solid residues; these values are used for calculating the yields of fermentable sugars from each pretreated biomass. Total hemicellulose contents (xylan, arabinan, and galactan) in ammonia-treated and organosolv-treated poplar were 5.3% and 11.2% lower, respectively, compared to the untreated poplar. Lignin contents of both pretreated poplar solids were also slightly lower than the content of untreated poplar. Resulting from the changes in hemicellulose and lignin contents, the relative cellulose content increased from 48.6% to 56.9% and 63.2% after ammonia pretreatment and organosolv pretreatment, respectively (Figure 37).
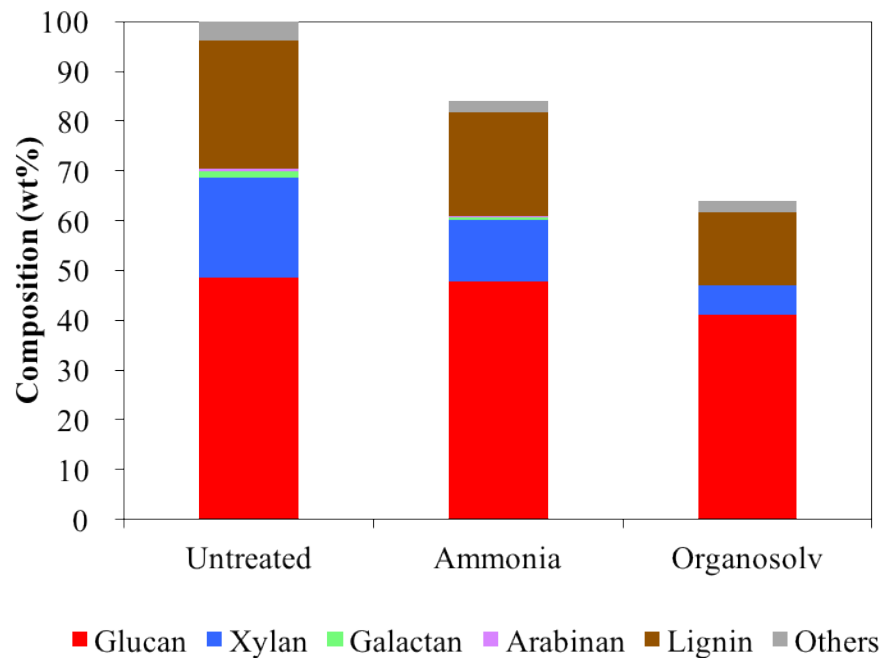
Figure 36. Chemical compositions of untreated, ammonia-treated, and organosolv-treated poplar based on oven-dry weight of untreated biomass.
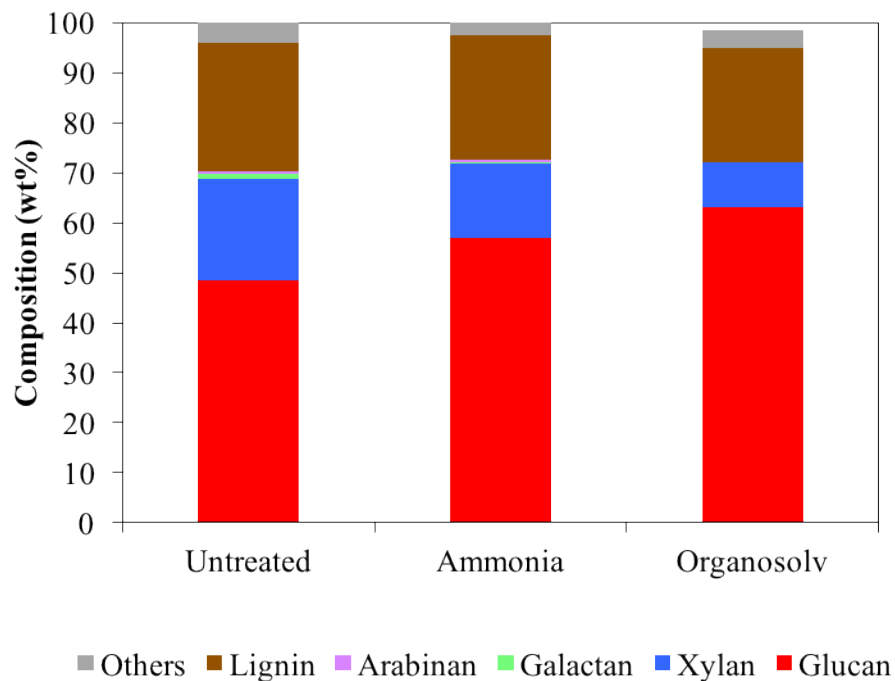
Figure 37. Chemical compositions of untreated, ammonia-treated, and organosolv-treated poplar based on oven-dry weight of the pretreated solid residues.

Table 21. Comparison of normalized polysaccharides and lignin contents by ToF-SIMS analysis and chemical composition analysis for untreated, ammonia, and organosolv

Composition	Analysis method	Untreated [%]	Ammonia-treated [%]	Organosolv-treated [%]
Polysaccharide	ToF-SIMS	55	46	57
	Chemical	73	74	76
Lignin	ToF-SIMS	45	54	43
	Chemical	27	26	24

pretreated poplar samples.

For direct comparison of the surface composition and the bulk composition of poplar, the aforementioned chemical compositional analysis results (Figure 37) were normalized using the sum of cellulose, hemicellulose, and lignin, excluding other compositions. Table 21 presents the normalized polysaccharide and lignin fractions for the untreated, ammonia-treated, and organosolv-treated poplar samples via the ToF-SIMS and chemical compositional analysis. The normalized polysaccharides and lignin contents by chemical compositional analysis for each sample did not vary significantly (< 3%), while the normalized compositions from the surface chemistry using ToF-SIMS presented up to an 11% difference. The contents of total polysaccharides and lignin by ToF-SIMS analysis did not correlate with the results from chemical compositional analysis; however, the cellulose peak intensities (*m/z* 127 and 145) on the poplar surface by ToF-SIMS (Figure 38) showed the same tendency as the bulk cellulose contents (Figure 37) — the cellulose content of organosolv-treated poplar was greater than that of ammonia-treated poplar and both were greater than that of untreated poplar sample.
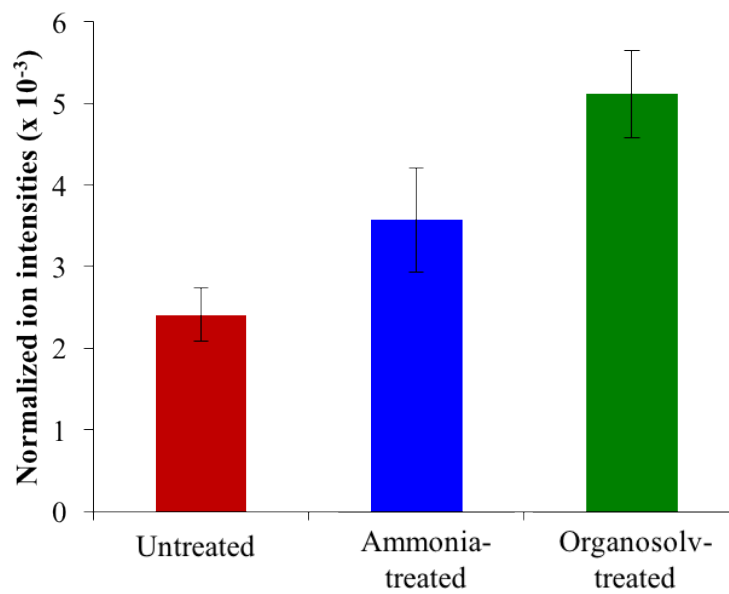
Figure 38. Cellulose (m/z 127 and 145) normalized ion intensities for untreated, ammonia-treated, and organosolv-treated samples.

5.3.2   Lignin S/G Ratio

Besides the changes to the compositions of bulk and biomass surface, other modifications to the chemistry could have occurred during biomass pretreatments. Lignin content based on the residual solids, for example, might not appear to be significantly altered from the previous analysis, but the structural and compositional information of lignin, like the lignin S/G ratio, could have changed. Studies have shown that the lignin S/G ratio can impact cellulose accessibility and/or sugar release during enzymatic hydrolysis.[100, 197] Specifically, the blocked C-5 position of S lignin allows for S-rich lignin to form more linear chains and minimizes cross-linkages that are more common with G-rich lignin, which allows microbes greater access to desired chemicals on the surface.[100, 197]

Therefore, the surface lignin S/G ratio for the untreated and pretreated samples were analyzed by ToF-SIMS and compared to the lignin S/G ratios determined by NMR

analysis. The ToF-SIMS lignin S/G ratios were calculated from the normalized ion intensities of the sum of S lignin peaks (m/z 167, 181) and the sum of G lignin peaks (m/z 137, 151). The pretreatments increased the detected lignin ion intensities on the surface of the samples, where the ammonia-treated poplar reported two and four times higher G and S lignin ion intensities, respectively, compared to the untreated sample (Figure 39). The changes of lignin composition (S and G contents) on the surface of ammonia-treated poplar resulted in the highest lignin S/G ratio (1.72). The S and G lignin ion intensities from the organosolv-treated surface also notably increased (Figure 39), and the resulting lignin S/G ratio of the organosolv-treated poplar (1.15) was higher than that of the untreated sample (0.93).
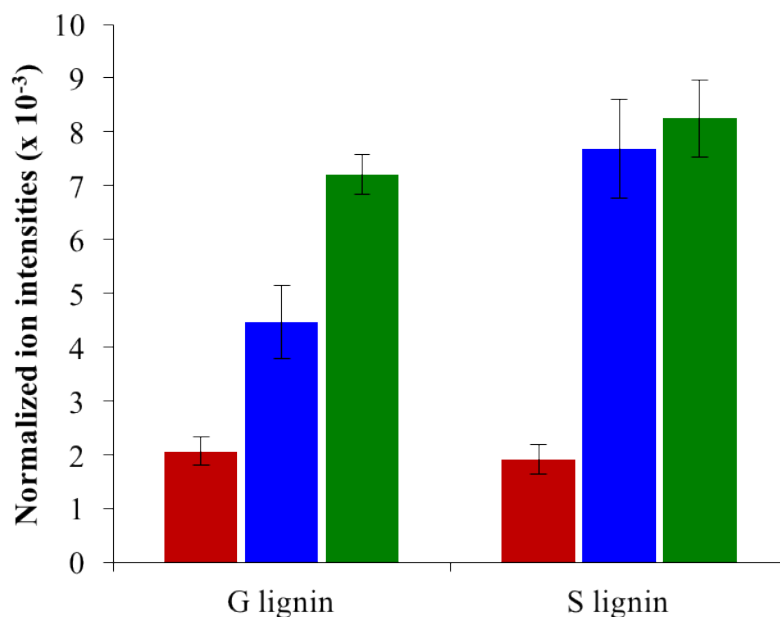
Figure 39. G lignin (m/z 137 and 151) and S lignin (m/z 167 and 181) normalized ion intensities for untreated (red), ammonia-treated (blue), and organosolv-treated (green) samples.

NMR analysis is a typical analysis method for understanding the structural characteristics of biomass, including lignin S/G ratio. Semi-quantitative analysis using ^{13}C–^1H HSQC NMR analysis was applied for monitoring the changes of lignin S/G ratio of the poplar samples. Aromatic regions of the NMR spectra from untreated, ammonia-treated, and organosolv-treated poplar (Figure 40) revealed syringyl (S), guaiacyl (G), and *p*-hydroxybenzoate (PB) contents. The correlation for $S_{2/6}$ and α-oxidized $S_{2/6}$ were assigned at δ_C/δ_H 104.0/6.74 ppm and δ_C/δ_H 106.3/7.25 ppm. The correlations of G unit (G_2, G_5, and G_6) were found at δ_C/δ_H 111.0/7.03 ppm, δ_C/δ_H 114.7/6.84 ppm and δ_C/δ_H 118.8/6.84 ppm, respectively. Changes to the relative contents of S and G units in the pretreated biomass were observed from the NMR analysis by quantifying the S and G units using $S_{2/6}$ and G_2. The S and G unit contents were 58% and 42% in the untreated poplar, respectively. Organosolv pretreatment increased S content to 70% with 30% G unit content, thereby the lignin S/G ratio increased to 2.35. Ammonia pretreatment changed this ratio further, resulting in a 3.20 lignin S/G ratio.

Figure 40. Aromatic regions of 2D ^{13}C – ^{1}H HSQC NMR spectra for untreated, ammonia-treated and organosolv-treated poplar samples.
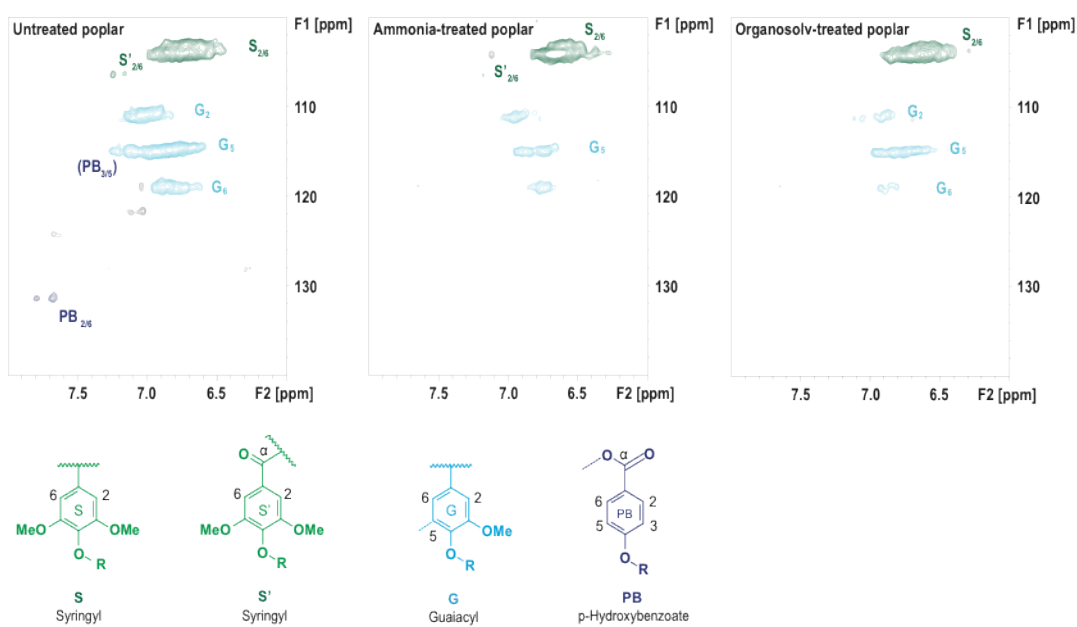
According to both ToF-SIMS analysis results from the cross-section of poplar samples and NMR analysis results from the whole plant cell wall, ammonia and organosolv pretreatments increased the lignin S/G ratio. Although the scale in each analysis method was different, the lignin S/G ratio from each analysis method shows a strong positive correlation ($R^2 = 0.9223$) (Figure 41). The order of lignin S/G ratio for these poplar samples was ammonia-treated poplar > organosolv-treated poplar > untreated poplar for both analysis methods.
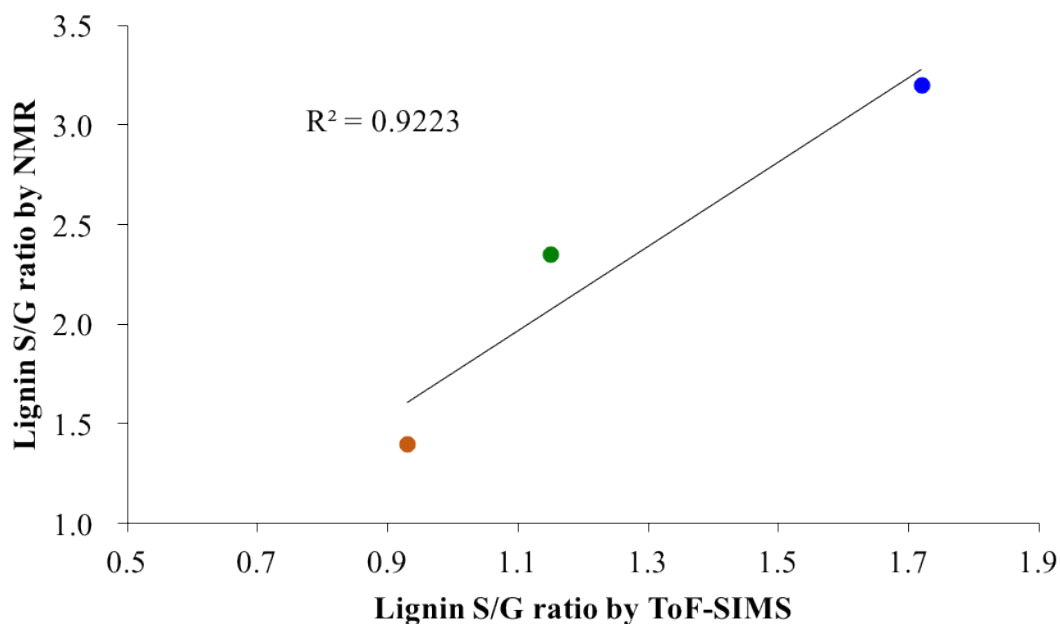
Figure 41. ToF-SIMS lignin S/G ratio vs. NMR lignin S/G ratio vs. for untreated (red point), organosolv pretreated (green point), and ammonia pretreated (blue point) poplar samples.

5.3.3   Sugar Release

The changes to the compositions and lignin S/G ratio by ammonia and organosolv pretreatments were evaluated by sugar release test. The glucose release performance of untreated, ammonia-treated, and organosolv-treated poplar was tested by enzymatic hydrolysis. Glucose release performances of pretreated poplar samples had a faster increase rate at the beginning of hydrolysis, and the difference between the samples' rates became larger over time (Figure 42). For instance, glucose releases at 6 h were 23, 26, and 27 mg from untreated, ammonia-treated, and organosolv-treated poplar, respectively, and the releases reached 40, 92, and 133 mg after 72 h enzymatic hydrolysis. The significant improvement in the sugar release of the pretreated samples indicates that the pretreatments assisted in overcoming some inhibiting barriers, possibly the presence of lignin and/or other characteristics of the biopolymer. The glucose release followed the same trend as the enzyme-accessible cellulose on the biomass surface detected by ToF-SIMS (Figure 38) and cellulose content from bulk compositional analysis results (Figure 37). Further surface characterization study analyzing enzymatically hydrolyzed biomass at various times may provide deeper insight into how enzymes consume cellulose on the biomass surface.
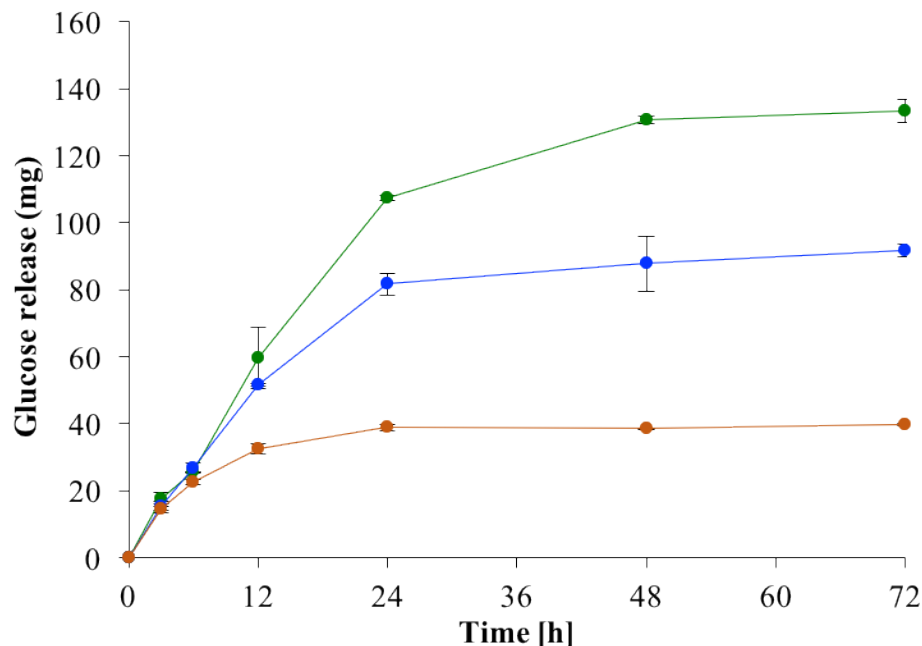
Figure 42. Glucose release of untreated (red), ammonia-treated (blue), and organosolv-treated (green) poplar samples.

5.4 Conclusion

In this chapter, ToF-SIMS was successfully used to understand the differences between surface and bulk chemistry of untreated, ammonia-treated, and organosolv-treated poplar samples. Jung et al. previously illustrated the similarity of carbohydrate and lignin content between milled and cross-sectioned poplar samples.[12] Therefore, both extractive-free milled ($\leq$ 42 mm) and cross-sectioned (60 μm thick) poplar stems were used in this study. The untreated and pretreated milled samples underwent compositional analysis, NMR analysis of the lignin S/G ratio, and sugar release from enzymatic hydrolysis, while the untreated and pretreated cross-sections were used for ToF-SIMS analysis since they had retained their cell wall structure.

The chemical information from the surface of a biomass sample can differ significantly from that of the whole plant cell wall.[12] This could explain the lack of correlation between the ToF-SIMS and bulk chemical compositions for polysaccharides and lignin. The bulk chemistry between the various samples did not vary considerably (≤ 3%), while the ToF-SIMS normalized chemistry revealed an 11% difference between the two pretreatment samples. Although the polysaccharide contents from the two techniques did not correlate well with each other, the discrepancies could indicate that the surface is being impacted differently by the chemical pretreatment than the bulk tissue.

Interestingly, the surface and bulk cellulose content did follow a similar trend. And while the lignin S/G ratios from ToF-SIMS and NMR analyses did not provide identical values, there was also a positive correlation detected between the values from the two methods. The ammonia-treated sample was show to possess the highest lignin S/G ratio, followed by the organosolv-treated sample. Enzymatic hydrolysis of the untreated and pretreated samples showed that higher glucose release correlated with the sample manifesting higher surface cellulose composition and lower surface lignin. ToF-SIMS analysis could expedite preliminary studies by identifying pretreatment conditions that result in specific outcomes; for example, high lignin S/G ratio or glucose release.

Overall, the ToF-SIMS provides a different perspective in understanding the pretreatment effects on properties of biomass and its sugar release, and could be a good predictor of cellulose content, lignin S/G ratio, and glucose release. Bulk characterization methods and ToF-SIMS provide different information about two important parts of the lignocellulosic biomass, and should be used together to present more comprehensive details about the samples and pretreatment processes. Not only would surface analysis by

ToF-SIMS provide depth and greater insight into pretreatment studies, it could also be useful in microbial studies where microorganisms directly interact with the biomass surface.

CHAPTER 6: SURFACE CHARACTERIZATION OF *POPULUS* DURING *CALDICELLULOSIRUPTOR BESCII* GROWTH BY TOF-SIMS ANALYSIS[§]

6.1   Introduction

One challenge in producing cost-efficient biofuels from lignocellulosic biomass is in overcoming its natural recalcitrance. Traditional methods to overcome recalcitrance incorporate various pretreatments to increase cellulose and hemicellulose accessibility by enzymes.[198] In place of standard purified enzymes cocktails, researchers have recently focused on engineering microorganisms for consolidated bioprocessing (CBP), a process that combines hydrolysis and fermentation of biomass to ethanol in one step with cellulase producing microorganisms, thus increasing efficiency and reducing costs.[199]

Members of the genus *Caldicellulosiruptor* are thermophilic, anaerobic bacteria known for their cellulolytic capabilities, making them potential CBP microorganisms.[200-201] Members of this genus have the specific ability to utilize complex polysaccharides such as crystalline cellulose and unpretreated plant biomass.[114, 200, 202] *Caldicellulosiruptor bescii*, is one of the most cellulolytic strains within this genus,[201] and recent genetic advances have resulted in engineering a strain capable of converting unpretreated biomass directly to ethanol.[90] The *C. bescii* genome contains 52 glycoside hydrolases, five pectate lyases, and seven carbohydrate esterases in combination with 22

carbohydrate binding modules contributing to their ability to break down plant biomass.[113, 201-202] Many of these enzymes are multifunctional enzymes that contain two catalytic modules connected by linker regions and CBM domains. In particular, *C. bescii* has a gene cluster (Cbes1853-1867) that together contains six multifunctional enzymes linked with CBM3s capable of assisting in the binding of 12 separate catalytic domains to insoluble substrates.[113] The cellulases are multi-functional somewhat similar to the cellulosome of organisms like *Clostridium thermocellum*,[203-204] but act as noncomplexed free enzymes.[113] The enzymes appear capable of degrading plant biomass by combining the ease of substrate access of the free cellulases with collective catalytic activities in one protein product.[205] Recently, a pectinase gene cluster (Cbes1853-1856) and a combination exo-/endoglucanase (CelA; Cbes1867) were both shown to play an important role in overcoming plant biomass recalcitrance.[122] CelA is the most abundant extracellular protein produced by *C. bescii* and was found to be more active than commercial enzyme cocktails.[206]

While *C. bescii* is known to bind to the surface of the biomass,[113] the mechanism of how the cells and their enzymes deconstruct the biomass is not well understood. Time-of-flight secondary ion mass spectrometry (ToF-SIMS) is a surface analysis technique that requires little sample preparation in order to detect secondary ions[159] from cellulose and lignin. High-resolution spectra and high spatial imaging provides valuable insight into biomass chemistry through normalized ion intensities, or counts, and image mapping of the fragmentation ions. Goacher et al.[165] developed an approach using ToF-SIMS to assess both enzyme activity on biomass and any subsequent biomass degradation. This study goes beyond the use of enzyme cocktails and apply a similar process using a

potential CBP organism, *C bescii*. SEM and ToF-SIMS are primarily utilized to gain insight into the physical and chemical impact of *C. bescii* and its extensive array of enzymes on the surface of juvenile poplar stems.

6.2　Experimental Section

6.2.1　Biomass Substrate and Extraction

Populus deltoides x nigra (DN34) was obtained from NREL and sectioned into 80 μm thick discs using a LEICA CM 3050S cryostat, for this study, as detailed in Chapter 4 (4.1.2 Biomass Substrate and 4.1.2.2 Cryotome Sectioned Poplar Stems). Extractives were subsequently removed from the sectioned samples through Soxhlet extraction with dichloromethane (~150 mL) at a reflux rate of 6 solvent cycles/h for 4 h, as described in Chapter 4 (4.2.1 Soxhlet Extraction).

6.2.2　C. bescii Incubation and Growth Analysis

Poplar cross-sections were incubated with or without *C. bescii* wild type in LOD medium at 75ºC for 0, 72, or 288 h, as described in Chapter 4 (4.2.3 *Caldicellulosiruptor bescii* Incubation). Poplar stems were then used as a sole carbon source for *C. bescii* in LOD media, and uninoculated controls were used to account for the effect of the growth conditions over time due to the temperature and media. To monitor growth on the poplar slices (0.5% (w/v)), cultures were periodically sampled and cell were counted, as described in Chapter 4 (4.3.2 *C. bescii* Cell Growth Analysis). After incubation, poplar

cross-sections were thoroughly washed with DI water and ethanol, then air dried between glass slides.

6.2.3 Scanning Electron Microscopy

Surface morphology of cross-sectioned samples incubated with and without *C. bescii* was observed using a Leo 1525 Field Emission (FE) SEM coated at 3 kV and various resolving powers, as described in Chapter 4 (4.3.5 Scanning Electron Microscopy).

6.2.4 ToF-SIMS Analysis

A TOF•SIMS V spectrometer equipped with a pulsing Bi_3^{2+} primary ion gun was used to obtain high mass resolution spectra and high spatial resolution images. High mass resolution spectra resulted from a total of 200 scans of each 500×500 μm area on the sample. Three data sets per sample were acquired from three replicates to reduce any site specificity. Spatial images were of a 100×100 μm area, and the different fragmentations were combined to form a cellulose ion image and a lignin ion image. The lignin ion image was given a green color and overlaid on the red total ion image. ToF-SIMS analysis occurred as described in Chapter 4 (4.3.7 ToF-SIMS Analysis).

6.3   Results and Discussion

6.3.1   C. bescii Cell Growth

Growth of *C. bescii* on poplar stems was monitored by cell counts using fluorescence microscopy after staining with Acridine Orange.[122] In the first 24 h, *C. bescii* grew quickly before temporarily plateauing around 24 h (Figure 43). We attribute this primary growth to utilization of easily accessible sugars, most likely soluble components of the biomass (such as xylan) released at high temperatures or by initial enzymatic degradation. Previous work has shown that incubation of poplar in liquid at 75°C can release about 7% soluble materials (by weight).[114] *C. bescii* is capable of growing on xylan as a sole carbon source and has the ability to utilize a wide range of sugar substrates found in plant biomass.[114, 116]

We observe a secondary growth phase starting around 30 h and peaking at 72 h. This is attributed to degradation of the more insoluble portion of the biomass as the enzymes produced during the primary growth phase provide a new release of usable carbon source. Washed materials and spent materials (residual substrate after previous growth with *C. bescii*) are both able to support growth of *C. bescii*.[114] In fact, we see cells attaching to the substrate at 48 h during this secondary growth phase (Figure 43 inset), potentially to better access sugars on the surface. Proximity of the microbe and the enzymes it produces to the substrate has been shown to create a favorable microenvironment for cellulose hydrolysis[207], presumably by increasing the local concentration of the enzymes trapped between the cell and the substrate. A structurally unique, non-catalytic protein has been described in *Caldicellulosiruptor* spp. involved in attachment to cellulose[208] and is

specific to the strongly cellulolytic strains within this genus, suggesting a link between attachment and cellulose degradation.
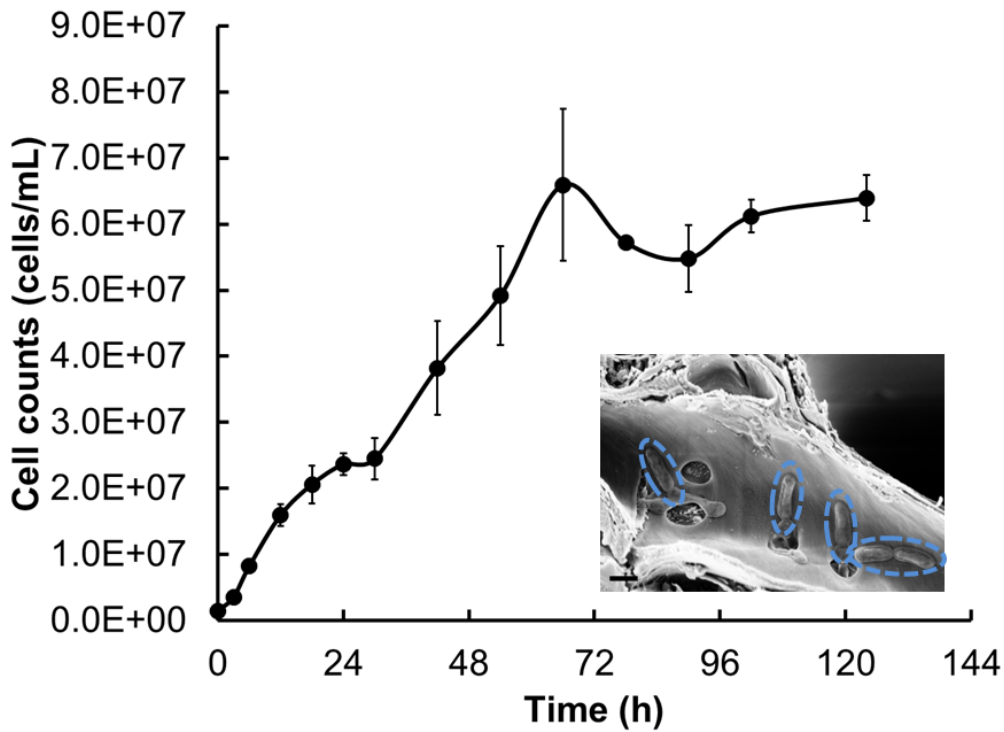
Figure 43. Growth properties of *C. bescii* on poplar slices. Growth measured by cell counts of cultures stained with Acridine Orange after growth on poplar slices as a sole carbon source in LOD medium. Inset: SEM image of *C. bescii* (denoted by blue circles) attached to cellulose walls at 48 h (scale bar 1μm).

6.3.2 Cell Wall Morphology

To determine the impact of *C. bescii* on cell wall structure, SEM was used to observe the surface morphology of the sectioned samples. To ascertain if the LOD medium or incubation temperature (75ºC) contributed to cell wall damage, uninoculated control samples were also analyzed, and underwent the same sample incubation conditions and incubation only without *C. bescii*. These controls do appear to have some surface roughness along the cell wall, likely the result of the sectioning process (Figure 44 a-b, e-f); however, they lack the degradation observed in the samples grown with *C. bescii* (Figure 44 c-d, g-h). After 72 h incubation with *C. bescii* (Figure 44 c-d), the poplar cell walls develop crevices that are not seen in the uninoculated controls (Figure 44 a-b). This corresponds well with the knowledge that CelA, the most abundant excreted enzyme of *C. bescii,*[209] is able to create cavities during digests of Avicel, a crystalline cellulose.[121] These crevices become even more prevalent at 288 h (Figure 44 g-h) and are primarily localized within the primary and secondary cell walls. This indicates that *C. bescii* enzymes have continued to digest the biomass after 72 h. *In vitro* work with CelA demonstrates that the thermophilic enzymes produced by *C. bescii* remain active up to at least 160 h at 75°C.[121] Proteomics of *Caldicellulosiruptor* spp. have also shown that the highest levels of extracellular proteins are observed in stationary phase.[209] Enzymes produced in stationary phase likely remain active for some time and would account for the continued degradation of the poplar slices after the end of the growth cycle.
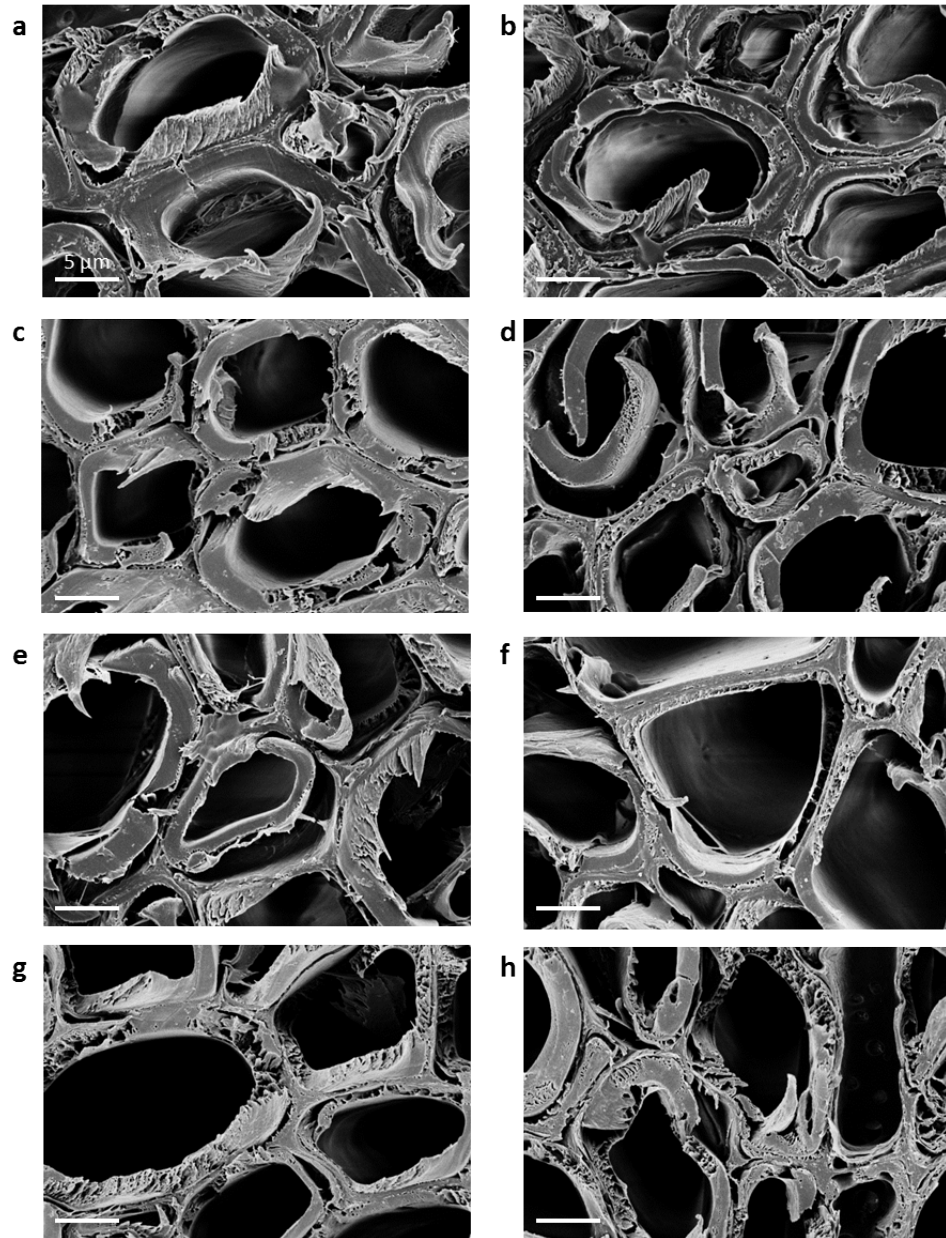
Figure 44. Electron micrograph of poplar slices after incubation in LOD medium at 75°C after 72 h without (a-b) and with *C. bescii* (c-d) and after 288 h without (e-f) and with *C. bescii* (g-h).

6.3.3   Cell Wall Chemistry

We also measured changes in the surface chemical composition during growth of *C. bescii* using ToF-SIMS. Average normalized ion intensities for cellulose (*m/z* 127 and 145), guaiacyl (G) lignin (*m/z* 137 and 151), and syringyl (S) lignin (*m/z* 167 and 181)[159] were obtained from high resolution spectra for the uninoculated controls and samples incubated with *C. bescii* for 0, 72, and 288 h. The normalized ion intensities for the controls (Figure 45 a) showed very little variation, indicating that the high incubation temperature and LOD medium alone do not impact the amount of cellulose and lignin measured on the surface. The changes in the cellulose and lignin ion count after incubation with *C. bescii* can be seen in Figure 45 b. Most notable was the increase in lignin ions between samples treated for 0 h and 72 h for G lignin and S lignin, 150% and 190% respectively. This trend was supported by the lignin ion images (Figure 46 a,c,e) where the pixels representing the lignin ions were scaled green and overlaid on the red total ion image. It is clear that for the 72 and 288 h samples (Figure 46 c,e), there is an increase in lignin ions within the middle lamellas and the cell corners of the plant cell wall. The increase in lignin can be attributed to the removal of other chemical components (hemicellulose and cellulose) allowing more lignin ions to be measured at the surface.
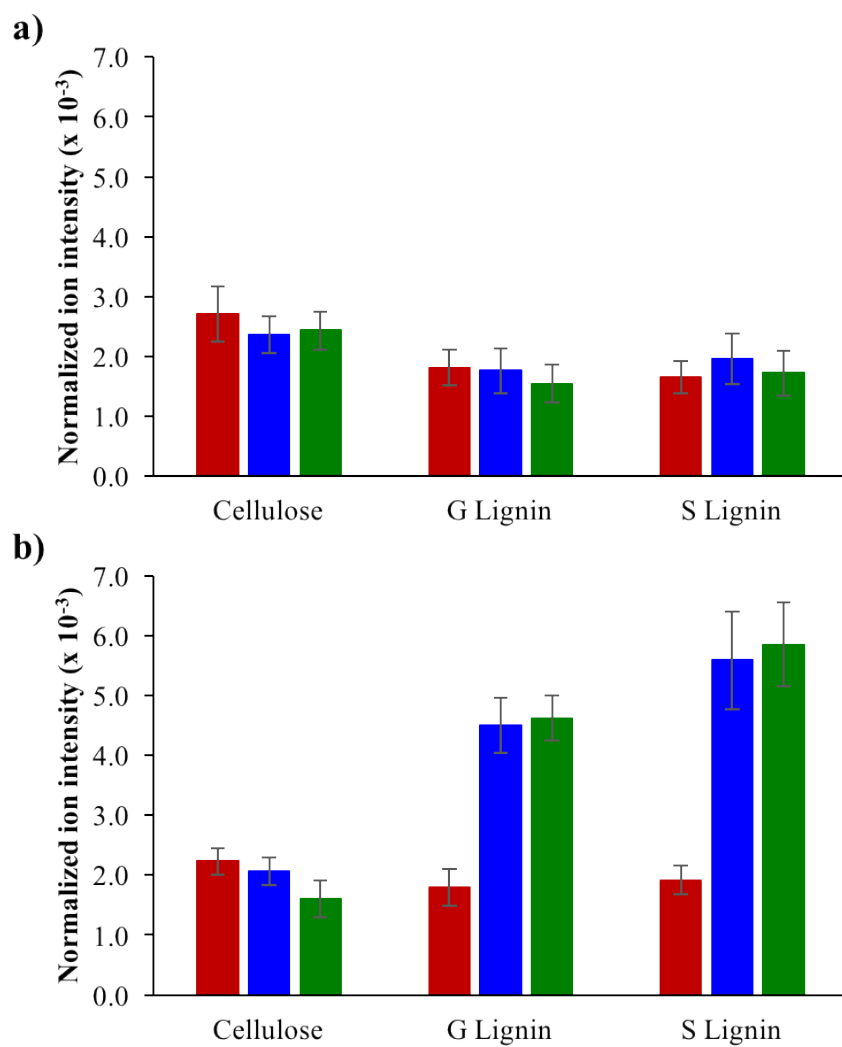
Figure 45. Normalized ion intensities for the surface components (cellulose, G and S-lignin) by ToF-SIMS for a) uninoculated controls for 0 h (red), 72 h (blue) and 288 h (green) And b) poplar cross-sections after growth with *C. bescii* for 0 h (red), 72 h (blue) and 288 h (green).
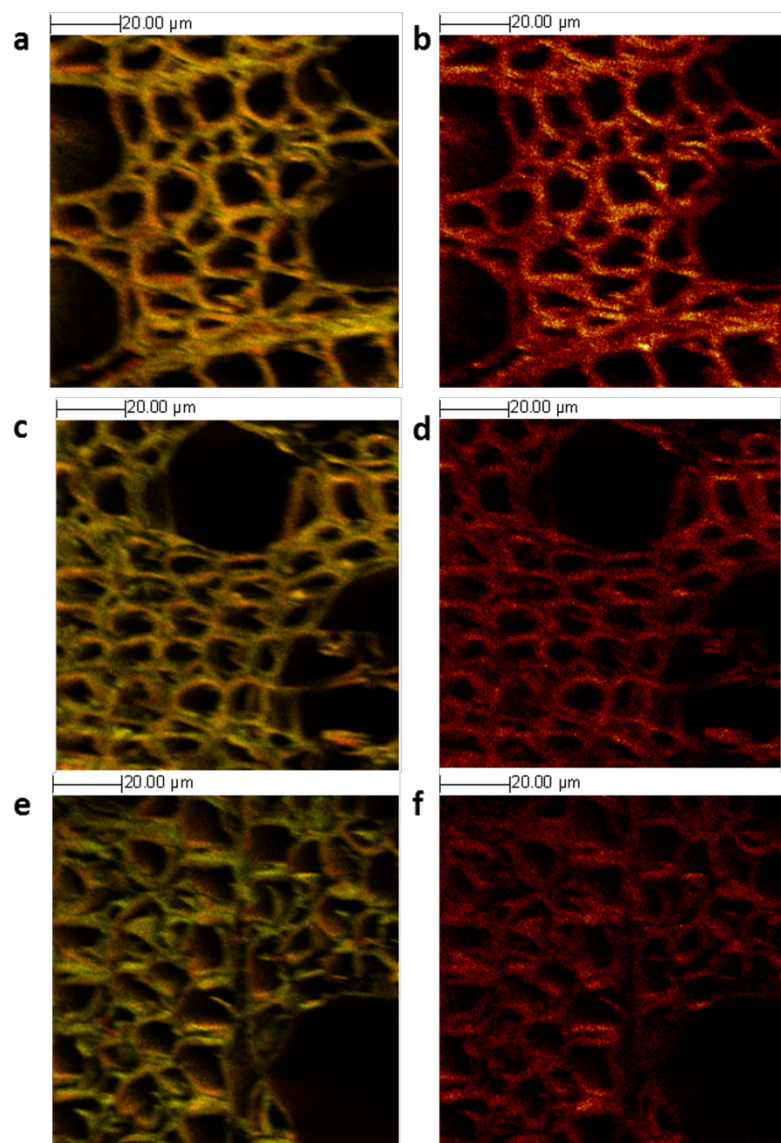
Figure 46. ToF-SIMS images of poplar cross-sections incubated with *C. bescii* in LOD medium at 75°C for a-b) 0 h, c-d) 72 h, and e-f) 288 h. The left column (a,c,e) show the lignin ions image (green) overlaid on the total ion image (red). The right column (b,d,f) is the cellulose ion image. Scale bar = 20 μm.

While the cellulose ion counts appear to remain relatively level over time (Figure 45 b), there was actually a decrease of 27% from 0 h to 288 h. This was supported with the ToF-SIMS images (Figure 46 b,d,f), where a decrease in cellulose ion intensity (brightness) occurs. In order to take into account the potential hemicellulose removal in addition to the cellulose, a more extensive analysis occurred to determine the sum of the polysaccharide (PS) and lignin (L) peaks.[165] The normalized ion intensities of approximately 30 ToF-SIMS peaks from each location were used to calculate the average polysaccharide peak fraction (PS/(PS+L)),[165] seen in Figure 47. There was a 41% and 48% difference in PS/(PS+L) from 0 h to 72h and 0 h to 288 h, respectively. The decrease in surface cellulose and polysaccharide peak fraction together with the sharp increase in surface lignin indicates that the microorganism is successfully removing both hemicellulose and cellulose.

Figure 47. The average ToF-SIMS polysaccharide peak fraction $(PS/(PS+L))$[165] for poplar cross-sections incubated with *C. bescii* for 0 h, 72 h, and 288 h.
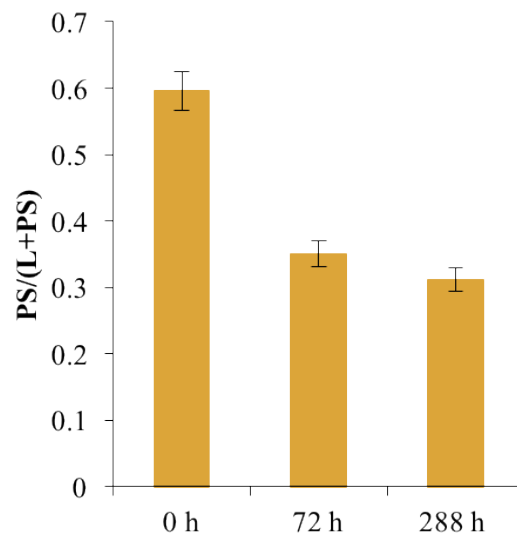
6.4 Conclusion

In this chapter, surface characterization techniques were used to determine the impact *C. bescii* has on the morphology and chemistry of poplar. Cell growth analysis determined that *C. bescii* possesses two growth phases. Therefore, the samples that underwent further analysis were at the end of the second growth phase (72 h) and at 288 h. Poplar cross-sections (80 μm thick) were also incubated in LOD medium at 75ºC for 0, 72, or 288 h, but without *C. bescii*.

SEM images revealed the formation of crevices within the cell walls of the *C. bescii* treated samples. The lack of similar physical deformations in the uninoculated samples showed that it was caused by the microorganism and not the temperature or medium.

Likewise, uninoculated controls proved that the temperature and medium did not alter the chemistry of the biomass. ToF-SIMS analysis revealed a decrease in cellulose ions and polysaccharide peak fractions as the incubation time increased, which indicates that *C. bescii* and its enzymes are targeting cellulose and hemicelluloses. As polysaccharides are removed from the surface, an increased amount of lignin becomes visible; this is seen in the significant increase in G lignin and S lignin by 150% and 190%, respectively. ToF-SIMS images reveal high concentrations of lignin within the middle lamella and the cell corners. While the detection of more lignin on the surface signify that the microorganism is removing hemicelluloses and cellulose, it could pose a problem by hindering further access to the sugars by *C. bescii*.

Overall, ToF-SIMS analysis provided additional insight into the consumption of untreated biomass by *C. bescii* through the surface chemistry. The greatest surface chemistry changes during the growth phases of *C. bescii* cells, as seen in the difference

between lignocellulosic ions at 0 h and 72 h. The microorganisms continue to degrade the biomass after 72 h, but not in great quantities. This indicates that the microorganism is most active and efficient while in its growth phases. It is possible that the increase of surface lignin inhibits access to polysaccharides and could contribute to the lack of continued cell growth. Similarly, *Clostridium thermocellum* ceases to hydrolyze lignocellulosic biomass despite approximately 70% of glucose remaining in the residue. Surface characterization techniques could provide a different perspective and determine if surface chemistry contributes to microbial fermentation cessation.

CHAPTER 7: MICROBIAL HYDROLYSIS OF *POPULUS* BIOMASS IS LIMITED BY CELLULOSE AND LIGNIN COLOCALIZATION AT THE PLANT CELL WALL SURFACE**

7.1   Introduction

Biorefinery valorization of lignocellulosic feedstock necessitates the deconstruction of plant cell wall biopolymers into simpler soluble components via the biological conversion platform. However, plant tissue presents an intrinsic resistance to deconstruction by purified enzymatic mixtures[210] or by specialized cellulolytic microbes,[64] which is largely due to the complex structure of the plant cell walls polymers, specifically cellulose and other heteropolysaccharides along with polyphenolic lignin.[211] While lignin has potential to add value to a biorefinery, at present it complicates biochemical processes for lignocellulosic biofuels.[212]

Undomesticated natural variants of *Populus deltoides* contain 16-28% w/w lignin, which has been negatively correlated to the extraction of sugars from non-pretreated biomass.[197] Conversely, increased cellulose exposure to hydrolytic agents has consistently been associated with improved solubilization. For example, mechanically cutting the biomass in a particular way, like tangential to the annual ring, can disrupt cellulose crystallinity and increase accessible surface area, leading to improved enzymatic hydrolysis.[213]

Clostridium thermocellum is a fast growing, anaerobic and thermophilic cellulolytic bacterium capable of growth on recalcitrant lignocellulosic material.[65] This well characterized biomass-hydrolyzing organism secretes a wide range of cell-bound and free glycoside hydrolases with an estimated 70 types of cellulosomal and 27 non-cellulosomal enzymes.[106, 214] Extracellular hydrolysis of biomass polysaccharides yields oligomeric hexose and pentose sugars, with the former utilized for energy and growth in anaerobic fermentation. The bacterium is known for efficient hydrolysis of crystalline cellulose to near-completion,[92, 215] and is capable of solubilizing 90% of xylan in dilute acid pretreated corn stover.[106] Although it is a robust cellulolytic microbe that commonly exceeds the performance of commercial fungal cellulase mixtures, it struggles to depolymerize the complex lignocellulose in the plant cell wall of typical energy grasses[102] and hard woods[100] without significant pretreatment of the feedstock.[103]

To realize the potential of feedstock bioconversion without costly or complex pre-treatments and to understand the major bottlenecks in lignocellulose solubilization, the cessation of microbial hydrolysis of juvenile poplar tissue by *C. thermocellum* and by cell-free microbial cellulase extracts, in the absence of known soluble inhibitors, was investigated. The changes in the colocalization and the relative proportion of lignin and cellulose on the surface of plant tissue was hypothesized to lead to the premature cessation of hydrolytic activity. To test this, 60 μm thick *C. thermocellum* hydrolyzed *Populus* sections were compared to non-hydrolyzed controls using quantitative fluorescence analysis in confocal laser scanning microscopy (CLSM) and surface chemical analysis in time-of-flight secondary ion mass spectrometry (TOF-SIMS).

7.2   Experimental Section

7.2.1   Biomass Substrate and Extraction

Populus deltoides were grown and harvested at ORNL, as described in Chapter 4 (4.1.2 Biomass Substrate). *Populus* stems (~4 cm length, ~2 cm diameter) were sectioned to 60 μm thick slices using a LEICA CM 1850 cryostat with an acetone-wiped disposable steel blade, as recounted in 4.1.2.2 Cryotome Sectioned Poplar Stems. *Populus* sections underwent Soxhlet extraction overnight with dichloromethane to remove the extractives in the lignocellulosic biomass (further details found in section 4.2.1 Soxhlet Extraction).

7.2.2   C. thermocellum Fermentation

The fermentation of extractive-free poplar cross-sections by freshly grown *Clostridium thermocellum* (ATCC 27405) in anaerobic prepared MTC media is described in Chapter 4 (4.2.4 *Clostridium thermocellum* Fermentation). Note the poplar discs are the only carbohydrate sources in the MTC media for the batch microbial reactions. The analysis of the liquid supernatant aliquots (detailed in section 4.3.3 Fermentation Products of *C. thermocellum*) tested for ethanol, acetic acid, formic acid, lactic acid, cellobiose, glucose, and xylose. Soluble sugars were not detectable in the incubated culture medium and only acetic acid and ethanol were produced by fermentation at above threshold concentrations.

7.2.3 Chemical Compositional Analysis

Average carbohydrate content of raw, control and fermented poplar biomass was determined using triplicates and processes adapted from NREL/TP-510-42618[187] and NREL/TP-510-42623[216] using a HPLC, as described in Chapter 4 (4.3.1 Chemical Compositional Analysis). Sugar degradation products (furfural and 5-hydroxymethyl furfural) were also quantified against known standards to ensure optimal acid solubilization with only trace amounts of degradative products detected.

7.2.4 Confocal Laser Scanning Microscopy

Control and fermented poplar samples were washed and rinsed three times in sterile saline solution. The cellulose in six controls and six fermented poplar cross-sections (randomly selected from biological replicate bottles) were fluorescently label and analyzed using a Zeiss LSM 710. Volume 3D images were reconstructed in Zen Black 2.1 and quantitative fluorescence and colocalization imaging was acquired and extracted using ImageJ in the Fiji distribution package. The Pearson's r[136] and Manders'[138] coefficients were calculate and the colocalization across plant cell walls and average fluorescence intensity were determined for the control and fermented samples. Processes were described in detailed in Chapter 4 (4.3.4 Confocal Laser Scanning Microscopy).

7.2.5 ToF-SIMS Analysis

A Bi_3^{2+} primary ion beam from a TOF·SIMS V instrument was randomly rastered across the *Populus* cross-sections and the ejected secondary ions analyzed in positive mode to produce a spectrum or an image, as described in Chapter 4 (4.3.7 ToF-SIMS Analysis). A total of 7 different locations on 2 control and 2 fermented cross-sections were analyzed and the normalized ion intensities for cellulose, S lignin, G lignin, and 25 additional ion peaks associated with polysaccharides and lignin (Table 18, peaks without protein fragment interference). The polysaccharide and lignin peak fractions are referred to as sugar and lignin normalized ion count fractions, respectively.

7.2.6 Enzymatic Hydrolysis

Biomass residues of fermented and control poplar were washed four times in sterile buffer (ph = 7.4) made of 50 mM Tris, 100 mM NaCl and 5 mM $CaCl_2$, in order to remove microbes and their enzymes from the surface - the absence of attached microbes in washed biomass was later verified by scanning electron microscopy. Enzymatic hydrolysis of the washed control and fermented poplar occurred with *C. thermocellum* cellulase exoproteome at 60 °C for 96 h, as described in Chapter 4 (4.2.5 Enzymatic Hydrolysis). To account for the potential presence of oligomeric sugar hydrolysates, aliquots of the hydrolysis supernatant were also acid-hydrolyzed with 4% H_2SO_4 for 1 h at 120 °C then neutralized to pH ~2.1 with 50% w/w NaOH. Resulting monosaccharides were quantified by HPLC in triplicates (7.2.3 Chemical Compositional Analysis). No

significant increase in total glucose was detected with this extra acid-hydrolysis of solutes; however, additional xylose was detected from supernatant xylooligomers and was reported accordingly.

7.3   Results

During growth on crystalline cellulose, *C. thermocellum* performs near-complete (95%) solubilization of typical 5 g/L Avicel loadings,[92] and similarly achieved 93% solubilization of industrially-relevant concentrations of 100 g/L Avicel.[215] However, due in part to its inability to deconstruct the lignin in biomass it performs only partial hydrolysis of raw lignocellulosic feedstock.

Partial hydrolytic activity of raw lignocellulose is common among cellulolytic microbes investigated for biorefinery applications, and microbial hydrolysis compares favorably with the performance of purified commercial fungal enzymes. Although the basis for limited hydrolysis is not fully elucidated, and while the causality may be situational, distinct general justifications have been demonstrated. Firstly, cellulases are inhibited by sugar hydrolysates[210, 217] and potentially by lignin-derived phenolic acids (e.g. gallic, vanillic, etc.).[218] Contraction of hydrolytic activity may also be linked to the inhibition of microbial metabolism by biomass degradation products – carboxylic acids, heterocyclic aldehydes and phenolic derivatives.[219] *C. thermocellum* can solubilize xylan to pentoses, which have recently been shown to accumulate intracellularly and inhibit growth and end-product formation in defined media[220] and to accumulate intracellularly in switchgrass fermentations.[221] Secondly, lignin in biomass provides sites for non-specific

and non-productive binding of glycoside hydrolases which restricts access to the cell wall sugars and leads to loss of activity.[222] Lastly, cellulases encounter a physical, mechanical barrier to carbohydrate accessibility. In this quantitative study, microbial inhibition was separated from enzymatic inhibition though our use of controls and sequential treatments. The latter two constraints to hydrolysis are intrinsic to the properties of ordinary biomass, namely the synthesis of lignin in the plant cell wall structure.

This study utilizes juvenile *Populus deltoides* stems sectioned in uniform slices of 60 μm thickness (raw poplar) to understand how biomass recalcitrance contributes to the limited hydrolysis by *C. thermocellum.* This was accomplished by incubating extractive-free poplar at 60 °C for 92 h with either microbe-free sterile media (control poplar) or with biomass-fermenting *Clostridium thermocellum* 27405 cells (fermented poplar), and analyzing the residual biomass of these two treatments for content and structure. Here, extractive-free biomass is used to represent non-pretreated poplar. Since biomass extractives and ash – as non-structural elements – make up less than 5% of the dry weight content;[7] their removal produced only a small increase in the relative proportion of carbohydrates in control biomass, as seen in the carbohydrate content of non-extracted raw tissue compared to the extractive-free control poplar (Table 22).

Table 22. Relative polysaccharide content in sectioned poplar biomass.

	Glucan	Xylan	Galactan	Arabinan	Mannan
Raw poplar (%)	42.9 (±1.4)	13.3 (±0.8)	2.4 (±0.1)	0.7 (±0.0)	1.7 (±0.0)
Control poplar (%)	45.5 (±0.9)	14.1 (±0.4)	2.3 (±0.2)	0.6 (±0.1)	1.9 (±0.0)
Fermented poplar (%)	39.5 (±1.1)	16.5 (±0.4)	2.3 (±0.2)	0.7 (±0.1)	1.5 (±0.1)

Sugars in %, g/g biomass (± standard deviation) in the initial unprocessed biomass (raw poplar) and in the extractive-free biomass incubated in buffered growth-medium without microbes (control poplar) and with *Clostridium thermocellum* (fermented poplar) for 92 h at 60°C. Fermentations and quantitative analysis of sugar content performed in triplicate biological replication.

7.3.1 Wet Chemical Analysis

As a result of its intrinsic recalcitrant nature of lignocellulose, microbial hydrolysis and fermentation of extractive-free poplar produced only a modest ($p < 0.05$) reduction in the relative glucan content of the residual fermented tissue (Table 22), which indicates that the residual poplar tissue still retained most of its bulk chemical composition. Compared to control poplar, microbial hydrolysis solubilized 17% (w/w) of the total solids (on a dry weight basis), the majority (83%) of which was glucan. Literature has reported 20% total solids solubilization of non-pretreated poplar[100] – with an estimated 35% glucan and 25% xylan hydrolysis. The predominant removal of glucan in this study owed in part to the preservation of the plant cell wall structure during cryotome sectioning, which exposed

polysaccharide-rich regions in the S2 and S3 layers (lumen side) of secondary cell walls (Figure 48).[190, 223]

Table 23. Microbial solubilization of polysaccharides in extractive-free *Populus* after incubation for 92 h at 60°C.

	Control Biomass (mg)	Fermented Biomass (mg)	Percent Reduction
Total Glucose	152.9	110.1	28.0%
Total Xylose	48.3	47.2	2.4%
Total Galactose	7.6	6.3	17.8%
Total Arabinose	2.2	2.0	7.5%
Total Mannose	6.3	4.3	32.5%
Total Six Carbon	166.9	120.7	27.7%
Total Five Carbon	50.5	49.2	2.7%
Total Sugars	217.4	169.8	21.9%

Total sugars (mg, monomeric equivalent) in biomass incubated with *Clostridium thermocellum* (fermented biomass) compared to biomass incubated in sterile culture media (control biomass).

Overall, the limited hydrolysis removed 22% of the total sugar equivalents supplied in the lignocellulosic material, with predominant consumption of six-carbon sugars (glucose, galactose, and mannose) and to a lesser degree of five-carbon sugars (Table 23). We note that glucan and mannan recorded the similar percent reduction, which may be related to the closer association between these polysaccharides in the secondary cell wall.
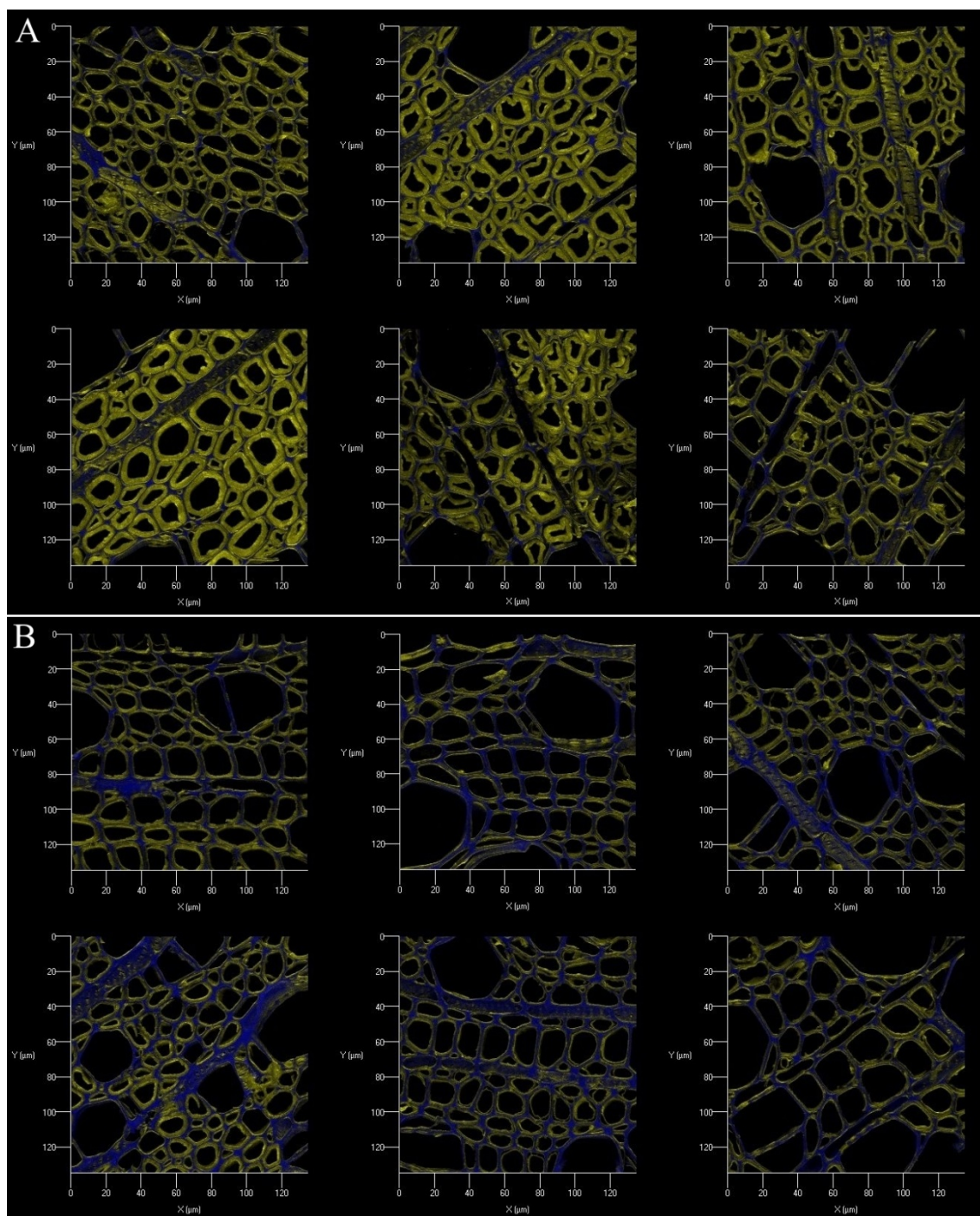
Figure 48. Confocal laser scanning micrographs of control (A) and fermented biomass (B) of cross-sectioned *Populus deltoides* showed the post-fermentation reduction of cellulose signal (yellow) in secondary cell walls, which revealed undigested lignin (blue). Cellulose labeled with Direct Red 23 (formerly, Pontamine Fast Scarlet 4B), lignin was autofluorescent.

Microbial utilization of solubilized glucan yielded detectable fermentation products in typical amounts and ratios (Figure 49) with ethanol calculated at 38% of the maximum theoretical yield (on a soluble glucan basis) – a typical value for wild-type strains in optimal growth conditions.[95] Soluble sugars were not detected and did not accumulate in the fermentation supernatant between the slowdown in fermentation output (48 h) and the end-point measurement (92 h), indicating non-inhibited microbial metabolism, which was not decoupled from hydrolysis. The bioconversion slowdown was therefore due to a hydrolytic bottleneck.

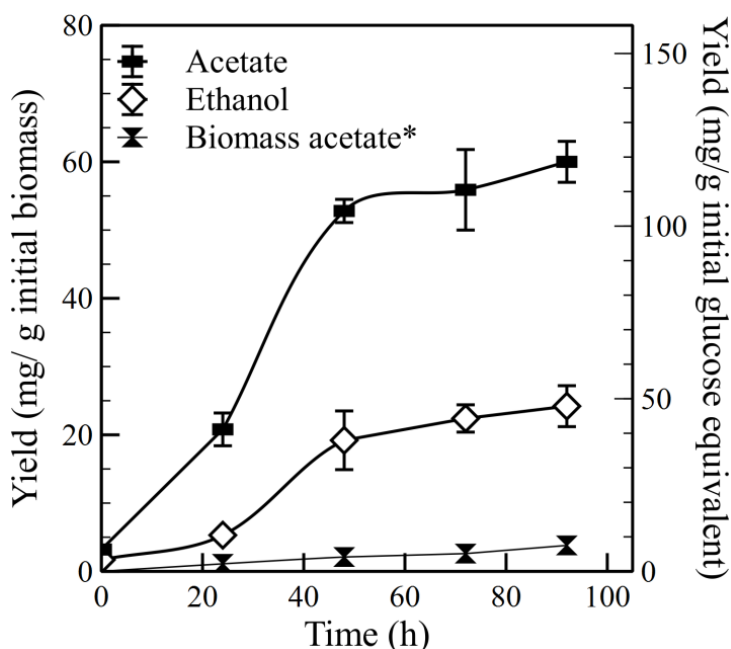Figure 49. Fermentation product yields. Microbial fermentation of extractive-free *Populus* incubated with *C. thermocellum* for 92 h at 60 °C yielded ethanol and acetate at a ratio typical of the bacterium wild-type phenotype. Small amounts of biomass-derived acetate were measured for control poplar sections incubated with sterile medium. Biological replication n = 3; error bars represent one standard deviation.

In a previous study,[100] metabolic inhibitors towards *C. thermocellum* were not detected when grown on non-pretreated *Populus* at similar or higher loadings to the current analysis and our fermentative performance further indicated unrestricted metabolism. While the initial observations of biomass solubilization (Table 23) and microbial fermentation yields (Figure 49) indicated a productive microbial metabolism and otherwise normal growth pattern, the possibility of a solubilization bottleneck due to a stalled cellular metabolism or an enzymatic inhibition was tested. To that end, fermented and control biomass was recovered and cleaned of cells and cellulases by gentle repeated washing with sterile saline solution. The washed biomass was then incubated for four days at 60°C with the purified (cell-free) cellulase exoproteome of *C. thermocellum* at 20 mg protein/g biomass and commercial *Aspergillus niger β*-glucosidase to test whether hydrolysis resumes equally unobstructed in both the previously fermented and the control feedstock. Cellulase inhibition by soluble components was invalidated by the results of Figure 50, where hydrolytic activity on washed residual biomass could not be significantly restored with cell-free cellulase preparations although the biomass still retained 72% of the original glucan content when compared to the control sample.
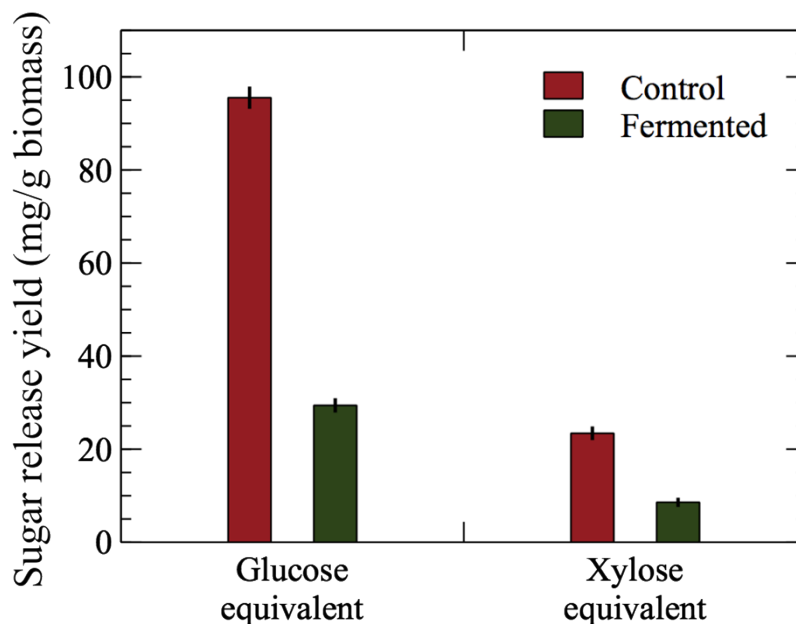
Figure 50. Sugar release from further hydrolysis of the control and fermented *Populus* biomass with purified, cell-free extracts of *C. thermocellum* cellulases. The a-priori microbially-fermented biomass with reduced surface cellulose and higher surface lignin yielded significantly lower sugars from further enzymatic hydrolysis compared to control biomass that was not "depleted" by microbes. Biological replication n = 5; error bars represent one standard deviation.

7.3.2 Colocalization of Lignin and Surface Characterization

Colocalization of lignin and cellulose by CLMS along with spatial mapping and ion counts by ToF-SIMS of the control and fermented poplar tissues were used to determine if the biopolymer network in the cell wall structure contribute to the limited hydrolysis. Both samples were washed and exposed to Direct Red 23 (DR23, formerly Pontamine Fast Scarlet 4B), a dye with high selectivity for β-1,4 linked polysaccharides and highly fluorescent upon cellulose binding, while significantly less fluorescent when bound to xyloglucan.[132, 134] In confocal laser scanning microscopy, DR23 emission was captured

in the 550-625 nm visible spectral band under λ_{exc}= 488 nm excitation. Lignin in plant tissue samples was visualized by autofluoresence under λ_{exc}= 405 nm excitation in the 410-480 nm emission band. In the experimental conditions selected, lignin and cellulose-bound DR23 fluorescent signals were independent and not cross-interfering. This was confirmed in spectral scans by the absence of cross-channel talk between the two, i.e., at λ_{exc}= 405 nm lignin had no significant emission above 550 nm, and at λ_{exc}= 488 nm no lignin autofluorescence was detected which is supported by existing literature.[132, 134]

Table 24. Colocalization coefficients of lignin and cellulose in control and fermented

Control poplar	Pearson's correlation, r	Manders split coefficient	Fermented poplar	Pearson's correlation, r	Manders split coefficient
1	0.28	0.80	1	0.27	0.84
2	0.07	0.55	2	0.51	0.94
3	0.24	0.76	3	0.50	0.95
4	0.00	0.47	4	0.54	0.96
5	0.14	0.57	5	0.56	0.96
6	0.36	0.85	6	0.39	0.87
Avg	**0.18**	**0.67**	**Avg**	**0.46**	**0.92**

Pearson's r coefficient represents the intensity correlation of colocalizing pixels; Manders split coefficient represents the fraction of cellulose-DR23 signal that had an overlapped lignin signal. Measurements made in z-stacks (of five frames) from images of the randomly sampled poplar presented in Figure 48.

poplar.

In the cross-sections, control poplar displayed glucan-rich (yellow) secondary cell walls with lignin-rich (blue) middle lamella between and at the corner of adjacent cells (Figure 48 A). In several of the examples provided, cellulose-rich G-layer formations may be observed, a common feature of poplar under normal growth conditions.[190] Fermented poplar showed a visually discernible reduction in cellulose signal near the lumen and a compensatory increase in lignin visibility across cells walls (Figure 48 B). This was confirmed in quantitative fluorescence and colocalization analysis by a significant ($p <$ 0.05) increase in the pixel intensity spatial correlation, i.e., the Pearson's r coefficient,[136] between lignin and cellulose-DR23 signals in the fermented poplar samples (Table 24).

The Manders split coefficients,[138] representative of the fraction of cellulose-DR23 signal that had an overlapping lignin signal, significantly increased ($p < 0.05$) in fermented poplar to near maximum values with an average 0.92 fractional overlap (Table 24). To better visualize the lignin colocalization with cellulose through secondary cell walls and in particular at the lumen surface, fluorescent intensities were also mapped across cell walls (Figure 51) at 18 randomly selected positions (Figure 52). The localization axis of each box (x-axis, in Figure 51) cut across three adjacent plant cells, and intersected cell walls (from lumen to lumen, e.g., arrows) and middle lamellas at a perpendicular angle.
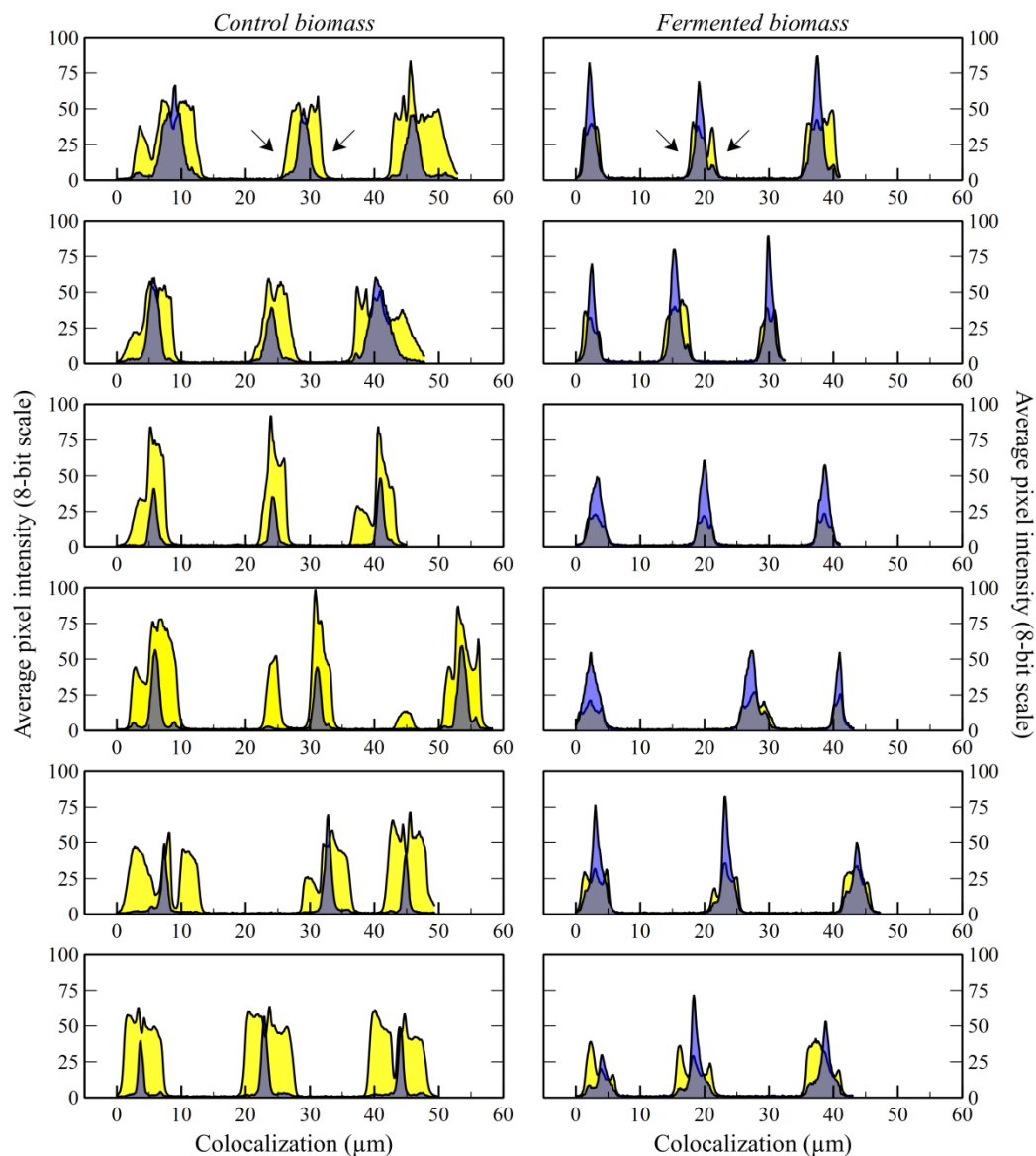
Figure 51. Colocalization of cellulose and lignin in plant cell walls of control (left) and fermented biomass (right). Colocalization measured across walls of adjacent plant cells (from lumen to lumen – e.g., arrows) and each histogram box captures the transverse sectioning of three cell wall regions. Control samples showed cellulose-rich regions on the lumen side (i.e., at secondary cell wall surface) and strong lignin signal intensity in the central region between adjacent cells (i.e., in the middle lamella). Post-fermentation, cellulose and lignin signals were well colocalized with high intensity on the lumen side (i.e., at cell wall surface).

In control poplar, a strong lignin signal of the middle lamella was flanked on each side by strong cellulose-DR23 fluorescence towards the lumen. Lignin was colocalized with cellulose at low intensity. In fermented samples, lignin strongly colocalized with cellulose signal throughout secondary cell walls up to the lumen side, indicative of increased exposure of the lignin polymer and a decline in surface cellulose.

Quantitative fluorescence of spatially-resolved signals (i.e., averaged pixel intensities normalized to total counts of pixels with a minimum threshold value, on an 8-bit scale) for each detection channel (in $n = 6$ randomly captured CLSM scans for each treatment, Figure 52), showed little change in DR23 fluorescence ($p = 0.07$) and an estimated 23% increase ($p < 0.05$) in lignin autofluorescence (Figure 53). This indicated that cellulose was similarly accessible after microbial hydrolysis to DR23 binding, within statistical error, which was in line with previous reports that document relatively unchanged chemical bond compositions in carbohydrates following enzymatic hydrolyses.[224] The increased signal visibility for the intrinsically autofluorescent lignin was caused by the removal of surface carbohydrates which obstructed lignin emission, and therefore denotes a higher exposure of superficial lignin.

Cell wall thickness (from lumen to lumen) was highly variable in each treatment (Figure 53); however, within the $n = 18$ randomly selected measurements, secondary cell wall thinning due to cellulose removal was found within statistical significance ($p < 0.05$). Variation in lignin signal location across the cell wall was minimal.
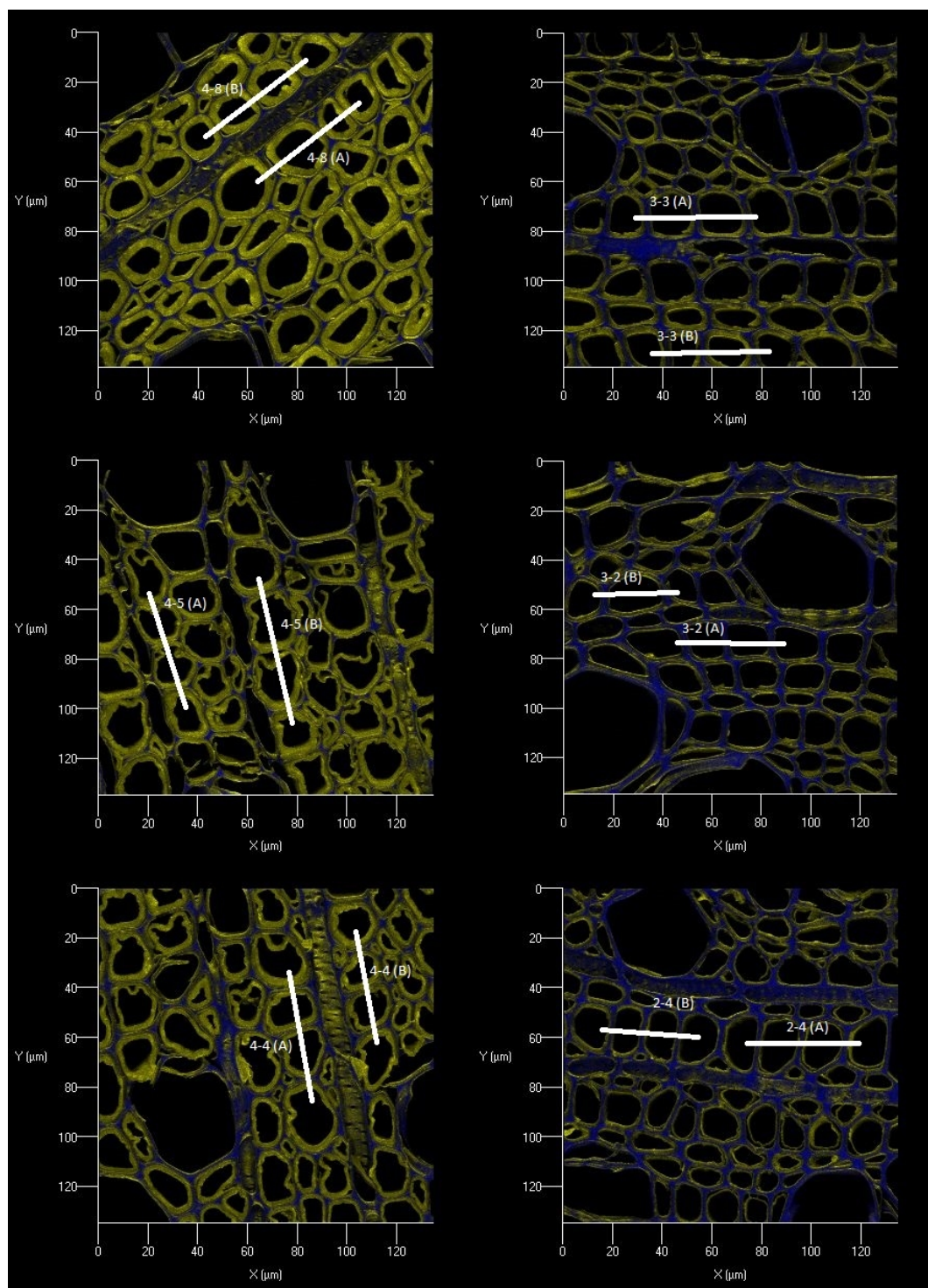
Figure 52. Microtome sections of poplar analyzed for co-localization of cellulose and lignin across cell walls (white lines). Control biomass (left side images) and fermented biomass (right side images).
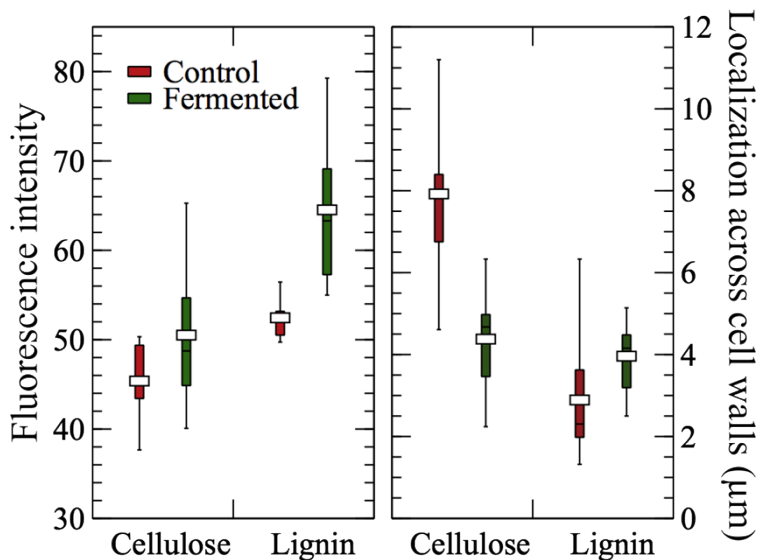

Figure 53. Average fluorescence intensity of spatially-resolved cellulose and lignin signals (left), as exemplified in Figure 48, showed the increased visibility of lignin autofluorescence in post-fermentation samples due to surface cellulose removal (left); and estimated localization of cellulose and lignin across the plant cell walls from lumen to lumen (as shown in Figure 51) confirmed a significant thinning in cellulose presence and the persistence of un-digestible lignin. Box plots of measurements in n = 6 (left) and n = 18 (right) independent and randomly selected samples, whiskers represent minimum and maximum, vertical solid bars are the interquartile range and the horizontal markers are the means.

Chemical imaging by ToF-SIMS quantifies and maps the distribution of surface chemical species,[165] which are detected and represented by their ion signatures. This was exemplified as heat maps of representative ions normalized to the total ion counts (Figure 54), where under visual inspection, cellulose detection decreased while S and G lignin increased post-fermentation. Comparing fermented and control poplar tissue in a more quantitative approach, of n = 7 randomly selected regions of poplar cross-sections,

revealed an average 49% reduction of cellulose normalized ion counts, and 30% and 11%

increase in S- and G- lignin normalized counts, respectively, in the cell walls of

microbially-hydrolyzed samples (Figure 55). An extended analysis of 30 ion signatures of

polysaccharides and lignin chemical species revealed the inversion of the relative

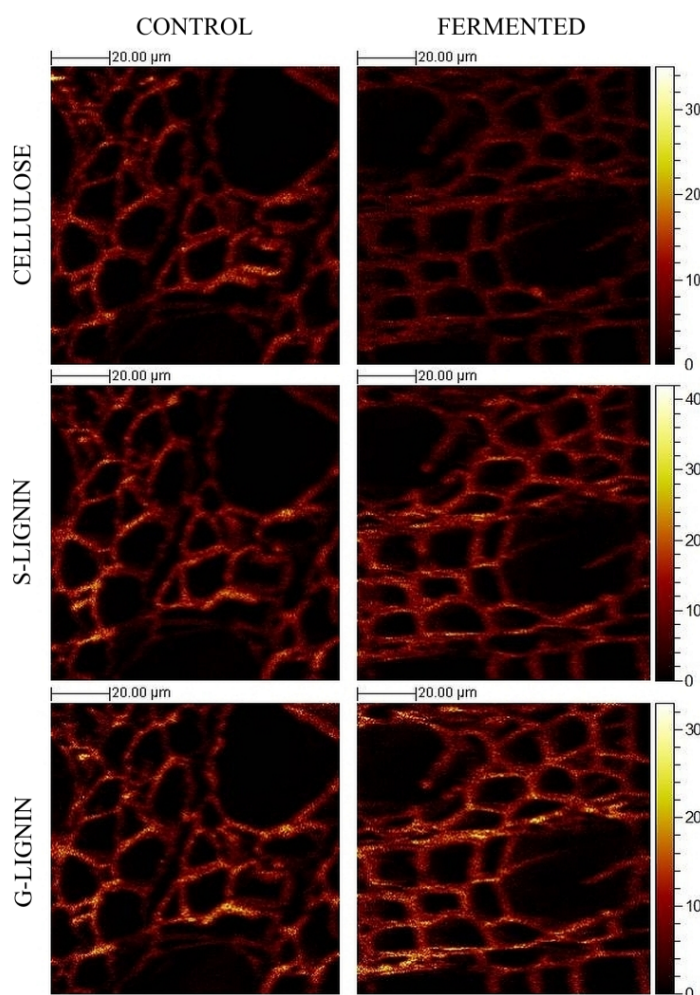proportions of the two groups, post-fermentation (Figure 55).

Figure 54. Sample micrographs obtained by ToF-SIMS of control (left) and fermented (right) biomass of *Populus* cross-sections showed the post-fermentation reduction in surface cellulose and the compensatory increase in S and G lignin. The Tof-SIMS technique quantifies and maps the presence of chemical species at sample surface.
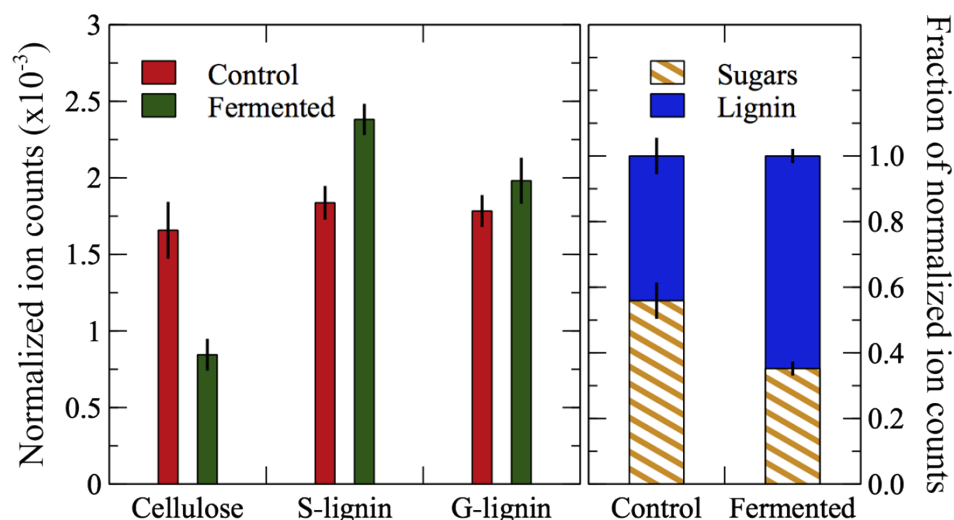
Figure 55. ToF-SIMS analysis of chemical species at the sample surface revealed a marked decrease in surface cellulose and a compensatory increase in surface S and G lignins at the end-point of microbial conversion (left); Sum of 30 ion count signatures of known polysaccharide and lignin chemical species represented as normalized fraction showed the inversion of their relative proportion post-fermentation (right). Data averaged across n = 7 randomly selected samples. Ion counts of each chemical species were normalized against total sample ion counts.

The total ion signatures of surface lignin species (Figure 55) showed an increase in relative proportion from 44% in control to 65% in fermented tissue. Limitation to hydrolysis occurred when the surface cellulose decreased to approximately half of its initial value. These are surprising novel observations of feedstock surface chemistry, which point to the severity of lignin interfering with sugar accessibility. Even results from further hydrolyzed microbially-processed biomass (Figure 50) confirmed an enzymatic bottleneck due to changes in biomass properties demonstrated above.

On the principle that increased lignin content in bulk tissue of milled poplar strongly correlates with reduced enzymatic solubilization,[197] we further provide direct, quantitative evidence that microbial hydrolysis was suspended by higher exposure of the lignin to the feedstock surface after the initial limited removal of accessible carbohydrates. We attempted cellulase adsorption measurements by BCA assay on fermented and control biomass without success due to interferences from matrix components (e.g., reduced sugars). Although we cannot comment whether enzyme binding was affected by higher lignin exposure we have demonstrated nonetheless that cellulases were significantly less productive.

7.4   Conclusion

In this chapter, the limited solubilization of *Populus deltoides* by the cellulolytic thermophile *Clostridium thermocellum* in the absence of solute inhibitors was investigated. Juvenile poplar cross-sections (60 μm thick) were fermented with and without *C. thermocellum*. The limit hydrolysis of the microbially-processed biomass along with the non-inhibiting fermentation supernatant confirms that the enzymatic bottleneck was not caused by soluble inhibitory compounds.

The decrease in available surface cellulose post-fermentation was associated with the increase in surface lignin and enzymatic inhibition of hydrolysis of non-pretreated poplar which was determined using quantitative analysis CLSM fluorescence images and ToF-SIMS. Compared to control samples, fermented poplar revealed that the hydrolysis of carbohydrates in cell walls ceased prematurely as lignin presence increased at the surface.

In quantitative fluorescence colocalization analysis by CLSM, the Manders' coefficient of fractional overlap between lignin and cellulose signals increased from an average of 0.67 to a near-maximum 0.92 in fermented tissue. Chemical imaging by ToF-SIMS revealed a 49% decline in surface cellulose and a compensatory 30% and 11% increase in surface S- and G- lignin, respectively. Although 72% of the initial glucan was still present in the lignocellulose matrix of this feedstock, subsequent treatments with cell-free purified cellulases did not significantly restore hydrolysis. This confirmed that biomass surfaces had become non-productive for the *C. thermocellum* hydrolytic exoproteome.

Therefore, microbial hydrolysis of raw woody feedstock was arrested prematurely by a critical shift in the ratio of carbohydrates and lignin at the biomass surface whereby the internal bulk regions of the plant tissue may retain relatively unaltered chemical composition. This study revealed how biomass recalcitrance can inhibit microbial fermentation and that *C. thermocellum* can be sensitive to the chemical changes occurring on the biomass surface. Surface characterization provides a new way to study plant tissue properties that impact biological solubilization.

CHAPTER 8: CONCLUSION

Lignocellulosic biomass is a valuable feedstock for biofuel production that can reduce the amount of fossil fuel-based transportation fuel consumed. The challenge of utilizing lignocellulosic biomass lies in understanding and overcoming its natural recalcitrance. Most research studies employ chemical and/or biological processes to reduce the recalcitrance and characterize the biomass residue with bulk chemical analysis methods to determine the changes that occurred. These analytical tools can provide important information about the biomass recalcitrance and the treatment process, but they do not allow for spatial distribution of key chemical components on the surface of the biomass residue. The chemical ions from the surface and their location within the cell wall can provide insightful information that is not available through more traditional analysis methods.

One goal of this thesis was to demonstrate the advantages of surface characterization during biomass utilization studies, including microbial fermentations, and to determine how surface chemistry and selected microorganisms impact each other. A comprehensive study occurred comparing ToF-SIMS surface analysis with traditional bulk chemical analyses of ammonia and organosolv pretreated poplar. While the ToF-SIMS polysaccharide and lignin content did not correlate well with the bulk data, both the surface and bulk cellulose possessed a similar trend (untreated < ammonia-treated < organosolv-treated). The samples with greater surface cellulose content resulted in higher glucose release during enzymatic hydrolysis. There was also a positive correlation between the lignin S/G ratio from ToF-SIMS and NMR. In this case, ToF-SIMS analysis

was revealed to be a good predictor of ordering samples from lowest to highest cellulose content, lignin S/G ratio, and glucose release. While the polysaccharide and lignin content on the surface differed from the bulk chemistry, this indicates that chemical changes due to pretreatments could be more severe on the surface than within the bulk tissue.

Not only can surface characterization be applied to pretreatment studies, but it is capable of providing insight into the workings of potential CBP microorganisms on lignocellulosic biomass. Interestingly, *C. bescii* possess two growth phases on untreated poplar. Previous *C. bescii* studies focused on the initial growth phase up to 24 h on untreated biomass; therefore, the impact *C. bescii* has on the physical structure and chemistry of poplar cross-sections after the second growth phase was evaluated primarily by SEM and ToF-SIMS. SEM analysis of uninoculated control and *C. bescii* treated samples revealed the microorganism disrupts the plant cell wall by forming crevices and continues this destruction well after the end of the second growth phase. *C. bescii* does appear to be targeting polysaccharides on the surface allowing for an increase in detectable lignin. This increase of lignin can inhibit cellulose and hemicellulose accessibility and possibly impact the cell growth and/or activity, as seen in the minor surface chemistry changes between samples incubated for 72 h and 288 h. *C. thermocellum* partially hydrolyzed untreated poplar; microbial hydrolysis ceased despite 72% of initial bulk glucan remaining in the sample and 50% of cellulose ions detected on the sample surface.

Another objective was to determine the impact surface chemistry has on enzymatic hydrolysis and microbial fermentations. With pretreated poplar, low lignin content, high

cellulose content, and high lignin S/G ratio on the surface improved enzymatic hydrolysis. The limited hydrolysis of *C. thermocellum* is a great concern for developing efficient CBP procedures with this microorganism. CLSM and ToF-SIMS were used to investigate how the surface chemistry of poplar might be impacting the efficiency of the microorganism. As expected, cellulose and polysaccharide content decreased on the surface of the fermented samples, while lignin content increased. Product yield and enzymatic hydrolysis failed to reveal any production of metabolic inhibitors or that any solubilized biomass components were hindering the microorganism. It was finally determined that the increase of surface lignin on the poplar along with the decrease of surface polysaccharides were contributing factors towards the hydrolysis cessation. At this time, efficient biomass conversion strategies will require the incorporation of a depolymerization step in order to utilize more of the biomass sugars.

In conclusion, biomass recalcitrance is a major barrier towards cost and time efficient biofuel production from lignocellulosic biomass. Surface characterization provides an important, but different point of view towards understanding the changes occurring to biomass chemistry during a chemical or microbial treatment. This type of characterization technique can provide additional information about the biomass that cannot be detected through bulk characterization methods. Instruments, like the ToF-SIMS, can greatly assist in advancing microbial research towards identifying or engineering an efficient CBP microorganism that produces large quantities of bioethanol from biomass.

CHAPTER 9: RECOMMENDATIONS FOR FUTURE WORK

The surface analytical characterization techniques discussed in this dissertation have greatly contributed toward obtaining comprehensive understanding of chemical pretreatments (ammonia and organosolv) and microbial treatments (*C. bescii* and *C. thermocellum*). The spatial mapping of lignocellulosic ions and corresponding ion counts via ToF-SIMS can provide additional insight into biomass utilization studies. There are several additional projects worth pursuing in order to improve our understanding of the impact pretreatments and bioconversions have on the biomass surface chemistry.

As addressed in Chapter 3, extractives are typically removed from a biomass sample prior to ToF-SIMS analysis. While some ToF-SIMS studies have analyzed biomass extractives,[158, 175] extractives have been shown to mask the detection of cellulose and lignin secondary ions.[172] Specifically, low molecular weight ion peaks (< 200 Da) of saturated hydrocarbons are characteristic not only of fatty acids, but lignin aromatic hydrocarbons.[158] Different polarity solvents solubilize different compounds; for example, dichloromethane is a medium polarity solvent capable of removing intermediate polarity compounds, like some alkaloids and flavonoids.[225] The higher polarity solvents, like acetone, ethanol, and water,[225] might remove more extractives, but they can cause structural changes to lignin, hemicellulose, and cellulose. Various extractive techniques have been used in ToF-SIMS studies, including acetone,[10, 159] dichloromethane,[12, 183] and a combination of water, ethanol, and acetone or toluene.[158, 172] Developing a standard extraction technique for lignocellulosic biomass for ToF-SIMS analysis is needed.

Lignin S/G ratio on the surface and in the bulk material of ammonia and organosolv pretreated poplar revealed a positive correlation between ToF-SIMS and NMR analysis (Chapter 5). Conducting a comprehensive pretreatment study should provide further insight into the connection between the surface and the bulk lignin S/G ratio. For example, determining the lignin S/G ratio via ToF-SIMS and NMR for LHW, DA, alkaline (NaOH), and organosolv pretreated poplar at various severities, reaction times, and temperatures should determine if ToF-SIMS can accurately predict the lignin S/G ratio in preliminary studies. While the ToF-SIMS would not be capable of providing the same lignin S/G ratio value as the other methods, it could rank the samples from least to greatest ratio.

Surface lignin can inhibit cellulose and hemicellulose accessibility, which could impact *C. bescii* cell growth (Chapter 6). Implementing a two-step pretreatment and microbial study should provide insight into the relationship between surface lignin and cell growth. An alkaline or dilute acid pretreatment of a biomass at various severities or reaction conditions should produce samples that retain different amounts of lignin. *C. bescii* cell growth would be monitored during incubation with pretreated samples, and the surface lignin of pretreated and pretreated + *C. bescii* samples should be analyzed by ToF-SIMS.

One difficulty with biomass utilization studies is the connection between the production of laboratory samples and the large-scale industrial production. For example, industry will never cut biomass to 60 μm thick sections or mill biomass to less than 0.42 mm. An interesting study would be to ferment larger wood chips with *C. thermocellum*. ToF-SIMS is capable of removing layers of the surface and could be used to determine a depth profile of the lignocellulosic ions. This analysis could provide insight into how *C.*

thermocellum penetrates the depth of the wood chip and its impact on the biomass chemistry further away from the surface.

APPENDIX A. COPYRIGHT PERMISSION

A.1 Acknowledgements for Figure Reprints

Figure 3 adapted by permission from Macmillan Publishers Ltd: Nature (Rubin, E. M., Genomics of cellulosic biofuels. *Nature* **2008,** *454* (7206), 841-845), copyright (2008).

Figure 13 reprinted with permission from Kumar, P.; Barrett, D. M.; Delwiche, M. J.; Stroeve, P., Methods for pretreatment of lignocellulosic biomass for efficient hydrolysis and biofuel production. *Industrial & Engineering Chemistry Research* **2009,** *48* (8), 3713-3729. Copyright (2009) American Chemical Society.

Figure 14 reprinted with permission from Dumitrache, A.; Akinosho, H.; Rodriguez, M.; Meng, X.; Yoo, C. G.; Natzke, J.; Engle, N. L.; Sykes, R. W.; Tschaplinski, T. J.; Muchero, W.; Ragauskas, A. J.; Davison, B. H.; Brown, S. D., Consolidated bioprocessing of Populus using Clostridium (Ruminiclostridium) thermocellum: a case study on the impact of lignin composition and structure. *Biotechnology for Biofuels* **2016,** *9* (31), 1-14. Copyright (2013) American Chemical Society.

Figure 15 reprinted with permission from Akinosho, H.; Yee, K.; Close, D.; Ragauskas, A., The emergence of *Clostridium thermocellum* as a high utility candidate for consolidated bioprocessing applications. *Frontiers in Chemistry* **2014,** *2*, 1-18 and CC BY 4.0.

Figure 16 reprinted from Olson, D. G.; Lynd, L. R., Transformation of Clostridium thermocellum by electroporation. In *Cellulases*, Abeson, J. N.; Simon, M. I.; Colowick, S. P.; Kaplan, N. O., Eds. Elsevier: San Diego, CA, Vol. 510, pp 317-330, Copyright (2012), with permission from Elsevier.

Figure 17 reprinted with permission from Biswas, R.; Zheng, T.; Olson, D. G.; Lynd, L. R.; Guss, A. M., Elimination of hydrogenase active site assembly blocks H 2 production and increases ethanol yield in Clostridium thermocellum. *Biotechnology for Biofuels* **2015,** *8* (20), 1-8 and CC BY 4.0

Figure 18 reprinted from Dam, P.; Kataeva, I.; Yang, S. J.; Zhou, F. F.; Yin, Y. B.; Chou, W. C.; Poole, F. L.; Westpheling, J.; Hettich, R.; Giannone, R.; Lewis, D. L.; Kelly, R.; Gilbert, H. J.; Henrissat, B.; Xu, Y.; Adams, M. W. W., Insights into plant biomass conversion from the genome of the anaerobic thermophilic bacterium

Caldicellulosiruptor bescii DSM 6725. *Nucleic Acids Research* **2011,** *39* (8), 3240-3254, by permission of Nuceic Acids research and Oxford University Press.

Figure 20 reprinted from Brunecky, R.; Alahuhta, M.; Xu, Q.; Donohoe, B. S.; Crowley, M. F.; Kataeva, I. A.; Yang, S.-J.; Resch, M. G.; Adams, M. W.; Lunin, V. V., Revealing nature's cellulase diversity: the digestion mechanism of Caldicellulosiruptor bescii CelA. *Science* **2013,** *342* (6165), 1513-1516, with permission from AAAS.

Figure 21 reprinted from Brunecky, R.; Alahuhta, M.; Xu, Q.; Donohoe, B. S.; Crowley, M. F.; Kataeva, I. A.; Yang, S.-J.; Resch, M. G.; Adams, M. W.; Lunin, V. V., Revealing nature's cellulase diversity: the digestion mechanism of Caldicellulosiruptor bescii CelA. *Science* **2013,** *342* (6165), 1513-1516, with permission from AAAS.

Figure 22 reprinted with permission from Chen, S.; Zhang, X.; Ling, Z.; Xu, F., Characterization of the micromorphology and topochemistry of poplar wood during mild ionic liquid pretreatment for improving enzymatic saccharification. *Molecules* **2017,** *22* (115), 1-15 and CC BY 4.0.

Figure 23 reprinted from Chundawat, S. P.; Donohoe, B. S.; da Costa Sousa, L.; Elder, T.; Agarwal, U. P.; Lu, F.; Ralph, J.; Himmel, M. E.; Balan, V.; Dale, B. E., Multi-scale visualization and characterization of lignocellulosic plant cell wall deconstruction during thermochemical pretreatment. *Energy & Environmental Science* **2011,** *4* (3), 973-984 with permission of The Royal Society of Chemistry.

Figure 24 reprinted from Belu, A. M.; Graham, D. J.; Castner, D. G., Time-of-flight secondary ion mass spectrometry: techniques and applications for the characterization of biomaterial surfaces. *Biomaterials, 24* (21), 3635-3653, Copyright (2003), with permission from Elsevier.

Figure 25 reprinted from Sodhi, R. N., Time-of-flight secondary ion mass spectrometry (TOF-SIMS):—versatility in chemical and imaging surface analysis. *Analyst* **2004,** *129* (6), 483-487 with permission of The Royal Society of Chemistry.

Figure 26 reprinted from Jung, S.; Foston, M.; Kalluri, U. C.; Tuskan, G. A.; Ragauskas, A. J., 3D chemical image using TOF-SIMS revealing the biopolymer component spatial and lateral distributions in biomass. *Angewandte Chemie International Edition* **2012,** *51* (48), 12005-12008 with permission from John Wiley and Sons.

A.2 Copyright Permission for Figure Reprints

License Number	4076581138475
License date	Mar 26, 2017
Licensed Content Publisher	Nature Publishing Group
Licensed Content Publication	Nature
Licensed Content Title	Genomics of cellulosic biofuels
Licensed Content Author	Edward M. Rubin
Licensed Content Date	Aug 14, 2008
Licensed Content Volume	454
Licensed Content Issue	7206
Type of Use	reuse in a dissertation / thesis
Requestor type	academic/educational
Format	print and electronic
Portion	figures/tables/illustrations
Number of figures/tables/illustrations	1
High-res required	no
Figures	Fig. 2
Author of this NPG article	no
Your reference number	
Title of your thesis / dissertation	Surface characterization of Pretreated and Microbial-treated Populus Cross-Sections
Expected completion date	Apr 2017
Estimated size (number of pages)	200
Requestor Location	Allison Tolbert 1 Bethel Vally Rd
	OAK RIDGE, TN 37830 United States Attn: Allison Tolbert
Billing Type	Invoice
Billing Address	Allison Tolbert 1 Bethel Valley Rd

169

Copyright
Clearance
Center

RightsLink®

Home		Account Info		Help

AMERICAN SOCIETY FOR MICROBIOLOGY

Title:		Form and Function of Clostridium thermocellum Biofilms

Author:		Alexandru Dumitrache, Gideon Wolfaardt, Grant Allen et al.

Publication:	Applied and Environmental Microbiology

Publisher:		American Society for Microbiology

Date:		Jan 1, 2013

Copyright © 2013, American Society for Microbiology

Logged in as:
Allison Tolbert
Account #:
3001050125

LOGOUT

Permissions Request

ASM authorizes an advanced degree candidate to republish the requested material in his/her doctoral thesis or dissertation. If your thesis, or dissertation, is to be published commercially, then you must reapply for permission.

BACK		CLOSE WINDOW

171

172

Jan 27, 2017

This Agreement between Allison Tolbert ("You") and Oxford University Press ("Oxford University Press") consists of your license details and the terms and conditions provided by Oxford University Press and Copyright Clearance Center.

License Number	4037170416094
License date	Jan 27, 2017
Licensed content publisher	Oxford University Press
Licensed content publication	Nucleic Acids Research
Licensed content title	Insights into plant biomass conversion from the genome of the anaerobic thermophilic bacterium Caldicellulosiruptor bescii DSM 6725
Licensed content author	Dam, Phuongan; Kataeva, Irina
Licensed content date	2011-01-10
Type of Use	Thesis/Dissertation
Institution name	
Title of your work	Surface characterization of Pretreated and Microbial-treated Populus Cross-Sections
Publisher of your work	n/a
Expected publication date	Apr 2017
Permissions cost	0.00 USD
Value added tax	0.00 USD
Total	0.00 USD
Requestor Location	Allison Tolbert 1 Bethel Vally Rd OAK RIDGE, TN 37830 United States Attn: Allison Tolbert
Publisher Tax ID	GB125506730
Billing Type	Invoice
Billing Address	Allison Tolbert 1 Bethel Valley Rd OAK RIDGE, TN 37830 United States Attn: Allison Tolbert

173

This Agreement between Allison Tolbert ("You") and The American Association for the Advancement of Science ("The American Association for the Advancement of Science") consists of your license details and the terms and conditions provided by The American Association for the Advancement of Science and Copyright Clearance Center.

License Number	4037180403804
License date	Jan 27, 2017
Licensed Content Publisher	The American Association for the Advancement of Science
Licensed Content Publication	Science
Licensed Content Title	Revealing Nature's Cellulase Diversity: The Digestion Mechanism of *Caldicellulosiruptor bescii* CelA
Licensed Content Author	Roman Brunecky,Markus Alahuhta,Qi Xu,Bryon S. Donohoe,Michael F. Crowley,Irina A. Kataeva,Sung-Jae Yang,Michael G. Resch,Michael W. W. Adams,Vladimir V. Lunin,Michael E. Himmel,Yannick J. Bomble
Licensed Content Date	Dec 20, 2013
Licensed Content Volume Number	342
Licensed Content Issue Number	6165
Volume number	342
Issue number	6165
Type of Use	Thesis / Dissertation
Requestor type	Scientist/individual at a research institution
Format	Print and electronic
Portion	Figure
Number of figures/tables	2
Order reference number	
Title of your thesis / dissertation	Surface characterization of Pretreated and Microbial-treated Populus Cross-Sections
Expected completion date	Apr 2017
Estimated size(pages)	200
Requestor Location	Allison Tolbert 1 Bethel Vally Rd OAK RIDGE, TN 37830 United States Attn: Allison Tolbert
Billing Type	Invoice

174

This Agreement between Allison Tolbert ("You") and Royal Society of Chemistry ("Royal Society of Chemistry") consists of your license details and the terms and conditions provided by Royal Society of Chemistry and Copyright Clearance Center.

License Number	4074570309780
License date	Mar 23, 2017
Licensed Content Publisher	Royal Society of Chemistry
Licensed Content Publication	Energy & Environmental Science
Licensed Content Title	Multi-scale visualization and characterization of lignocellulosic plant cell wall deconstruction during thermochemical pretreatment
Licensed Content Author	Shishir P. S. Chundawat,Bryon S. Donohoe,Leonardo da Costa Sousa,Thomas Elder,Umesh P. Agarwal,Fachuang Lu,John Ralph,Michael E. Himmel,Venkatesh Balan,Bruce E. Dale
Licensed Content Date	Jan 11, 2011
Licensed Content Volume	4
Licensed Content Issue	3
Type of Use	Thesis/Dissertation
Requestor type	academic/educational
Portion	figures/tables/images
Number of figures/tables/images	1
Format	print and electronic
Distribution quantity	10
Will you be translating?	no
Order reference number	
Title of the thesis/dissertation	Surface characterization of Pretreated and Microbial-treated Populus Cross-Sections
Expected completion date	Apr 2017
Estimated size	200
Requestor Location	Allison Tolbert 1 Bethel Vally Rd

OAK RIDGE, TN 37830 United States Attn: Allison Tolbert |
| Billing Type | Invoice |
| Billing Address | Allison Tolbert 1 Bethel Valley Rd |

175

This Agreement between Allison Tolbert ("You") and Elsevier ("Elsevier") consists of your license details and the terms and conditions provided by Elsevier and Copyright Clearance Center.

License Number	4071661330012
License date	Mar 17, 2017
Licensed Content Publisher	Elsevier
Licensed Content Publication	Biomaterials
Licensed Content Title	Time-of-flight secondary ion mass spectrometry: techniques and applications for the characterization of biomaterial surfaces
Licensed Content Author	Anna M. Belu,Daniel J. Graham,David G. Castner
Licensed Content Date	September 2003
Licensed Content Volume	24
Licensed Content Issue	21
Licensed Content Pages	19
Start Page	3635
End Page	3653
Type of Use	reuse in a thesis/dissertation
Intended publisher of new work	other
Portion	figures/tables/illustrations
Number of figures/tables/illustrations	1
Format	both print and electronic
Are you the author of this Elsevier article?	No
Will you be translating?	No
Order reference number	
Original figure numbers	Figure 1
Title of your thesis/dissertation	Surface characterization of Pretreated and Microbial-treated Populus Cross-Sections
Expected completion date	Apr 2017
Estimated size (number of pages)	200
Elsevier VAT number	GB 494 6272 12
Requestor Location	Allison Tolbert 1 Bethel Vally Rd

This Agreement between Allison Tolbert ("You") and Royal Society of Chemistry ("Royal Society of Chemistry") consists of your license details and the terms and conditions provided by Royal Society of Chemistry and Copyright Clearance Center.

License Number	4074801223878
License date	Mar 23, 2017
Licensed Content Publisher	Royal Society of Chemistry
Licensed Content Publication	Analyst
Licensed Content Title	Time-of-flight secondary ion mass spectrometry (TOF-SIMS):— versatility in chemical and imaging surface analysis
Licensed Content Author	Rana N. S. Sodhi
Licensed Content Date	May 10, 2004
Licensed Content Volume	129
Licensed Content Issue	6
Type of Use	Thesis/Dissertation
Requestor type	academic/educational
Portion	figures/tables/images
Number of figures/tables/images	1
Format	print and electronic
Distribution quantity	100
Will you be translating?	no
Order reference number	
Title of the thesis/dissertation	Surface characterization of Pretreated and Microbial-treated Populus Cross-Sections
Expected completion date	Apr 2017
Estimated size	200
Requestor Location	Allison Tolbert 1 Bethel Vally Rd OAK RIDGE, TN 37830 United States Attn: Allison Tolbert
Billing Type	Invoice
Billing Address	Allison Tolbert 1 Bethel Valley Rd

This Agreement between Allison Tolbert ("You") and John Wiley and Sons ("John Wiley and Sons") consists of your license details and the terms and conditions provided by John Wiley and Sons and Copyright Clearance Center.

License Number	4071670021341
License date	Mar 17, 2017
Licensed Content Publisher	John Wiley and Sons
Licensed Content Publication	Angewandte Chemie International Edition
Licensed Content Title	3D Chemical Image using TOF-SIMS Revealing the Biopolymer Component Spatial and Lateral Distributions in Biomass
Licensed Content Author	Seokwon Jung,Marcus Foston,Udaya C. Kalluri,Gerald A. Tuskan,Arthur J. Ragauskas
Licensed Content Date	Oct 25, 2012
Licensed Content Pages	4
Type of use	Dissertation/Thesis
Requestor type	University/Academic
Format	Print and electronic
Portion	Figure/table
Number of figures/tables	1
Original Wiley figure/table number(s)	Figure 3
Will you be translating?	No
Title of your thesis / dissertation	Surface characterization of Pretreated and Microbial-treated Populus Cross-Sections
Expected completion date	Apr 2017
Expected size (number of pages)	200
Requestor Location	Allison Tolbert 1 Bethel Vally Rd OAK RIDGE, TN 37830 United States Attn: Allison Tolbert
Publisher Tax ID	EU826007151
Billing Type	Invoice
Billing Address	Allison Tolbert 1 Bethel Valley Rd

178

ACS Publications
Most Trusted. Most Cited. Most Read.

Title: Identifying the Characteristic Secondary Ions of Lignin Polymer Using ToF−SIMS

Author: Kaori Saito, Toshiyuki Kato, Yukiko Tsuji, et al

Publication: Biomacromolecules

Publisher: American Chemical Society

Date: Mar 1, 2005

Copyright © 2005, American Chemical Society

BACK | CLOSE WINDOW

Title: Chemical and Spatial Differentiation of Syringyl and Guaiacyl Lignins in Poplar Wood via Time-of-Flight Secondary Ion Mass Spectrometry

Author: Chuanzhen Zhou, Quanzi Li, Vincent L. Chiang, et al

Publication: Analytical Chemistry

Publisher: American Chemical Society

Date: Sep 1, 2011

Copyright © 2011, American Chemical Society

PERMISSION/LICENSE IS GRANTED FOR YOUR ORDER AT NO CHARGE

This type of permission/license, instead of the standard Terms & Conditions, is sent to you because no fee is being charged for your order. Please note the following:

- Permission is granted for your request in both print and electronic formats, and translations.
- If figures and/or tables were requested, they may be adapted or used in part.
- Please print this page for your records and send a copy of it to your publisher/graduate school.
- Appropriate credit for the requested material should be given as follows: "Reprinted (adapted) with permission from (COMPLETE REFERENCE CITATION). Copyright (YEAR) American Chemical Society." Insert appropriate information in place of the capitalized words.
- One-time permission is granted only for the use specified in your request. No additional uses are granted (such as derivative works or other editions). For any other uses, please submit a new request.

If credit is given to another source for the material you requested, permission must be obtained from that source.

BACK | CLOSE WINDOW

A.3 Copyright Permission for Reprints of Publications

This Agreement between Allison Tolbert ("You") and John Wiley and Sons ("John Wiley and Sons") consists of your license details and the terms and conditions provided by John Wiley and Sons and Copyright Clearance Center.

License Number	4037181296105
License date	Jan 27, 2017
Licensed Content Publisher	John Wiley and Sons
Licensed Content Publication	Biofuels, Bioproducts and Biorefining
Licensed Content Title	Characterization and analysis of the molecular weight of lignin for biorefining studies
Licensed Content Author	Allison Tolbert,Hannah Akinosho,Ratayakorn Khunsupat,Amit K. Naskar,Arthur J. Ragauskas
Licensed Content Date	Jun 4, 2014
Licensed Content Pages	21
Type of use	Dissertation/Thesis
Requestor type	Author of this Wiley article
Format	Print and electronic
Portion	Figure/table
Number of figures/tables	2
Original Wiley figure/table number(s)	Figure 1, Table 2
Will you be translating?	No
Title of your thesis / dissertation	Surface characterization of Pretreated and Microbial-treated Populus Cross-Sections
Expected completion date	Apr 2017
Expected size (number of pages)	200
Requestor Location	Allison Tolbert 1 Bethel Vally Rd

OAK RIDGE, TN 37830 United States Attn: Allison Tolbert |
| Publisher Tax ID | EU826007151 |
| Billing Type | Invoice |

183

WILEY

Title: Advances in understanding the surface chemistry of lignocellulosic biomass via time of flight secondary ion mass spectrometry

Author: Allison Tolbert, Arthur J. Ragauskas

Publication: Energy Science & Engineering

Publisher: John Wiley and Sons

Date: Dec 12, 2016

© 2016 The Authors. Energy Science & Engineering published by the Society of Chemical Industry and John Wiley & Sons Ltd.

Welcome to RightsLink

Wiley offers a professional reprint service for high quality reproduction of articles from over 1400 scientific and medical journals. Wiley's reprint service offers:

• Peer reviewed research or reviews
• Tailored collections of articles
• A professional high quality finish
• Glossy journal style color covers
• Company or brand customisation
• Language translations
• Prompt turnaround times and delivery directly to your office, warehouse or congress.

Please contact our Reprints department for a quotation. Email corporatesaleseurope@wiley.com or corporatesalesusa@wiley.com or corporatesalesDE@wiley.com .

CLOSE WINDOW

This Agreement between Allison Tolbert ("You") and John Wiley and Sons ("John Wiley and Sons") consists of your license details and the terms and conditions provided by John Wiley and Sons and Copyright Clearance Center.

License Number	4091440061499
License date	Apr 17, 2017
Licensed Content Publisher	John Wiley and Sons
Licensed Content Publication	CHEMPLUSCHEM
Licensed Content Title	Understanding the Changes to Biomass Surface Characteristics after Ammonia and Organosolv Pretreatments by Using Time-of-Flight Secondary-Ion Mass Spectrometry (TOF-SIMS)
Licensed Content Author	Allison K. Tolbert,Chang Geun Yoo,Arthur J. Ragauskas
Licensed Content Date	Apr 11, 2017
Licensed Content Pages	1
Type of use	Dissertation/Thesis
Requestor type	Author of this Wiley article
Format	Print and electronic
Portion	Full article
Will you be translating?	No
Title of your thesis / dissertation	Surface characterization of Pretreated and Microbial-treated Populus Cross-Sections
Expected completion date	Apr 2017
Expected size (number of pages)	200
Requestor Location	Allison Tolbert 1 Bethel Vally Rd
	OAK RIDGE, TN 37830 United States Attn: Allison Tolbert
Publisher Tax ID	EU826007151
Billing Type	Invoice
Billing Address	Allison Tolbert 1 Bethel Valley Rd
	OAK RIDGE, TN 37830 United States Attn: Allison Tolbert
Total	0.00 USD

Cellulose and lignin colocalization at the plant cell wall surface limits microbial hydrolysis of *Populus* biomass

A. Dumitrache, A. Tolbert, J. Natzke, S. D. Brown, B. H. Davison and A. J. Ragauskas, *Green Chem.*, 2017, Advance Article , **DOI:** 10.1039/C7GC00346C

If you are the author of this article you do not need to formally request permission to reproduce figures, diagrams etc. contained in this article in third party publications or in a thesis or dissertation provided that the correct acknowledgement is given with the reproduced material.

REFERENCES

1. Ragauskas, A. J.; Williams, C. K.; Davison, B. H.; Britovsek, G.; Cairney, J.; Eckert, C. A.; Frederick, W. J.; Hallett, J. P.; Leak, D. J.; Liotta, C. L.; Mielenz, J. R.; Murphy, R.; Templer, R.; Tschaplinski, T., The path forward for biofuels and biomaterials. *Science* **2006,** *311* (5760), 484-489.

2. Long, H.; Li, X.; Wang, H.; Jia, J., Biomass resources and their bioenergy potential estimation: a review. *Renewable and Sustainable Energy Reviews* **2013,** *26*, 344-352.

3. Ellabban, O.; Abu-Rub, H.; Blaabjerg, F., Renewable energy resources: current status, future prospects and their enabling technology. *Renewable and Sustainable Energy Reviews* **2014,** *39*, 748-764.

4. Limayem, A.; Ricke, S. C., Lignocellulosic biomass for bioethanol production: current perspectives, potential issues and future prospects. *Progress in Energy and Combustion Science* **2012,** *38* (4), 449-467.

5. Cherubini, F., The biorefinery concept: using biomass instead of oil for producing energy and chemicals. *Energy Conversion and Management* **2010,** *51* (7), 1412-1421.

6. Himmel, M. E.; Ding, S.-Y.; Johnson, D. K.; Adney, W. S.; Nimlos, M. R.; Brady, J. W.; Foust, T. D., Biomass recalcitrance: engineering plants and enzymes for biofuels production. *Science* **2007,** *315* (5813), 804-807.

7. Sannigrahi, P.; Ragauskas, A. J.; Tuskan, G. A., Poplar as a feedstock for biofuels: a review of compositional characteristics. *Biofuels, Bioproducts and Biorefining* **2010,** *4* (2), 209-226.

8. Langholtz, M.; Stokes, B.; Eaton, L. *2016 Billion-ton report: Advancing domestic resources for a thriving bioeconomy, Volume 1: Economic availability of feedstock*; U.S. Department of Energy: 2016.

9. Hatfield, R.; Vermerris, W., Lignin formation in plants. The dilemma of linkage specificity. *Plant Physiology* **2001,** *126* (4), 1351-1357.

10. Mou, H.-Y.; Orblin, E.; Kruus, K.; Fardim, P., Topochemical pretreatment of wood biomass to enhance enzymatic hydrolysis of polysaccharides to sugars. *Bioresource Technology* **2013,** *142*, 540-545.

11. Mou, H. Y.; Heikkilä, E.; Fardim, P., Topochemistry of alkaline, alkaline-peroxide and hydrotropic pretreatments of common reed to enhance enzymatic hydrolysis efficiency. *Bioresource Technology* **2013,** *150*, 36-41.

12.	Jung, S.; Foston, M.; Sullards, M. C.; Ragauskas, A. J., Surface characterization of dilute acid pretreated Populus deltoides by ToF-SIMS. *Energy & Fuels* **2010,** *24* (2), 1347-1357.

13.	Sluiter, J. B.; Ruiz, R. O.; Scarlata, C. J.; Sluiter, A. D.; Templeton, D. W., Compositional analysis of lignocellulosic feedstocks. 1. Review and description of methods. *Journal of Agricultural and Food Chemistry* **2010,** *58* (16), 9043-9053.

14.	Jordan, D. B.; Bowman, M. J.; Braker, J. D.; Dien, B. S.; Hector, R. E.; Lee, C. C.; Mertens, J. A.; Wagschal, K., Plant cell walls to ethanol. *Biochemical Journal* **2012,** *442* (2), 241-252.

15.	Khalil, H. S. A.; Alwani, M. S.; Omar, A. K. M., Chemical composition, anatomy, lignin distribution, and cell wall structure of Malaysian plant waste fibers. *BioResources* **2007,** *1* (2), 220-232.

16.	Wimmer, R.; Lucas, B. N., Comparing mechanical properties of secondary wall and cell corner middle lamella in spruce wood. *IAWA Journal* **1997,** *18* (1), 77-88.

17.	Davison, B. H.; Parks, J.; Davis, M. F.; Donohoe, B. S., Plant cell walls: basics of structure, chemistry, accessibility and the influence on conversion. *Aqueous Pretreatment of Plant Biomass for Biological and Chemical Conversion to Fuels and Chemicals* **2013**, 23-38.

18.	Rubin, E. M., Genomics of cellulosic biofuels. *Nature* **2008,** *454* (7206), 841-845.

19.	Singh, R.; Shukla, A.; Tiwari, S.; Srivastava, M., A review on delignification of lignocellulosic biomass for enhancement of ethanol production potential. *Renewable and Sustainable Energy Reviews* **2014,** *32*, 713-728.

20.	Huber, G. W.; Iborra, S.; Corma, A., Synthesis of transportation fuels from biomass: chemistry, catalysts, and engineering. *Chemical Reviews* **2006,** *106* (9), 4044-4098.

21.	Saha, B. C., Hemicellulose bioconversion. *Journal of Industrial Microbiology and Biotechnology* **2003,** *30* (5), 279-291.

22.	Ballesteros, I.; Negro, M. J.; Oliva, J. M.; Cabañas, A.; Manzanares, P.; Ballesteros, M., Ethanol production from steam-explosion pretreated wheat straw. *Applied Biochemistry and Biotechnology* **2006,** *130* (1), 496-508.

23.	Akinosho, H.; Yee, K.; Close, D.; Ragauskas, A., The emergence of *Clostridium thermocellum* as a high utility candidate for consolidated bioprocessing applications. *Frontiers in Chemistry* **2014,** *2*, 1-18.

24.	Klemm, D.; Heublein, B.; Fink, H. P.; Bohn, A., Cellulose: fascinating biopolymer and sustainable raw material. *Angewandte Chemie International Edition* **2005,** *44* (22), 3358-3393.

25.   Hallac, B. B.; Ragauskas, A. J., Analyzing cellulose degree of polymerization and its relevancy to cellulosic ethanol. *Biofuels, Bioproducts and Biorefining* **2011,** *5* (2), 215-225.

26.   Kamel, S.; Ali, N.; Jahangir, K.; Shah, S.; El-Gendy, A., Pharmaceutical significance of cellulose: a review. *eXPRESS Polymer Letters* **2008,** *2* (11), 758-778.

27.   Pu, Y.; Zhang, D.; Singh, P. M.; Ragauskas, A. J., The new forestry biofuels sector. *Biofuels, Bioproducts and Biorefining* **2008,** *2* (1), 58-73.

28.   Nishiyama, Y.; Sugiyama, J.; Chanzy, H.; Langan, P., Crystal structure and hydrogen bonding system in cellulose Iα from synchrotron X-ray and neutron fiber diffraction. *Journal of the American Chemical Society* **2003,** *125* (47), 14300-14306.

29.   Baker, A. A.; Helbert, W.; Sugiyama, J.; Miles, M. J., High-resolution atomic force microscopy of nativeValoniacellulose I microcrystals. *Journal of Structural Biology* **1997,** *119* (2), 129-138.

30.   Nishiyama, Y.; Langan, P.; Chanzy, H., Crystal structure and hydrogen-bonding system in cellulose Iβ from synchrotron X-ray and neutron fiber diffraction. *Journal of the American Chemical Society* **2002,** *124* (31), 9074-9082.

31.   O'sullivan, A. C., Cellulose: the structure slowly unravels. *Cellulose* **1997,** *4* (3), 173-207.

32.   Zhou, C.; Wu, Q., Recent development in applications of cellulose nanocrystals for advanced polymer-based nanocomposites by novel fabrication strategies. In *Nanocrystals - Synthesis, Characterization and Applications*, Neralla, S., Ed. InTech: Rijeka, Croatia, 2012; pp 103-120.

33.   Sannigrahi, P.; Ragauskas, A. J.; Miller, S. J., Effects of two-stage dilute acid pretreatment on the structure and composition of lignin and cellulose in loblolly pine. *BioEnergy Research* **2008,** *1* (3-4), 205-214.

34.   Foston, M.; Hubbell, C. A.; Davis, M.; Ragauskas, A. J., Variations in cellulosic ultrastructure of poplar. *BioEnergy Research* **2009,** *2* (4), 193-197.

35.   Samuel, R.; Pu, Y.; Foston, M.; Ragauskas, A. J., Solid-state NMR characterization of switchgrass cellulose after dilute acid pretreatment. *Biofuels* **2010,** *1* (1), 85-90.

36.   Pauly, M.; Gille, S.; Liu, L.; Mansoori, N.; de Souza, A.; Schultink, A.; Xiong, G., Hemicellulose biosynthesis. *Planta* **2013,** *238* (4), 627-642.

37.   Mood, S. H.; Golfeshan, A. H.; Tabatabaei, M.; Jouzani, G. S.; Najafi, G. H.; Gholami, M.; Ardjmand, M., Lignocellulosic biomass to bioethanol, a comprehensive review with a focus on pretreatment. *Renewable and Sustainable Energy Reviews* **2013,** *27*, 77-93.

38.   Tolbert, A.; Akinosho, H.; Khunsupat, R.; Naskar, A. K.; Ragauskas, A. J., Characterization and analysis of the molecular weight of lignin for biorefining studies. *Biofuels, Bioproducts and Biorefining* **2014,** *8* (6), 836-856.

39.   Ragauskas, A. J.; Nagy, M.; Kim, D. H.; Eckert, C. A.; Hallett, J. P.; Liotta, C. L., From wood to fuels: integrating biofuels and pulp production. *Industrial Biotechnology* **2006,** *2* (1), 55-65.

40.   Gírio, F. M.; Fonseca, C.; Carvalheiro, F.; Duarte, L. C.; Marques, S.; Bogel-Łukasik, R., Hemicelluloses for fuel ethanol: a review. *Bioresource Technology* **2010,** *101* (13), 4775-4800.

41.   Barakat, A.; Winter, H.; Rondeau-Mouro, C.; Saake, B.; Chabbert, B.; Cathala, B., Studies of xylan interactions and cross-linking to synthetic lignins formed by bulk and end-wise polymerization: a model study of lignin carbohydrate complex formation. *Planta* **2007,** *226* (1), 267-281.

42.   Foston, M.; Ragauskas, A. J., Biomass characterization: recent progress in understanding biomass recalcitrance. *Industrial Biotechnology* **2012,** *8* (4), 191-208.

43.   Doherty, W. O. S.; Mousavioun, P.; Fellows, C. M., Value-adding to cellulosic ethanol: Lignin polymers. *Industrial Crops and Products* **2011,** *33* (2), 259-276.

44.   Pu, Y.; Hu, F.; Huang, F.; Davison, B. H.; Ragauskas, A. J., Assessing the molecular structure basis for biomass recalcitrance during dilute acid and hydrothermal pretreatments. *Biotechnology for Biofuels* **2013,** *6* (1-13), 15.

45.   Suhas; Carrott, P. J. M.; Ribeiro Carrott, M. M. L., Lignin – from natural adsorbent to activated carbon: A review. *Bioresource Technology* **2007,** *98* (12), 2301-2312.

46.   Chakar, F. S.; Ragauskas, A. J., Review of current and future softwood kraft lignin process chemistry. *Industrial Crops and Products* **2004,** *20* (2), 131-141.

47.   Ziebell, A.; Gracom, K.; Katahira, R.; Chen, F.; Pu, Y.; Ragauskas, A.; Dixon, R. A.; Davis, M., Increase in 4-coumaryl alcohol units during lignification in alfalfa (Medicago sativa) alters the extractability and molecular weight of lignin. *Journal of Biological Chemistry* **2010,** *285* (50), 38961-38968.

48.   Lapierre, C.; Pollet, B.; Rolando, C., New insights into the molecular architecture of hardwood lignins by chemical degradative methods. *Research on Chemical Intermediates* **1995,** *21* (3), 397-412.

49.   El Hage, R.; Brosse, N.; Chrusciel, L.; Sanchez, C.; Sannigrahi, P.; Ragauskas, A., Characterization of milled wood lignin and ethanol organosolv lignin from miscanthus. *Polymer Degradation and Stability* **2009,** *94* (10), 1632-1638.

50.   Sannigrahi, P.; Pu, Y.; Ragauskas, A., Cellulosic biorefineries—unleashing lignin opportunities. *Current Opinion in Environmental Sustainability* **2010,** *2* (5–6), 383-393.

51.   Achyuthan, K. E.; Achyuthan, A. M.; Adams, P. D.; Dirk, S. M.; Harper, J. C.; Simmons, B. A.; Singh, A. K., Supramolecular self-assembled chaos: polyphenolic lignin's barrier to cost-effective lignocellulosic biofuels. *Molecules* **2010,** *15* (12), 8641-8688.

52.   Kukkola, E. M.; Koutaniemi, S.; Pöllänen, E.; Gustafsson, M.; Karhunen, P.; Lundell, T. K.; Saranpää, P.; Kilpeläinen, I.; Teeri, T. H.; Fagerstedt, K. V., The dibenzodioxocin lignin substructure is abundant in the inner part of the secondary wall in Norway spruce and silver birch xylem. *Planta* **2004,** *218* (3), 497-500.

53.   Kim, J.-Y.; Shin, E.-J.; Eom, I.-Y.; Won, K.; Kim, Y. H.; Choi, D.; Choi, I.-G.; Choi, J. W., Structural features of lignin macromolecules extracted with ionic liquid from poplar wood. *Bioresource Technology* **2011,** *102* (19), 9020-9025.

54.   Zhu, L.; O'Dwyer, J. P.; Chang, V. S.; Granda, C. B.; Holtzapple, M. T., Structural features affecting biomass enzymatic digestibility. *Bioresource Technology* **2008,** *99* (9), 3817-3828.

55.   Pandey, M. P.; Kim, C. S., Lignin depolymerization and conversion: a review of thermochemical methods. *Chemical Engineering & Technology* **2011,** *34* (1), 29-41.

56.   Karhunen, P.; Rummakko, P.; Sipilä, J.; Brunow, G.; Kilpeläinen, I., Dibenzodioxocins; a novel type of linkage in softwood lignins. *Tetrahedron Letters* **1995,** *36* (1), 169-170.

57.   Buranov, A. U.; Mazza, G., Lignin in straw of herbaceous crops. *Industrial Crops and Products* **2008,** *28* (3), 237-259.

58.   Adler, E., Lignin chemistry—past, present and future. *Wood Science and Technology* **1977,** *11* (3), 169-218.

59.   Yuan, T.-Q.; Sun, S.-N.; Xu, F.; Sun, R.-C., Characterization of lignin structures and lignin–carbohydrate complex (LCC) linkages by quantitative 13C and 2D HSQC NMR spectroscopy. *Journal of Agricultural and Food Chemistry* **2011,** *59* (19), 10604-10614.

60.   Zhao, X.; Zhang, L.; Liu, D., Biomass recalcitrance. Part I: the chemical compositions and physical structures affecting the enzymatic hydrolysis of lignocellulose. *Biofuels, Bioproducts and Biorefining* **2012,** *6* (4), 465-482.

61.   Mosier, N.; Wyman, C.; Dale, B.; Elander, R.; Lee, Y.; Holtzapple, M.; Ladisch, M., Features of promising technologies for pretreatment of lignocellulosic biomass. *Bioresource Technology* **2005,** *96* (6), 673-686.

62.	Sun, Y.; Cheng, J., Hydrolysis of lignocellulosic materials for ethanol production: a review. *Bioresource Technology* **2002,** *83* (1), 1-11.

63.	Hu, F.; Ragauskas, A., Pretreatment and lignocellulosic chemistry. *BioEnergy Research* **2012,** *5* (4), 1043-1066.

64.	Mbaneme-Smith, V.; Chinn, M. S., Consolidated bioprocessing for biofuel production: recent advances. *Energy and Emission Control Technologies* **2015,** *3*, 23-44.

65.	Lynd, L. R.; Weimer, P. J.; Van Zyl, W. H.; Pretorius, I. S., Microbial cellulose utilization: fundamentals and biotechnology. *Microbiology and Molecular Biology Reviews* **2002,** *66* (3), 506-577.

66.	Wyman, C. E., What is (and is not) vital to advancing cellulosic ethanol. *Trends in Biotechnology* **2007,** *25* (4), 153-157.

67.	Hendriks, A.; Zeeman, G., Pretreatments to enhance the digestibility of lignocellulosic biomass. *Bioresource Technology* **2009,** *100* (1), 10-18.

68.	Kumar, P.; Barrett, D. M.; Delwiche, M. J.; Stroeve, P., Methods for pretreatment of lignocellulosic biomass for efficient hydrolysis and biofuel production. *Industrial & Engineering Chemistry Research* **2009,** *48* (8), 3713-3729.

69.	Zhao, X.; Zhang, L.; Liu, D., Biomass recalcitrance. Part II: Fundamentals of different pre-treatments to increase the enzymatic digestibility of lignocellulose. *Biofuels, Bioproducts and Biorefining* **2012,** *6* (5), 561-579.

70.	Agbor, V. B.; Cicek, N.; Sparling, R.; Berlin, A.; Levin, D. B., Biomass pretreatment: fundamentals toward application. *Biotechnology Advances* **2011,** *29* (6), 675-685.

71.	Ma, H.; Liu, W.-W.; Chen, X.; Wu, Y.-J.; Yu, Z.-L., Enhanced enzymatic saccharification of rice straw by microwave pretreatment. *Bioresource Technology* **2009,** *100* (3), 1279-1284.

72.	Sanchez, O. J.; Cardona, C. A., Trends in biotechnological production of fuel ethanol from different feedstocks. *Bioresource Technology* **2008,** *99* (13), 5270-5295.

73.	Hu, F.; Jung, S.; Ragauskas, A., Pseudo-lignin formation and its impact on enzymatic hydrolysis. *Bioresource Technology* **2012,** *117*, 7-12.

74.	Kim, T. H.; Kim, J. S.; Sunwoo, C.; Lee, Y., Pretreatment of corn stover by aqueous ammonia. *Bioresource Technology* **2003,** *90* (1), 39-47.

75.	Zheng, Y.; Pan, Z.; Zhang, R., Overview of biomass pretreatment for cellulosic ethanol production. *International Journal of Agricultural and Biological Engineering* **2009,** *2* (3), 51-68.

76.   Silverstein, R. A.; Chen, Y.; Sharma-Shivappa, R. R.; Boyette, M. D.; Osborne, J., A comparison of chemical pretreatment methods for improving saccharification of cotton stalks. *Bioresource Technology* **2007,** *98* (16), 3000-3011.

77.   Pawar, P. M.-A.; Koutaniemi, S.; Tenkanen, M.; Mellerowicz, E. J., Acetylation of woody lignocellulose: significance and regulation. *Frontiers in Plant Science* **2013,** *4* (118), 1-8.

78.   Kim, J. S.; Lee, Y.; Kim, T. H., A review on alkaline pretreatment technology for bioconversion of lignocellulosic biomass. *Bioresource Technology* **2016,** *199*, 42-48.

79.   Carvalheiro, F.; Duarte, L. C.; Gírio, F. M., Hemicellulose biorefineries: a review on biomass pretreatments. *Journal of Scientific & Industrial Research* **2008**, 849-864.

80.   Park, Y. C.; Kim, J. S., Comparison of various alkaline pretreatment methods of lignocellulosic biomass. *Energy* **2012,** *47* (1), 31-35.

81.   Zhao, X.; Cheng, K.; Liu, D., Organosolv pretreatment of lignocellulosic biomass for enzymatic hydrolysis. *Applied Microbiology and Biotechnology* **2009,** *82* (5), 815-827.

82.   Koo, B.-W.; Kim, H.-Y.; Park, N.; Lee, S.-M.; Yeo, H.; Choi, I.-G., Organosolv pretreatment of Liriodendron tulipifera and simultaneous saccharification and fermentation for bioethanol production. *Biomass and Bioenergy* **2011,** *35* (5), 1833-1840.

83.   Duff, S. J.; Murray, W. D., Bioconversion of forest products industry waste cellulosics to fuel ethanol: a review. *Bioresource Technology* **1996,** *55* (1), 1-33.

84.   Pan, X.; Gilkes, N.; Kadla, J.; Pye, K.; Saka, S.; Gregg, D.; Ehara, K.; Xie, D.; Lam, D.; Saddler, J., Bioconversion of hybrid poplar to ethanol and co-products using an organosolv fractionation process: Optimization of process yields. *Biotechnology and Bioengineering* **2006,** *94* (5), 851-861.

85.   Brosse, N.; El Hage, R.; Sannigrahi, P.; Ragauskas, A., Dilute sulphuric acid and ethanol organosol pretreatment of Miscanthus x Giganteus. *Cellulose Chemistry & Technology* **2010,** *44* (1), 71-78.

86.   Teramoto, Y.; Lee, S.-H.; Endo, T., Pretreatment of woody and herbaceous biomass for enzymatic saccharification using sulfuric acid-free ethanol cooking. *Bioresource Technology* **2008,** *99* (18), 8856-8863.

87.   Zhang, K.; Pei, Z.; Wang, D., Organic solvent pretreatment of lignocellulosic biomass for biofuels and biochemicals: a review. *Bioresource Technology* **2016,** *199*, 21-33.

88.   Raman, B.; McKeown, C. K.; Rodriguez, M.; Brown, S. D.; Mielenz, J. R., Transcriptomic analysis of Clostridium thermocellum ATCC 27405 cellulose fermentation. *BMC Microbiology* **2011,** *11* (134), 1-15.

89.   Tian, L.; Papanek, B.; Olson, D. G.; Rydzak, T.; Holwerda, E. K.; Zheng, T.; Zhou, J.; Maloney, M.; Jiang, N.; Giannone, R. J., Simultaneous achievement of high ethanol yield and titer in Clostridium thermocellum. *Biotechnology for Biofuels* **2016,** *9* (116), 1-11.

90.   Chung, D.; Cha, M.; Guss, A. M.; Westpheling, J., Direct conversion of plant biomass to ethanol by engineered *Caldicellulosiruptor bescii. Proceedings of the National Academy of Sciences* **2014,** *111* (24), 8931-8936.

91.   Tripathi, S. A.; Olson, D. G.; Argyros, D. A.; Miller, B. B.; Barrett, T. F.; Murphy, D. M.; McCool, J. D.; Warner, A. K.; Rajgarhia, V. B.; Lynd, L. R., Development of pyrF-based genetic system for targeted gene deletion in Clostridium thermocellum and creation of a pta mutant. *Applied and Environmental Microbiology* **2010,** *76* (19), 6591-6599.

92.   Ellis, L. D.; Holwerda, E. K.; Hogsett, D.; Rogers, S.; Shao, X.; Tschaplinski, T.; Thorne, P.; Lynd, L. R., Closing the carbon balance for fermentation by Clostridium thermocellum (ATCC 27405). *Bioresource Technology* **2012,** *103* (1), 293-299.

93.   Freier, D.; Mothershed, C. P.; Wiegel, J., Characterization of Clostridium thermocellum JW20. *Applied and Environmental Microbiology* **1988,** *54* (1), 204-211.

94.   Olson, D. G.; Sparling, R.; Lynd, L. R., Ethanol production by engineered thermophiles. *Current Opinion in Biotechnology* **2015,** *33*, 130-141.

95.   Biswas, R.; Zheng, T.; Olson, D. G.; Lynd, L. R.; Guss, A. M., Elimination of hydrogenase active site assembly blocks H 2 production and increases ethanol yield in Clostridium thermocellum. *Biotechnology for Biofuels* **2015,** *8* (20), 1-8.

96.   Dumitrache, A.; Wolfaardt, G.; Allen, G.; Liss, S. N.; Lynd, L. R., Form and function of Clostridium thermocellum biofilms. *Applied and Environmental Microbiology* **2013,** *79* (1), 231-239.

97.   Wilson, C. M.; Rodriguez, M.; Johnson, C. M.; Martin, S. L.; Chu, T. M.; Wolfinger, R. D.; Hauser, L. J.; Land, M. L.; Klingeman, D. M.; Syed, M. H., Global transcriptome analysis of Clostridium thermocellum ATCC 27405 during growth on dilute acid pretreated Populus and switchgrass. *Biotechnology for Biofuels* **2013,** *6* (1), 179.

98.   Basen, M.; Rhaesa, A. M.; Kataeva, I.; Prybol, C. J.; Scott, I. M.; Poole, F. L.; Adams, M. W., Degradation of high loads of crystalline cellulose and of unpretreated plant biomass by the thermophilic bacterium Caldicellulosiruptor bescii. *Bioresource Technology* **2014,** *152*, 384-392.

99.   Paye, J. M.; Guseva, A.; Hammer, S. K.; Gjersing, E.; Davis, M. F.; Davison, B. H.; Olstad, J.; Donohoe, B. S.; Nguyen, T. Y.; Wyman, C. E., Biological lignocellulose solubilization: comparative evaluation of biocatalysts and enhancement via cotreatment. *Biotechnology for Biofuels* **2016,** *9* (8), 1-13.

100.   Dumitrache, A.; Akinosho, H.; Rodriguez, M.; Meng, X.; Yoo, C. G.; Natzke, J.; Engle, N. L.; Sykes, R. W.; Tschaplinski, T. J.; Muchero, W.; Ragauskas, A. J.; Davison, B. H.; Brown, S. D., Consolidated bioprocessing of Populus using Clostridium (Ruminiclostridium) thermocellum: a case study on the impact of lignin composition and structure. *Biotechnology for Biofuels* **2016,** *9* (31), 1-14.

101.   Izquierdo, J. A.; Pattathil, S.; Guseva, A.; Hahn, M. G.; Lynd, L. R., Comparative analysis of the ability of Clostridium clariflavum strains and Clostridium thermocellum to utilize hemicellulose and unpretreated plant material. *Biotechnology for Biofuels* **2014,** *7* (136), 1-8.

102.   Paye, J. M.; Guseva, A.; Hammer, S. K.; Gjersing, E.; Davis, M. F.; Davison, B. H.; Olstad, J.; Donohoe, B. S.; Nguyen, T. Y.; Wyman, C. E.; Pattathil, S.; Hahn, M. G.; Lynd, L. R., Biological lignocellulose solubilization: comparative evaluation of biocatalysts and enhancement via cotreatment. *Biotechnology for Biofuels* **2016,** *9* (1), 1-13.

103.   Shao, X.; Jin, M.; Guseva, A.; Liu, C.; Balan, V.; Hogsett, D.; Dale, B. E.; Lynd, L., Conversion for Avicel and AFEX pretreated corn stover by Clostridium thermocellum and simultaneous saccharification and fermentation: Insights into microbial conversion of pretreated cellulosic biomass. *Bioresource Technology* **2011,** *102* (17), 8040-8045.

104.   Raman, B.; Pan, C.; Hurst, G. B.; Rodriguez Jr, M.; McKeown, C. K.; Lankford, P. K.; Samatova, N. F.; Mielenz, J. R., Impact of pretreated switchgrass and biomass carbohydrates on Clostridium thermocellum ATCC 27405 cellulosome composition: a quantitative proteomic analysis. *PLOS ONE* **2009,** *4* (4), e5271.

105.   Blumer-Schuette, S. E.; Brown, S. D.; Sander, K. B.; Bayer, E. A.; Kataeva, I.; Zurawski, J. V.; Conway, J. M.; Adams, M. W.; Kelly, R. M., Thermophilic lignocellulose deconstruction. *FEMS Microbiology Reviews* **2014,** *38* (3), 393-448.

106.   Xu, Q.; Resch, M. G.; Podkaminer, K.; Yang, S.; Baker, J. O.; Donohoe, B. S.; Wilson, C.; Klingeman, D. M.; Olson, D. G.; Decker, S. R.; Giannone, R. J.; Hettich, R. L.; Brown, S. D.; Lynd, L. R.; Bayer, E. A.; Himmel, M. E.; Bomble, Y. J., Dramatic performance of Clostridium thermocellum explained by its wide range of cellulase modalities. *Science Advances* **2016,** *2* (e1501254), 1-12.

107.   Argyros, D. A.; Tripathi, S. A.; Barrett, T. F.; Rogers, S. R.; Feinberg, L. F.; Olson, D. G.; Foden, J. M.; Miller, B. B.; Lynd, L. R.; Hogsett, D. A., High ethanol titers from cellulose by using metabolically engineered thermophilic, anaerobic microbes. *Applied and Environmental Microbiology* **2011,** *77* (23), 8288-8294.

108.   Olson, D. G.; Lynd, L. R., Transformation of Clostridium thermocellum by electroporation. In *Cellulases*, Abeson, J. N.; Simon, M. I.; Colowick, S. P.; Kaplan, N. O., Eds. Elsevier: San Diego, CA, 2012; Vol. 510, pp 317-330.

109.   Herrero, A. A.; Gomez, R. F., Development of ethanol tolerance in Clostridium thermocellum: effect of growth temperature. *Applied and Environmental Microbiology* **1980,** *40* (3), 571-577.

110.   Tailliez, P.; Girard, H.; Longin, R.; Beguin, P.; Millet, J., Cellulose fermentation by an asporogenous mutant and an ethanol-tolerant mutant of Clostridium thermocellum. *Applied and Environmental Microbiology* **1989,** *55* (1), 203-206.

111.   Brown, S. D.; Guss, A. M.; Karpinets, T. V.; Parks, J. M.; Smolin, N.; Yang, S.; Land, M. L.; Klingeman, D. M.; Bhandiwad, A.; Rodriguez, M., Mutant alcohol dehydrogenase leads to improved ethanol tolerance in Clostridium thermocellum. *Proceedings of the National Academy of Sciences* **2011,** *108* (33), 13752-13757.

112.   Linville, J. L.; Rodriguez Jr, M.; Land, M.; Syed, M. H.; Engle, N. L.; Tschaplinski, T. J.; Mielenz, J. R.; Cox, C. D., Industrial robustness: understanding the mechanism of tolerance for the Populus hydrolysate-tolerant mutant strain of Clostridium thermocellum. *PLOS ONE* **2013,** *8* (10), e78829.

113.   Dam, P.; Kataeva, I.; Yang, S. J.; Zhou, F. F.; Yin, Y. B.; Chou, W. C.; Poole, F. L.; Westpheling, J.; Hettich, R.; Giannone, R.; Lewis, D. L.; Kelly, R.; Gilbert, H. J.; Henrissat, B.; Xu, Y.; Adams, M. W. W., Insights into plant biomass conversion from the genome of the anaerobic thermophilic bacterium *Caldicellulosiruptor bescii* DSM 6725. *Nucleic Acids Research* **2011,** *39* (8), 3240-3254.

114.   Yang, S.-J.; Kataeva, I.; Hamilton-Brehm, S. D.; Engle, N. L.; Tschaplinski, T. J.; Doeppke, C.; Davis, M.; Westpheling, J.; Adams, M. W., Efficient degradation of lignocellulosic plant biomass, without pretreatment, by the thermophilic anaerobe "*Anaerocellum thermophilum*" DSM 6725. *Applied and Environmental Microbiology* **2009,** *75* (14), 4762-4769.

115.   Chung, D.; Farkas, J.; Westpheling, J., Overcoming restriction as a barrier to DNA transformation in Caldicellulosiruptor species results in efficient marker replacement. *Biotechnology for Biofuels* **2013,** *6* (82), 1-9.

116.   Yang, S.-J.; Kataeva, I.; Wiegel, J.; Yin, Y.; Dam, P.; Xu, Y.; Westpheling, J.; Adams, M. W., Classification of 'Anaerocellum thermophilum'strain DSM 6725 as Caldicellulosiruptor bescii sp. nov. *International Journal of Systematic and Evolutionary Microbiology* **2010,** *60* (9), 2011-2015.

117.   Kataeva, I.; Foston, M. B.; Yang, S.-J.; Pattathil, S.; Biswal, A. K.; Poole II, F. L.; Basen, M.; Rhaesa, A. M.; Thomas, T. P.; Azadi, P., Carbohydrate and lignin are simultaneously solubilized from unpretreated switchgrass by microbial action at high temperature. *Energy & Environmental Science* **2013,** *6* (7), 2186-2195.

118.   Yee, K. L.; Rodriguez Jr, M.; Tschaplinski, T. J.; Engle, N. L.; Martin, M. Z.; Fu, C.; Wang, Z.-Y.; Hamilton-Brehm, S. D.; Mielenz, J. R., Evaluation of the bioconversion of genetically modified switchgrass using simultaneous saccharification and fermentation and a consolidated bioprocessing approach. *Biotechnology for Biofuels* **2012,** *5* (1), 81.

119.   Taylor, M. P.; Eley, K. L.; Martin, S.; Tuffin, M. I.; Burton, S. G.; Cowan, D. A., Thermophilic ethanologenesis: future prospects for second-generation bioethanol production. *Trends in Biotechnology* **2009,** *27* (7), 398-405.

120.   Egorova, K.; Antranikian, G., Industrial relevance of thermophilic Archaea. *Current Opinion in Microbiology* **2005,** *8* (6), 649-655.

121.   Brunecky, R.; Alahuhta, M.; Xu, Q.; Donohoe, B. S.; Crowley, M. F.; Kataeva, I. A.; Yang, S. J.; Resch, M. G.; Adams, M. W.; Lunin, V. V.; Himmel, M. E.; Bomble, Y. J., Revealing nature's cellulase diversity: the digestion mechanism of *Caldicellulosiruptor bescii* CelA. *Science* **2013,** *342* (6165), 1513-6.

122.   Young, J.; Chung, D.; Bomble, Y. J.; Himmel, M. E.; Westpheling, J., Deletion of *Caldicellulosiruptor bescii* CelA reveals its crucial role in the deconstruction of lignocellulosic biomass. *Biotechnology for Biofuels* **2014,** *7* (1), 142.

123.   Binnig, G.; Quate, C. F.; Gerber, C., Atomic force microscope. *Physical Review Letters* **1986,** *56* (9), 930.

124.   Jalili, N.; Laxminarayana, K., A review of atomic force microscopy imaging systems: application to molecular metrology and biological sciences. *Mechatronics* **2004,** *14* (8), 907-945.

125.   Ding, S.-Y.; Himmel, M. E., The maize primary cell wall microfibril: a new model derived from direct visualization. *Journal of Agricultural and Food Chemistry* **2006,** *54* (3), 597-606.

126.   Kirby, A. R.; Gunning, A. P.; Waldron, K. W.; Morris, V. J.; Ng, A., Visualization of plant cell walls by atomic force microscopy. *Biophysical Journal* **1996,** *70* (3), 1138-1143.

127.   Yan, L.; Li, W.; Yang, J.; Zhu, Q., Direct visualization of straw cell walls by AFM. *Macromolecular Bioscience* **2004,** *4* (2), 112-118.

128.   Paddock, S. W., Principles and practices of laser scanning confocal microscopy. *Molecular Biotechnology* **2000,** *16* (2), 127-149.

129.   Donaldson, L.; Hague, J.; Snell, R., Lignin distribution in coppice poplar, linseed and wheat straw. *Holzforschung* **2001,** *55* (4), 379-385.

130.   Sant'Anna, C.; de Souza, W., Microscopy as a tool to follow deconstruction of lignocellulosic biomass. *Formatex Research Center, Espanha* **2012**, 639-645.

131.   Donaldson, L. A., Lignification and lignin topochemistry—an ultrastructural view. *Phytochemistry* **2001,** *57* (6), 859-873.

132.   Thomas, J.; Ingerfeld, M.; Nair, H.; Chauhan, S. S.; Collings, D. A., Pontamine fast scarlet 4B: a new fluorescent dye for visualising cell wall organisation in radiata pine tracheids. *Wood Science and Technology* **2013,** *47* (1), 59-75.

133.   Voiniciuc, C.; Schmidt, M. H.-W.; Berger, A.; Yang, B.; Ebert, B.; Scheller, H. V.; North, H. M.; Usadel, B.; Günl, M., MUCIlAGE-RELATED10 produces galactoglucomannan that maintains pectin and cellulose architecture in Arabidopsis seed mucilage. *Plant Physiology* **2015,** *169* (1), 403-420.

134.   Anderson, C. T.; Carroll, A.; Akhmetova, L.; Somerville, C., Real-time imaging of cellulose reorientation during cell wall expansion in Arabidopsis roots. *Plant Physiology* **2010,** *152* (2), 787-796.

135.   Zhu, P.; Moran-Mirabal, J. M.; Luterbacher, J. S.; Walker, L. P.; Craighead, H. G., Observing Thermobifida fusca cellulase binding to pretreated wood particles using time-lapse confocal laser scanning microscopy. *Cellulose* **2011,** *18* (3), 749-758.

136.   Costes, S. V.; Daelemans, D.; Cho, E. H.; Dobbin, Z.; Pavlakis, G.; Lockett, S., Automatic and quantitative measurement of protein-protein colocalization in live cells. *Biophysical Journal* **2004,** *86* (6), 3993-4003.

137.   Manders, E.; Stap, J.; Brakenhoff, G.; Van Driel, R.; Aten, J., Dynamics of three-dimensional replication patterns during the S-phase, analysed by double labelling of DNA and confocal microscopy. *Journal of Cell Science* **1992,** *103* (3), 857-862.

138.   Manders, E.; Verbeek, F.; Aten, J., Measurement of co-localization of objects in dual-colour confocal images. *Journal of Microscopy* **1993,** *169* (3), 375-382.

139.   Chen, S.; Zhang, X.; Ling, Z.; Xu, F., Characterization of the micromorphology and topochemistry of poplar wood during mild ionic liquid pretreatment for improving enzymatic saccharification. *Molecules* **2017,** *22* (115), 1-15.

140.   Selig, M. J.; Viamajala, S.; Decker, S. R.; Tucker, M. P.; Himmel, M. E.; Vinzant, T. B., Deposition of lignin droplets produced during dilute acid pretreatment of maize stems retards enzymatic hydrolysis of cellulose. *Biotechnology Progress* **2007,** *23* (6), 1333-1339.

141.   Donohoe, B. S.; Decker, S. R.; Tucker, M. P.; Himmel, M. E.; Vinzant, T. B., Visualizing lignin coalescence and migration through maize cell walls following thermochemical pretreatment. *Biotechnology and Bioengineering* **2008,** *101* (5), 913-925.

142.   Singh, S.; Simmons, B. A.; Vogel, K. P., Visualization of biomass solubilization and cellulose regeneration during ionic liquid pretreatment of switchgrass. *Biotechnology and Bioengineering* **2009,** *104* (1), 68-75.

143.   Chundawat, S. P.; Donohoe, B. S.; da Costa Sousa, L.; Elder, T.; Agarwal, U. P.; Lu, F.; Ralph, J.; Himmel, M. E.; Balan, V.; Dale, B. E., Multi-scale visualization and

characterization of lignocellulosic plant cell wall deconstruction during thermochemical pretreatment. *Energy & Environmental Science* **2011,** *4* (3), 973-984.

144.   Xu, F.; Yu, J.; Tesso, T.; Dowell, F.; Wang, D., Qualitative and quantitative analysis of lignocellulosic biomass using infrared techniques: a mini-review. *Applied Energy* **2013,** *104*, 801-809.

145.   Yu, H.; Fu, G.; He, B., Preparation and adsorption properties of PAA-grafted cellulose adsorbent for low-density lipoprotein from human plasma. *Cellulose* **2007,** *14* (2), 99-107.

146.   Owen, N.; Thomas, D., Infrared studies of "hard" and "soft" woods. *Applied Spectroscopy* **1989,** *43* (3), 451-455.

147.   Yin, Y.; Berglund, L.; Salmén, L., Effect of steam treatment on the properties of wood cell walls. *Biomacromolecules* **2010,** *12* (1), 194-202.

148.   Sun, Q.; Foston, M.; Meng, X.; Sawada, D.; Pingali, S. V.; O'Neill, H. M.; Li, H.; Wyman, C. E.; Langan, P.; Ragauskas, A. J., Effect of lignin content on changes occurring in poplar cellulose ultrastructure during dilute acid pretreatment. *Biotechnology for Biofuels* **2014,** *7* (1), 1.

149.   Yáñez-S, M.; Matsuhiro, B.; Nunez, C.; Pan, S.; Hubbell, C. A.; Sannigrahi, P.; Ragauskas, A. J., Physicochemical characterization of ethanol organosolv lignin (EOL) from Eucalyptus globulus: Effect of extraction conditions on the molecular structure. *Polymer Degradation and Stability* **2014,** *110*, 184-194.

150.   Zhang, W.; Yi, Z.; Huang, J.; Li, F.; Hao, B.; Li, M.; Hong, S.; Lv, Y.; Sun, W.; Ragauskas, A., Three lignocellulose features that distinctively affect biomass enzymatic digestibility under NaOH and H 2 SO 4 pretreatments in Miscanthus. *Bioresource Technology* **2013,** *130*, 30-37.

151.   Hong, J.; Ye, X.; Zhang, Y. H. P., Quantitative Determination of Cellulose Accessibility to Cellulase Based on Adsorption of a Nonhydrolytic Fusion Protein Containing CBM and GFP with Its Applications. *Langmuir* **2007,** *23* (25), 12535-12540.

152.   Wang, Q. Q.; He, Z.; Zhu, Z.; Zhang, Y. H. P.; Ni, Y.; Luo, X. L.; Zhu, J. Y., Evaluations of cellulose accessibilities of lignocelluloses by solute exclusion and protein adsorption techniques. *Biotechnology and Bioengineering* **2012,** *109* (2), 381-389.

153.   Rollin, J. A.; Zhu, Z.; Sathitsuksanoh, N.; Zhang, Y. H. P., Increasing cellulose accessibility is more important than removing lignin: A comparison of cellulose solvent-based lignocellulose fractionation and soaking in aqueous ammonia. *Biotechnology and Bioengineering* **2011,** *108* (1), 22-30.

154.   Li, C.; Knierim, B.; Manisseri, C.; Arora, R.; Scheller, H. V.; Auer, M.; Vogel, K. P.; Simmons, B. A.; Singh, S., Comparison of dilute acid and ionic liquid pretreatment of

switchgrass: biomass recalcitrance, delignification and enzymatic saccharification. *Bioresource Technology* **2010,** *101* (13), 4900-4906.

155.　Zhu, Z.; Sathitsuksanoh, N.; Vinzant, T.; Schell, D. J.; McMillan, J. D.; Zhang, Y. H. P., Comparative study of corn stover pretreated by dilute acid and cellulose solvent-based lignocellulose fractionation: Enzymatic hydrolysis, supramolecular structure, and substrate accessibility. *Biotechnology and Bioengineering* **2009,** *103* (4), 715-724.

156.　Tsai, A. Y. L.; Goacher, R. E.; Master, E. R., Detecting changes in arabidopsis cell wall composition using time-of-flight secondary ion mass spectrometry. *Surface and Interface Analysis* **2015,** *47* (5), 626-631.

157.　Saito, K.; Kato, T.; Takamori, H.; Kishimoto, T.; Fukushima, K., A new analysis of the depolymerized fragments of lignin polymer using ToF-SIMS. *Biomacromolecules* **2005,** *6* (5), 2688-2696.

158.　Goacher, R. E.; Tsai, A. Y.-L.; Master, E. R., Towards practical time-of-flight secondary ion mass spectrometry lignocellulolytic enzyme assays. *Biotechnology for Biofuels* **2013,** *6* (1), 1.

159.　Goacher, R. E.; Jeremic, D.; Master, E. R., Expanding the Library of Secondary Ions That Distinguish Lignin and Polysaccharides in Time-of-Flight Secondary Ion Mass Spectrometry Analysis of Wood. *Analytical Chemistry* **2011,** *83* (3), 804-812.

160.　Saito, K.; Kato, T.; Tsuji, Y.; Fukushima, K., Identifying the characteristic secondary ions of lignin polymer using ToF-SIMS. *Biomacromolecules* **2005,** *6* (2), 678-683.

161.　Belu, A. M.; Graham, D. J.; Castner, D. G., Time-of-flight secondary ion mass spectrometry: techniques and applications for the characterization of biomaterial surfaces. *Biomaterials* **2003,** *24* (21), 3635-3653.

162.　Kuroda, K.; Fujiwara, T.; Imai, T.; Takama, R.; Saito, K.; Matsushita, Y.; Fukushima, K., The cryo-TOF-SIMS/SEM system for the analysis of the chemical distribution in freeze-fixed Cryptomeria japonica wood. *Surface and Interface Analysis* **2013,** *45* (1), 215-219.

163.　Saito, K.; Kato, T.; Takamori, H.; Kishimoto, T.; Yamamoto, A.; Fukushima, K., A new analysis of the depolymerized fragments of lignin polymer in the plant cell walls using ToF-SIMS. *Applied Surface Science* **2006,** *252* (19), 6734-6737.

164.　Karuna, N.; Zhang, L.; Walton, J. H.; Couturier, M.; Oztop, M. H.; Master, E. R.; McCarthy, M. J.; Jeoh, T., The impact of alkali pretreatment and post-pretreatment conditioning on the surface properties of rice straw affecting cellulose accessibility to cellulases. *Bioresource Technology* **2014,** *167*, 232-240.

165.　Goacher, R. E.; Edwards, E. A.; Yakunin, A. F.; Mims, C. A.; Master, E. R., Application of Time-of-Flight-Secondary Ion Mass Spectrometry for the Detection of

Enzyme Activity on Solid Wood Substrates. *Analytical Chemistry* **2012,** *84* (10), 4443-4451.

166.	Mahajan, S.; Jeremic, D.; Goacher, R. E.; Master, E. R., Mode of coniferous wood decay by the white rot fungus Phanerochaete carnosa as elucidated by FTIR and ToF-SIMS. *Applied Microbiology and Biotechnology* **2012,** *94* (5), 1303-1311.

167.	Jung, S.; Foston, M.; Kalluri, U. C.; Tuskan, G. A.; Ragauskas, A. J., 3D chemical image using TOF-SIMS revealing the biopolymer component spatial and lateral distributions in biomass. *Angewandte Chemie International Edition* **2012,** *51* (48), 12005-12008.

168.	Zhou, C.; Li, Q.; Chiang, V. L.; Lucia, L. A.; Griffis, D. P., Chemical and spatial differentiation of syringyl and guaiacyl lignins in poplar wood via time-of-flight secondary ion mass spectrometry. *Analytical Chemistry* **2011,** *83* (18), 7020-7026.

169.	Jeremic, D.; Goacher, R. E.; Yan, R.; Karunakaran, C.; Master, E. R., Direct and up-close views of plant cell walls show a leading role for lignin-modifying enzymes on ensuing xylanases. *Biotechnology for Biofuels* **2014,** *7* (1), 1.

170.	Sodhi, R. N., Time-of-flight secondary ion mass spectrometry (TOF-SIMS):— versatility in chemical and imaging surface analysis. *Analyst* **2004,** *129* (6), 483-487.

171.	Saito, K.; Mitsutani, T.; Imai, T.; Matsushita, Y.; Yamamoto, A.; Fukushima, K., Chemical differences between sapwood and heartwood of Chamaecyparis obtusa detected by ToF-SIMS. *Applied Surface Science* **2008,** *255* (4), 1088-1091.

172.	Tokareva, E.; Fardim, P.; Pranovich, A.; Fagerholm, H.-P.; Daniel, G.; Holmbom, B., Imaging of wood tissue by ToF-SIMS: Critical evaluation and development of sample preparation techniques. *Applied Surface Science* **2007,** *253* (18), 7569-7577.

173.	Gerber, L.; Hoang, V. M.; Tran, L.; Kiet, H. A. T.; Malmberg, P.; Hanrieder, J.; Ewing, A., Using imaging ToF-SIMS data to determine the cell wall thickness of fibers in wood. *Surface and Interface Analysis* **2014,** *46* (S1), 225-228.

174.	Slutier, A.; Ruiz, R.; Scarlata, C.; Sluiter, J.; Templeton, D.; Crocker, D., Determination of extractives in biomass. *Laboratory Analytical Procedure* **2005**.

175.	Fardim, P.; Durán, N., Modification of fibre surfaces during pulping and refining as analysed by SEM, XPS and ToF-SIMS. *Colloids and Surfaces A: Physicochemical and Engineering Aspects* **2003,** *223* (1), 263-276.

176.	Braham, E. J.; Goacher, R. E., Identifying and minimizing buffer interferences in ToF-SIMS analyses of lignocellulose. *Surface and Interface Analysis* **2015,** *47* (1), 120-126.

177. Tokareva, E. N.; Pranovich, A. V.; Holmbom, B. R., Characteristic fragment ions from lignin and polysaccharides in ToF–SIMS. *Wood Science and Technology* **2011,** *45* (4), 767-785.

178. Berman, E. S. F.; Kulp, K. S.; Knize, M. G.; Wu, L.; Nelson, E. J.; Nelson, D. O.; Wu, K. J., Distinguishing Monosaccharide Stereo- and Structural Isomers with TOF-SIMS and Multivariate Statistical Analysis. *Analytical Chemistry* **2006,** *78* (18), 6497-6503.

179. Imai, T.; Tanabe, K.; Kato, T.; Fukushima, K., Localization of ferruginol, a diterpene phenol, in Cryptomeria japonica heartwood by time-of-flight secondary ion mass spectrometry. *Planta* **2005,** *221* (4), 549-556.

180. Müller-Maatsch, J.; Bencivenni, M.; Caligiani, A.; Tedeschi, T.; Bruggeman, G.; Bosch, M.; Petrusan, J.; Van Droogenbroeck, B.; Elst, K.; Sforza, S., Pectin content and composition from different food waste streams. *Food Chemistry* **2016,** *201*, 37-45.

181. Tokareva, E. N.; Pranovich, A. V.; Ek, P.; Holmbom, B., Determination of anionic groups in wood by time-of-flight secondary ion mass spectrometry and laser ablation-inductively coupled plasma-mass spectrometry. *Holzforschung* **2010,** *64* (1), 35-43.

182. Saito, K.; Watanabe, Y.; Shirakawa, M.; Matsushita, Y.; Imai, T.; Koike, T.; Sano, Y.; Funada, R.; Fukazawa, K.; Fukushima, K., Direct mapping of morphological distribution of syringyl and guaiacyl lignin in the xylem of maple by time-of-flight secondary ion mass spectrometry. *The Plant Journal* **2012,** *69* (3), 542-552.

183. Tolbert, A. K.; Ma, T.; Kalluri, U. C.; Ragauskas, A. J., Determining the syringyl/guaiacyl lignin ratio in the vessel and fiber cell walls of transgenic Populus plants. *Energy & Fuels* **2016,** *30* (7), 5716-5720.

184. Sathitsuksanoh, N.; Zhu, Z.; Zhang, Y.-H. P., Cellulose solvent-based pretreatment for corn stover and avicel: concentrated phosphoric acid versus ionic liquid [BMIM] Cl. *Cellulose* **2012,** *19* (4), 1161-1172.

185. Farkas, J.; Chung, D. W.; Cha, M.; Copeland, J.; Grayeski, P.; Westpheling, J., Improved growth media and culture techniques for genetic analysis and assessment of biomass utilization by *Caldicellulosiruptor bescii*. *Journal of Industrial Microbiology and Biotechnology* **2013,** *40* (1), 41-49.

186. Kádár, Z.; De Vrije, T.; Budde, M. A.; Szengyel, Z.; Réczey, K.; Claassen, P. A., Hydrogen production from paper sludge hydrolysate. *Applied Biochemistry and Biotechnology* **2003,** *107* (1-3), 557-566.

187. Sluiter, A.; Hames, B.; Ruiz, R.; Scarlata, C.; Sluiter, J.; Templeton, D.; Crocker, D., Determination of structural carbohydrates and lignin in biomass. *Laboratory Analytical Procedure* **2008,** *1617*.

188.   Yoo, C. G.; Pu, Y.; Li, M.; Ragauskas, A. J., Elucidating Structural Characteristics of Biomass using Solution-State 2 D NMR with a Mixture of Deuterated Dimethylsulfoxide and Hexamethylphosphoramide. *ChemSusChem* **2016,** *9* (10), 1090-1095.

189.   Donohoe, B. S.; Vinzant, T. B.; Elander, R. T.; Pallapolu, V. R.; Lee, Y.; Garlock, R. J.; Balan, V.; Dale, B. E.; Kim, Y.; Mosier, N. S., Surface and ultrastructural characterization of raw and pretreated switchgrass. *Bioresource Technology* **2011,** *102* (24), 11097-11104.

190.   Schmidt, M.; Schwartzberg, A.; Perera, P.; Weber-Bargioni, A.; Carroll, A.; Sarkar, P.; Bosneaga, E.; Urban, J.; Song, J.; Balakshin, M., Label-free in situ imaging of lignification in the cell wall of low lignin transgenic Populus trichocarpa. *Planta* **2009,** *230* (3), 589-597.

191.   Tetard, L.; Passian, A.; Farahi, R.; Kalluri, U.; Davison, B.; Thundat, T., Spectroscopy and atomic force microscopy of biomass. *Ultramicroscopy* **2010,** *110* (6), 701-707.

192.   Hanrieder, J. r.; Phan, N. T.; Kurczy, M. E.; Ewing, A. G., Imaging mass spectrometry in neuroscience. *ACS Chemical Neuroscience* **2013,** *4* (5), 666-679.

193.   Belu, A. M.; Davies, M. C.; Newton, J. M.; Patel, N., TOF-SIMS Characterization and Imaging of Controlled-Release Drug Delivery Systems. *Analytical Chemistry* **2000,** *72* (22), 5625-5638.

194.   Goacher, R. E.; Jeremic, D.; Master, E. R., Expanding the library of secondary ions that distinguish lignin and polysaccharides in time-of-flight secondary ion mass spectrometry analysis of wood. *Analytical Chemistry* **2010,** *83* (3), 804-812.

195.   Kim, T. H.; Lee, Y., Pretreatment of corn stover by soaking in aqueous ammonia at moderate temperatures. *Applied Biochemistry and Biotechnology* **2007,** *137* (1-12), 81-92.

196.   Hu, G.; Cateto, C.; Pu, Y.; Samuel, R.; Ragauskas, A. J., Structural characterization of switchgrass lignin after ethanol organosolv pretreatment. *Energy & Fuels* **2011,** *26* (1), 740-745.

197.   Studer, M. H.; DeMartini, J. D.; Davis, M. F.; Sykes, R. W.; Davison, B.; Keller, M.; Tuskan, G. A.; Wyman, C. E., Lignin content in natural Populus variants affects sugar release. *Proceedings of the National Academy of Sciences* **2011,** *108* (15), 6300-6305.

198.   Yang, B.; Wyman, C. E., Pretreatment: the key to unlocking low-cost cellulosic ethanol. *Biofuels, Bioproducts and Biorefining* **2008,** *2* (1), 26-40.

199.   Lynd, L. R.; van Zyl, W. H.; McBride, J. E.; Laser, M., Consolidated bioprocessing of cellulosic biomass: an update. *Current Opinion in Biotechnology* **2005,** *16* (5), 577-83.

200.   Blumer-Schuette, S. E.; Kataeva, I.; Westpheling, J.; Adams, M. W. W.; Kelly, R. M., Extremely thermophilic microorganisms for biomass conversion: status and prospects. *Current Opinion in Biotechnology* **2008,** *19* (3), 210-217.

201.   Blumer-Schuette, S. E.; Giannone, R. J.; Zurawski, J. V.; Ozdemir, I.; Ma, Q.; Yin, Y. B.; Xu, Y.; Kataeva, I.; Poole, F. L.; Adams, M. W. W.; Hamilton-Brehm, S. D.; Elkins, J. G.; Larimer, F. W.; Land, M. L.; Hauser, L. J.; Cottingham, R. W.; Hettich, R. L.; Kelly, R. M., *Caldicellulosiruptor* core and pangenomes reveal determinants for noncellulosomal thermophilic deconstruction of plant biomass. *Journal of Bacteriology* **2012,** *194* (15), 4015-4028.

202.   Blumer-Schuette, S. E.; Lewis, D. L.; Kelly, R. M., Phylogenetic, Microbiological, and Glycoside Hydrolase Diversities within the Extremely Thermophilic, Plant Biomass-Degrading Genus *Caldicellulosiruptor*. *Applied and Environmental Microbiology* **2010,** *76* (24), 8084-8092.

203.   Bayer, E. A.; Morag, E.; Lamed, R., The dellulosome - A treasure trove for biotechnology. *Trends in Biotechnology* **1994,** *12* (9), 379-386.

204.   Bayer, E. A.; Setter, E.; Lamed, R., Organization and distribution of the cellulosome in *Clostridium thermocellum*. *Journal of Bacteriology* **1985,** *163* (2), 552-559.

205.   Olson, D. G.; McBride, J. E.; Shaw, A. J.; Lynd, L. R., Recent progress in consolidated bioprocessing. *Current Opinion in Biotechnology* **2012,** *23* (3), 396-405.

206.   Brunecky, R.; Alahuhta, M.; Xu, Q.; Donohoe, B. S.; Crowley, M. F.; Kataeva, I. A.; Yang, S.-J.; Resch, M. G.; Adams, M. W.; Lunin, V. V., Revealing nature's cellulase diversity: the digestion mechanism of Caldicellulosiruptor bescii CelA. *Science* **2013,** *342* (6165), 1513-1516.

207.   Lu, Y.; Zhang, Y.-H. P.; Lynd, L. R., Enzyme–microbe synergy during cellulose hydrolysis by Clostridium thermocellum. *Proceedings of the National Academy of Sciences* **2006,** *103* (44), 16165-16169.

208.   Blumer-Schuette, S. E.; Alahuhta, M.; Conway, J. M.; Lee, L. L.; Zurawski, J. V.; Giannone, R. J.; Hettich, R. L.; Lunin, V. V.; Himmel, M. E.; Kelly, R. M., Discrete and structurally unique proteins (tapirins) mediate attachment of extremely thermophilic *Caldicellulosiruptor* species to cellulose. *Journal of Biological Chemistry* **2015,** *290* (17), 10645-10656.

209.   Lochner, A.; Giannone, R. J.; Rodriguez, M., Jr.; Shah, M. B.; Mielenz, J. R.; Keller, M.; Antranikian, G.; Graham, D. E.; Hettich, R. L., Use of label-free quantitative proteomics to distinguish the secreted cellulolytic systems of *Caldicellulosiruptor bescii*

and *Caldicellosiruptor obsidiansis. Applied and Environmental Microbiology* **2011,** *77* (12), 4042-54.

210. Van Dyk, J.; Pletschke, B., A review of lignocellulose bioconversion using enzymatic hydrolysis and synergistic cooperation between enzymes—factors affecting enzymes, conversion and synergy. *Biotechnology Advances* **2012,** *30* (6), 1458-1480.

211. Ragauskas, A. J.; Beckham, G. T.; Biddy, M. J.; Chandra, R.; Chen, F.; Davis, M. F.; Davison, B. H.; Dixon, R. A.; Gilna, P.; Keller, M., Lignin valorization: improving lignin processing in the biorefinery. *Science* **2014,** *344* (6185), 1246843.

212. Zeng, Y.; Zhao, S.; Yang, S.; Ding, S.-Y., Lignin plays a negative role in the biochemical process for producing lignocellulosic biofuels. *Current Opinion in Biotechnology* **2014,** *27*, 38-45.

213. Zhang, M.; Ju, X.; Song, X.; Zhang, X.; Pei, Z.; Wang, D., Effects of cutting orientation in poplar wood biomass size reduction on enzymatic hydrolysis sugar yield. *Bioresource Technology* **2015,** *194*, 407-410.

214. Bayer, E. A.; Lamed, R.; White, B. A.; Flint, H. J., From cellulosomes to cellulosomics. *The Chemical Record* **2008,** *8* (6), 364-377.

215. Holwerda, E. K.; Thorne, P. G.; Olson, D. G.; Amador-Noguez, D.; Engle, N. L.; Tschaplinski, T. J.; van Dijken, J. P.; Lynd, L. R., The exometabolome of Clostridium thermocellum reveals overflow metabolism at high cellulose loading. *Biotechnology for Biofuels* **2014,** *7* (155), 1-11.

216. Sluiter, A.; Hames, B.; Ruiz, R.; Scarlata, C.; Sluiter, J.; Templeton, D., Determination of sugars, byproducts, and degradation products in liquid fraction process samples. *Laboratory Analytical Procedure* **2006**.

217. Xu, Q.; Singh, A.; Himmel, M. E., Perspectives and new directions for the production of bioethanol using consolidated bioprocessing of lignocellulose. *Current Opinion in Biotechnology* **2009,** *20* (3), 364-371.

218. Frederick, N.; Zhang, N.; Ge, X.; Xu, J.; Pelkki, M.; Martin, E.; Carrier, D. J., Poplar (Populus deltoides L.): The effect of washing pretreated biomass on enzymatic hydrolysis and fermentation to ethanol. *ACS Sustainable Chemistry & Engineering* **2014,** *2* (7), 1835-1842.

219. Palmqvist, E.; Hahn-Hägerdal, B., Fermentation of lignocellulosic hydrolysates. II: inhibitors and mechanisms of inhibition. *Bioresource Technology* **2000,** *74* (1), 25-33.

220. Verbeke, T. J.; Giannone, R. J.; Klingeman, D. M.; Engle, N. L.; Rydzak, T.; Guss, A. M.; Tschaplinski, T. J.; Brown, S. D.; Hettich, R. L.; Elkins, J. G., Pentose sugars inhibit metabolism and increase expression of an AgrD-type cyclic pentapeptide in Clostridium thermocellum. *Scientific Reports* **2017,** *7*.

221. Poudel, S.; Giannone, R. J.; Rodriguez, M.; Raman, B.; Martin, M. Z.; Engle, N. L.; Mielenz, J. R.; Nookaew, I.; Brown, S. D.; Tschaplinski, T. J., Integrated omics analyses reveal the details of metabolic adaptation of Clostridium thermocellum to lignocellulose-derived growth inhibitors released during the deconstruction of switchgrass. *Biotechnology for Biofuels* **2017,** *10* (1), 14.

222. Yarbrough, J. M.; Mittal, A.; Mansfield, E.; Taylor, L. E.; Hobdey, S. E.; Sammond, D. W.; Bomble, Y. J.; Crowley, M. F.; Decker, S. R.; Himmel, M. E., New perspective on glycoside hydrolase binding to lignin from pretreated corn stover. *Biotechnology for Biofuels* **2015,** *8* (214), 1-14.

223. Donaldson, L. A.; Knox, J. P., Localization of cell wall polysaccharides in normal and compression wood of radiata pine: relationships with lignification and microfibril orientation. *Plant Physiology* **2012,** *158* (2), 642-653.

224. Alcántara, M. Á. B.; Dobruchowska, J.; Azadi, P.; García, B. D.; Molina-Heredia, F. P.; Reyes-Sosa, F. M., Recalcitrant carbohydrates after enzymatic hydrolysis of pretreated lignocellulosic biomass. *Biotechnology for Biofuels* **2016,** *9* (207), 1-10.

225. *Natural Products Isolation*. 2 ed.; Humana Press Totowa, NJ, 2006; p 515.